BIOCOMPATIBILITY EVALUATIONS AND BIOMEDICAL SENSING APPLICATIONS OF NITRIC OXIDE-RELEASING/GENERATING POLYMERIC MATERIALS

by

Yiduo Wu

A dissertation submitted in partial fulfillment
of the requirements for the degree of
Doctor of Philosophy
(Chemistry)
in The University of Michigan
2008

Doctoral Committee:

Professor Mark E. Meyerhoff, Chair
Professor Carol A. Fierke
Assistant Professor Marc J. A. Johnson
Associate Professor Shuichi Takayama

To my mom

Chunhong Wang

ACKNOWLEDGEMENTS

First and foremost, I would like to express my sincerest gratitude to my mentor, Dr. Mark Meyerhoff, whose guidance, understanding and inspiration were invaluable in the completion of this study. I would also like to extend my thanks to Drs. Carol Fierke, Marc Johnson and Shuichi Takayama for serving on my dissertation committee.

I am indebt to our collaborators for their wonderful support and assistance. The implantable sensor and extracorporeal circulation experiments were performed in the ExtraCorporeal Membrane Oxygenation (ECMO) lab at the University of Michigan Medical School, lead by Drs. Robert Bartlett and Gail Annich. Dr. Bartlett's surgical team, including Dr. Alvaro Rojas, Grant Griffith, Nathan Lafayette, Amy Skrzypchak, Joshua Pohlmann and Candice Hall, offered tremendous help for the successful execution of the animal studies. The *S*-nitrosothiol measurements in porcine blood were carried out in Dr. Prabir Roy-Chaudhury's lab at the University of Cincinnati, with the great help of Yang Wang and Mehash Krishnamoorthy. In addition, I am grateful for the support and direction from Dr. Barry Bleske at the U of M College of Pharmacy. The research presented in this dissertation would not have been possible without their contribution.

My genuine appreciation goes to all my colleagues at the Meyerhoff group. In particular, I wish to thank Dr. Megan Frost for her coaching in the implantable sensor studies and Dr. Wansik Cha for his pioneering work in RSNO sensors. During my graduate career, I am thankful for the encouragement from all previous and current

members of the Meyerhoff group, including Dr. Melissa Reynolds, Dr. Zhengrong Zhou, Dr. Hyoungsik Yim, Dr. Wei Zhang, Dr. Jeremy Mitchell-Koch, Dr. Sangyeul Hwang, Dr. Fenghua Zhang, Dr. Jason Bennett, Biyun Wu, Lin Wang, Dongxuan Shen, Jun Yang, Youngjea Kang, Laura Zimmerman and Qinyi Yan. We take pride in being a very happy family at the Meyerhoff lab.

I would like to acknowledge the financial support provided by the National Institutes of Health and Michigan Critical Care Consultant (MC3), Inc.

Last but not least, I owe many thanks to my family. I want to say a big 'thank-you' to my fiancée, Ziyang Su, whose love, patience and encouragement kept me moving forward during the most challenging moments of Ph.D study. I am also grateful for the love and support from other family members back in China, including my dad, step-mother, and the soon-to-be parent-in-laws.

TABLE OF CONTENTS

LIST OF FIGURES

FIGURE

LIST OF TABLES

TABLE

LIST OF ABBREVIATIONS

ABG	Arterial Blood Gas
ACT	Activated Clotting Time
AlbSNO	*S*-Nitrosoalbumin
BSA	Bovine Serum Albumin
cGMP	Cyclic Guanosine Monophosphate
Cu(II)-DTTCT	Cu(II)-Dibenzo-[e,k]-2,3,8,9-Tetraphenyl-1,4,7,10-Tetraaza-Cyclododeca-1,3,7,9-Tetraene
CVP	Central Venous Pressure
CysNO	*S*-Nitrosocysteine
DACA	Diaminoalkyltrimethoxylsilane
DBHD	*N,N'*-Dibutyl-1,6-Hexanediamine
DMHD	*N,N*'-Dimethyl-1,6-Hexanediamine
DOS	Sebacic Acid Di(2-Ethylhexyl) Ester
DTT	1,4-Dithiothreitol
EC	Endothelial Cell
ECC	Extracorporeal Circulation
EDC	*N*-(3-Dimethylaminopropyl)-*N'*-Ethylcarbodiimide Hydrochloride
EDTA	Ethylenediaminetetraacetic Acid
ELISA	Enzyme-Linked Immunosorbent Assay
GPx	Glutathione Peroxidase
GSH	Glutathione
GSNO	*S*-Nitrosoglutathione
Hct	Hematocrit
HMW	High Molecular Weight
HPPU	Hydrophilic Polyurethane

HRP	Horseradish Peroxidase
KTpClPB	Potassium Tetrakis(4-chlorophenyl)borate
LDH	Lactate Dehydrogenase
LMW	Low Molecular Weight
NHS	*N*-Hydroxylsuccinimide
NOA	Nitric Oxide Analyzer
NOS	Nitric Oxide Synthase
NPOE	2-Nitrophenyl Octyl Ether
PBS	Phosphate Buffered Saline
PDMS	Polydimethylsiloxane
PEI	Polyethylenimine
PPP	Platelet Poor Plasma
PRP	Platelet Rich Plasma
PTFE	Polytetrafluoroethylene
PU	Polyurethane
PVC	Poly(Vinyl Chloride)
RCF	Relative Centrifugation Force
RSePEI	Selenium-Immobilized Polyethylenimine
RSNO	*S*-Nitrosothiol
RXNO	Total Nitroso- Species
SeDPA	3,3’-Dipropionic Acid Diselenide
SEM	Scanning Electron Microscopy
SNAC	*S*-Nitroso-*N*-Acetyl-Cysteine
SNAP	*S*-Nitroso-*N*-Acetyl-Penicillamine
SR	Silicone Rubber
THF	Tetrahydrofuran
vWF	von Willebrand Factor

ABSTRACT

BIOCOMPATIBILITY EVALUATIONS AND BIOMEDICAL SENSING APPLICATIONS OF NITRIC OXIDE-RELEASING/GENERATING POLYMERIC MATERIALS

by

Yiduo Wu

Chair: Mark E. Meyerhoff

Nitric oxide (NO) is a potent signaling molecule secreted by healthy vascular endothelial cells (EC) that is capable of inhibiting the activation and adhesion of platelets, preventing inflammation and inducing vasodilation. Polymeric materials that mimic the EC through the continuous release or generation of NO are expected to exhibit enhanced biocompatibility *in vivo*. In this dissertation research, the biocompatibility of novel NO-releasing/generating materials has been evaluated via both *in vitro* and *in vivo* studies.

A new *in vitro* platelet adhesion assay has been designed to quantify platelet adhesion on NO-releasing/generating polymer surfaces via their innate lactate dehydrogenase (LDH) content. Using this assay, it was discovered that continuous NO fluxes of up to 7.05 $\times 10^{-10}$ mol cm^{-2} min^{-1} emitted from the polymer surfaces could reduce platelet adhesion by almost 80%. Such an *in vitro* biocompatibility assay can be employed as a preliminary screening method in the development of new NO-releasing/generating materials.

In addition, the first *in vivo* biocompatibility evaluation of NO-generating polymers was conducted in a porcine artery model for intravascular oxygen sensing catheters. The Cu(I)-catalyzed decomposition of endogenous *S*-nitrosothiols (RSNOs) generated NO *in situ* at the polymer/blood interface and offered enhanced biocompatibility to the NO-generating catheters along with more accurate analytical results for intra-arterial measurements of PO_2 levels.

NO-generating polymers can also be utilized to fabricate electrochemical RSNO sensors based on the amperometric detection of NO generated by the reaction of RSNOs with immobilized catalysts. Unlike conventional methodologies employed to measure labile RSNO, the advantage of the RSNO sensor method is that measurement in whole blood samples is possible and this minimizes sample processing artifacts in RSNO measurements. An electrochemical RSNO sensor with organoselenium crosslinked polyethylenimine (RSePEI) catalyst was used to determine the endogenous RSNO levels in the whole blood of rabbits and pigs, and substantial variations of RSNO levels were found within the same animal species. The photo-decomposition of RSNOs during sample collection was also studied. The results show that complete insulation from external light during the blood sampling step is critical for the accurate determination of endogenous RSNOs.

CHAPTER 1

INTRODUCTION

1.1. Overview and Scope of Areas Examined by this Thesis Research

The development of reliable *in vivo* chemical sensors for real-time clinical monitoring of blood gases, electrolytes, glucose, etc. in critically ill and diabetic patients remains a great challenge owing to inherent biocompatibility problems that can cause errant analytical results upon sensor implantation (e.g., cell adhesion, thrombosis, inflammation) [1, 2]. Nitric oxide (NO) is a well-known inhibitor of platelet activation and adhesion, and also a potent inhibitor of smooth muscle cell proliferation [3]. In addition, NO mediates inflammatory response [4] and promotes angiogenesis [5]. Polymers that release or generate NO at their surfaces have been shown to exhibit greatly enhanced thromboresistance *in vivo* when in contact with flowing blood [6, 7], as well as reduce inflammatory response when placed subcutaneously [8], and thus have the potential to improve the biocompatibility of implanted chemical sensors. Locally elevated NO levels at the surface of implanted devices can be achieved by using polymers that incorporate NO donor species that can decompose and release NO

spontaneously when in contact with physiological fluids, or NO-generating polymers that possess an immobilized catalyst that decompose endogenous *S*-nitrosothiols (RSNOs) to generate NO *in situ*. The structures of some endogenous RSNOs are illustrated in Figure 4.1.

Although *in vivo* study remains the 'gold standard' for the determination of biocompatibility, *in vitro* biocompatibility assays are still an attractive approach for the sake of time and cost. Therefore, it is the focus of this dissertation research to evaluate the biocompatibility of NO-releasing/generating biomaterials both *in vitro* and *in vivo*. Moreover, since RSNOs serve as substrates for the NO-generating polymeric materials, their endogenous concentrations are a critical factor in determining the biocompatibility of NO-generating materials. However, there is lack of consensus regarding the endogenous concentrations of RSNO species in the literature. The reported values range from nM to μM levels [9]. Thus, another goal of this dissertation research is to employ the new electrochemical RSNO sensors developed in the Meyerhoff lab to determine blood RSNO concentrations in various animals and to help provide insight regarding the potential function of NO-generating materials *in vivo*.

1.2. Current Challenge to the Development of Implantable Chemical Sensors

The care of critically ill hospitalized patients requires frequent and accurate measurements of arterial blood gases (pH, PO_2, PCO_2), electrolytes (Na^+, K^+, Ca^{2+}) and glucose/lactate levels in undiluted whole blood. To date, such values are usually obtained from *in vitro* tests using discrete blood samples drawn intermittently from

patients and analyzed on benchtop instruments or smaller point-of–care devices [2, 10, 11]. However, intermittent sampling can miss events that can be life-threatening to the patient. Indeed, isolated measurements are not able to provide the desired real-time monitoring of minute-to-minute physiological changes that can occur in unstable critically ill patients [2]. Therefore, continuous intravascular sensing of clinically important species would be of great value to improve the quality of health care for such patients.

At the same time, reliable *in vivo* monitoring of glucose concentrations in blood or the interstitial fluid could significantly enhance the quality of life for millions of non-hospitalized patients with diabetes mellitus. A successful implantable glucose sensor must: i) be small enough to be placed intravascularly or subcutaneously; ii) provide long-term stable analytical signals so that re-calibration can be minimized; iii) yield accurate measurements of glucose that correlate well with *in vitro* tests based on discrete blood samples so that therapeutic action can be taken based on the measured values (e.g., infusion of insulin); and iv) be compatible with the biological environment in which it is implanted (i.e., 'biocompatible').

Advances in the miniaturization of optical and electrochemical sensors for blood gases, electrolytes and glucose/lactate have made it possible to place such devices within blood vessels or under the skin. However, despite significant efforts toward developing implantable intravascular and/or subcutaneous chemical sensors suitable for continuous *in vivo* monitoring, the routine clinical use of such devices has not yet been realized [1]. The major challenge to be overcome for success in this area is the erratic analytical results obtained from sensors implanted *in vivo*. Errant analytical results are generally

attributed to the adverse biological responses to such implanted devices [2, 11-13], which usually relates to the lack of biocompatibility of the implanted optical or electrochemical probes. This problem has been reviewed previously [13]. Here, greater emphasis is given to a newer strategy involving coatings that generate nitric oxide (a species that can dramatically improve biocompatibility) from endogenous physiological species.

The biocompatibility of an implantable medical device refers to the ability of the device to perform its intended function, with the desired degree of incorporation within the host, without eliciting any undesirable local or systemic effects in that host [14]. The biological response to implanted sensors depends largely on the site of implantation. Intravascular placement is the most desirable for blood chemistry measurements. The biocompatibility problems associated with sensors implanted intravascularly have been reviewed previously [1, 2, 10, 11]. When an intravascular sensor is in contact with blood, the initial biological response is the rapid adsorption of plasma proteins (e.g., fibrinogen, fibronectin and von Willebrand's factor (vWF)) onto the surface, followed by the adhesion and activation of platelets (see Figure 1.1) [15]. Once activated, platelets undergo shape change and secretion of the granular contents. The activated platelet is a key player in the coagulation cascade and will ultimately lead to the formation of a blood clot on the surface of the device [16].

Such biofouling of the sensing membrane can restrict the diffusion of analyte to the sensor surface [17]. Moreover, the metabolic activities of adhered cells consume oxygen and glucose while producing carbon dioxide, thus changing the local concentration of blood gases and glucose levels sensed by the implanted device [13].

Figure 1.2 illustrates the typical patterns of deviation for sensors implanted

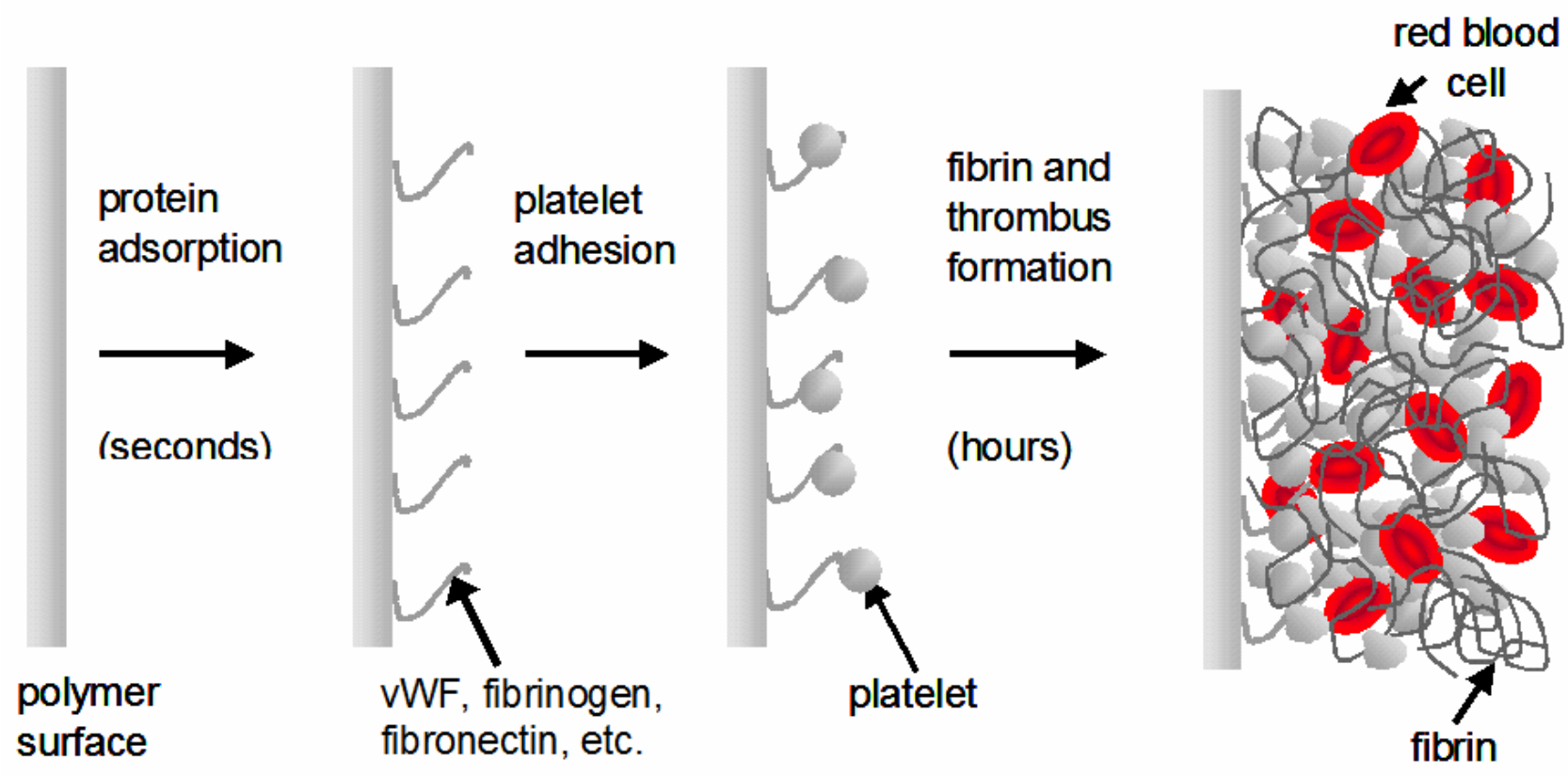

Figure 1.1. Sequence of events leading to thrombus formation on surface of intravascularly implanted sensor

intravascularly. Even a monolayer of cells adhered onto the sensor surface is sufficient to produce the behavior illustrated in Figure 1.2.

Similar patterns of deviation can also be observed when blood flow is reduced in the blood vessel where the sensor is placed, or when the sensor touches the wall of blood vessels where inherent metabolism of endothelial cells can affect sensor performance in the same way as adhered blood cells ("wall effect") [2, 13]. Moreover, thrombus formation in patients can occur randomly since it also depends on factors such as the native coagulation propensity of a particular patient and the velocity of blood-flow within the lumen of the vessel in which the sensor is placed. The unpredictability of intravascular sensor performance due to these biological factors makes the measurements unreliable, preventing timely therapeutic intervention. Sensors implanted under the skin (subcutaneous measurements), such as those often developed for monitoring glucose levels, do not encounter the same issues of platelet activation and thrombus formation. However, such sensors are subject to their own biocompatibility problems, primarily from inflammatory responses that can affect their accuracy. The size, shape and physical/chemical properties of the implanted devices contribute to variations in the intensity and time duration of the inflammatory and wound-healing process [18]. Acute inflammatory response starts immediately after sensor implantation as fluids, plasma proteins and inflammatory cells migrate to the implant site [19]. The first event that occurs is protein adsorption, followed by the attack of phagocytic cells (neutrophils, monocytes and macrophages) to the implanted sensor, attempting to destroy it. However, since the sensor is large, only 'frustrated phagocytosis' occurs [18, 19]. Acute inflammatory response (24 – 48 h) is characterized by the predominance of neutrophils,

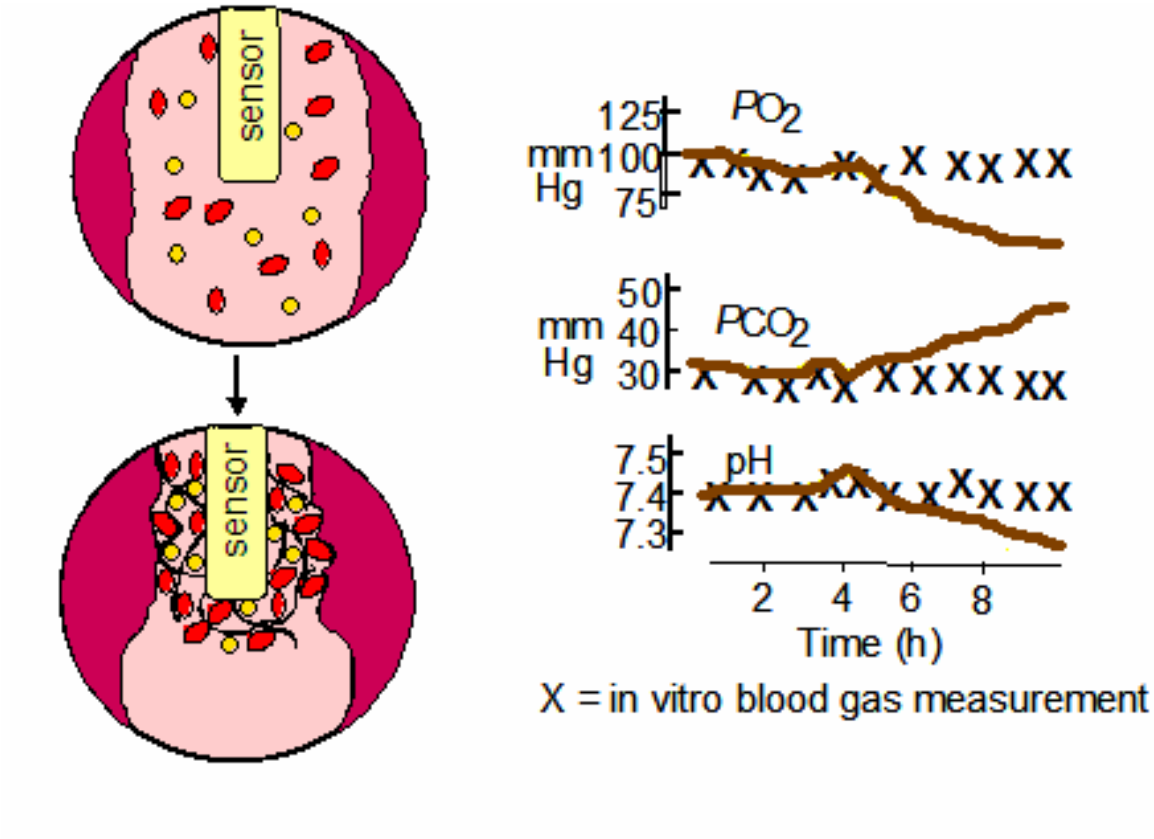

Figure 1.2. Deviations in implanted sensor measurements of blood gases/pH due to cell adhesion and/or low blood flow at the implant site.

which are later replaced by macrophages, monocytes and lymphocytes during the chronic inflammation stage [19]. Ultimately, fibrous encapsulation of the subcutaneously implanted device by primarily macrophages and fibrin indicates the end-stage of the wound-healing process. The fibrous capsule can change the analyte levels in the vicinity of the sensor through metabolic activities (e.g., faster glucose consumption). It also can affect the transport of analyte to the sensor surface as well as that between the blood and the interstitial fluid. This can lead to significant changes in the calibration curve (i.e., lowering the sensitivity) as well as affecting the lag time of the sensor's response to the fluctuations of glucose levels in bulk blood for both optical [20, 21] and electrochemical sensors [12, 18, 22]. Angiogenesis around the site of tissue injury caused by implanted sensor is also part of the wound-healing process. Since more blood vessels around the implanted sensors will facilitate the diffusion of the analyte from blood to the subcutaneous fluids (so interstitial fluid levels of the analyte more closely resemble blood levels), the degree of angiogenesis after implantation will also influence the output of sensors placed subcutaneously [23]

1.3. Strategies for Improving Biocompatibility

1.3.1. Surface Modifications

The surface of an implanted device is thought by many to be of critical importance in determining the *in vivo* performance of any implant. Surface modification strategies employed to address biocompatibility issues have been reviewed by Wisniewski et al. [17]. These approaches include hydrogel overlays, phospholipid-based biomimicry,

flow-based systems, Nafion coatings, surfactants, covalent attachments, diamond-like carbons, and topology treatments. Surfaces with high water content are found to be more inert to protein adsorption and cell adhesion as a result of low interfacial energy [24]. Hydrogels and other hydrophilic surface modifications are aimed at minimizing protein adsorption, since such adsorption initiates a series of biological responses [15, 19]. Biomaterials with the surface immobilized biological molecules, such as albumin [25], heparin [26], thrombomodulin [27], prostacyclin [28] and hyaluronic acid [29] have all been shown to exhibit some effectiveness in enhancing biocompatibility.

1.3.2. Potential for Utilizing Nitric Oxide (NO) with *In Vivo* Sensors

Unfortunately, hydrophilic surfaces by themselves may retard, but do not completely prevent the adsorption of proteins on artificial surfaces *in vivo*. Eventually, the proteins that can initiate platelet adhesion/activation or those that mediate inflammatory responses will still adsorb onto the surface of the implanted sensor, leading to thrombus formation and/or inflammation. The biological environments in which the sensors are implanted involve a myriad of activities besides the cell surface expression of certain molecules. In the case of the vascular endothelium that lines the inner walls of all blood vessels (and is known to be the best example of a completely non-thrombogenic surface), a number of active molecules such as thrombomodulin, prostacyclin, heparan sulfate, and nitric oxide (NO) are either expressed at the surface or are continuously being secreted to mediate the biological responses underlining biocompatibility [16].

Over the past twenty years, NO has received considerable interest from the pharmacological and biomedical research communities owing to its diverse physiological

functions as a protective, regulatory and signaling molecule involved in the regulation of blood pressure, clotting, neurotransmission and immune response. Indeed, NO is widely recognized as a key anti-platelet, anti-inflammatory and vasodilating agent [30-34]. In addition, NO is also known to inhibit bacterial growth [35, 36] and promote angiogenesis [5].

Nitric oxide is produced endogenously from L-arginine and oxygen by enzymes known as nitric oxide synthases (NOS) [37]. NO exerts its vasodilation and anti-platelet function by binding to the heme iron of soluble guanylate cyclase and subsequently increasing the production and intracellular concentrations of cyclic guanosine monophosphate (cGMP), a secondary messenger [38]. The endogenous concentration of NO as a dissolved gas is very low (~3 nM) [39]. Under physiological conditions, oxidized NO (in the form of NO^+ or N_2O_3) reacts with thiol groups in cysteine or cysteine-containing peptides and proteins (e.g., glutathione, albumin and hemoglobin) to yield *S*-nitrosothiols (RSNOs) [40, 41]. RSNOs act as carriers of NO in the body and are thought to be responsible for the storage and bioavailability of NO [39, 42] (see Section **1.5** below).

Vasoconstriction can occur at the site where the intravascular sensor is implanted as a biological response to reduce bleeding at the implant site. Meanwhile, platelets are activated and recruited to repair the vascular injury [43]. NO is synthesized in the endothelial cells that line the wall of healthy blood vessel and diffuses in all directions. When NO reaches the underlying vascular smooth muscle cells, NO stimulates cGMP production and, in turn, decreases the Ca^{2+} levels in the smooth muscle cells, leading to vascular relaxation [44]. Muscle relaxation allows the blood vessel to dilate and lowers

the blood pressure. NO also diffuses into circulating platelets, especially when they approach the surface of the endothelium. Platelet activation is also Ca^{2+} dependent [45] and is thus inhibited by NO [34, 46]. The lifetime of NO in whole blood is very short (< 1 sec) due to its reaction with heme-containing compounds such as oxyhemoglobin [3]. Therefore the anti-platelet effect occurs only locally when platelets are in close proximity to the endothelium, as the presence of red blood cells would block the NO transfer to platelets. It has been estimated that the endothelial derived NO flux is in the range of 0.5-4.0 $\times 10^{-10}$ mol cm^{-2} min^{-1} [47]. Therefore, if the surface of an intravascular sensor can release or generate NO at or above this range of fluxes, it is expected to display enhanced thromboresistance. Furthermore, the released NO will be effective only locally at the blood/polymer interface, which is ideal for biocompatibility purposes. Owing to the low NO fluxes, the small dimension of the intravascular sensor, and the very short half-life of NO in blood, the locally released NO is unlikely to cause any systemic effect that may lead to cytotoxicity or hemorrhage.

Nitric oxide also is involved in virtually every step of the inflammatory process [4]. In fact, NO plays a crucial role in wound healing and down regulates mediators of inflammatory response. Low concentrations of NO can inhibit adhesive molecule expression, cytokine and chemokine synthesis as well as leukocyte adhesion and transmigration [4]. Nitric oxide also promotes angiogenesis and disruption of the NOS-based NO generation pathway is known to impair neovascularization [5]. Subcutaneous implantation also brings the risk of infection, which can also be inhibited by NO [36]. Therefore, an active surface that can continuously release or generate NO in the interstitial fluid may also benefit greatly from a locally enhanced level of NO, with

respect to reducing inflammatory cell migration and promotion of neovascularization that could increase the exchange of glucose and other analytes into the subcutaneous fluid adjacent to the implanted sensor.

1.4. Implantable Sensors with NO-Releasing/Generating Coatings

1.4.1. NO-Releasing Materials

Since the discovery of the anti-thrombogenic role of NO, the possibility of improving biocompatibility by incorporating NO-releasing/generating function into biomedical polymers has been explored by several research groups. Ramamurthi and Lewis [46] used the direct infusion of gaseous $NO_{(g)}$ (0.1 ppm) through a semi-permeable membrane to produce surface NO fluxes ranging between 3-6.6 $\times 10^{-8}$ mol cm^{-2} min^{-1}. These low levels of NO were shown to inhibit platelet adhesion by as much as 87%. However, it would be quite difficult to deliver gaseous NO (from a reservoir of NO gas) to the surface of an implanted sensor, once it was placed in an artery/vein or under the skin. Fortunately, a number of NO donor compounds have been developed to deliver NO *in vivo* and study its biological effects [48]. For implantable sensor applications, the NO donors must be incorporated in the polymer either as a thin outer coating or into the bulk polymer from which the medical sensor is made (e.g., polymeric tubing for certain catheter style sensors). The duration of NO release should match the implant lifetime of the device itself. In addition, it is critical that the NO release rate be controllable, as excess exposure to the NO donor, NO and any reaction products can be cytotoxic, mutagenic or carcinogenic.

To date, the two most widely investigated NO donors for biomedical applications are *S*-nitrosothiols (RSNO) and *N*-diazeniumdiolates (so-called NONOates). *S*-Nitrosothiols can be prepared by reacting thiols with nitrous acid. *S*-Nitrosoglutathione (GSNO) and *S*-nitroso-*N*-acetyl-cysteine (SNAC) have been blended into various polymers (e.g., poly(vinyl alcohol), poly(vinyl pyrrolidone), poly(ethylene glycol)) by de Oliveira and coworkers for targeted delivery of NO and parent RSNOs [49-51]. Bohl and West demonstrated that *S*-nitrosocysteine (CysNO) immobilized within a poly(ethylene glycol) hydrogel reduced platelet adhesion and smooth muscle cell proliferation *in vitro* [52].

A *N*-diazeniumdiolate is an NO adduct with secondary amines [53]. One equivalent of amine reacts with two equivalents of NO to form the corresponding diazeniumdiolate under high $NO_{(g)}$ pressure (e.g., 80 psi). The NO release from diazeniumdiolates is proton-driven and follows pseudo-first order kinetics at physiological pH [54]. Three general procedures have been used in the preparation of diazeniumdiolate-based NO-releasing polymers: 1) dispersion of small amine-based diazeniumdiolate molecules into polymer matrices (e.g., DBHD/N_2O_2) [55]; 2) diazeniumdiolation of covalently linked amine sites on pendant polymer side chains, or on the polymer backbone [56, 57]; and 3) covalent binding of diazeniumdiolate groups to micro- or nano-particles, and use of such particles as polymer fillers [58]. The half-life of NO release can be modulated by selecting different secondary amine structures [59] and the NO fluxes can be tuned by changing the diazeniumdiolate dopant amount or hydrophobicity of the polymer matrices or by applying topcoats of polymers to control the diffusion of water into the layer containing the NONOate. The leaching of

non-covalently bound small molecule diazeniumdiolates can be greatly reduced by using highly lipophilic diazeniumdiolates blended into the polymer matrix [55]. The potential application of diazeniumdiolate-based NO release to implantable sensors has recently been reviewed [13].

A key assumption with respect to potentially using NO-release polymers to prepare implantable sensors is that the NO release chemistry should not interfere with the sensing chemistry of the device. Since NO is a redox active species, it is necessary to establish that the initial NO donors and the released NO from the outer coating do not interfere with the analyte measurement by significantly changing the sensitivity, selectivity or lifetime of the implantable chemical sensor, especially electrochemical devices.

Initial work with NO-releasing chemical sensors focused on using a small molecule NO donor, dimethylhexane diamine diazeniumdiolate (DMHD/N_2O_2), dispersed into plasticized poly(vinyl chloride) (PVC) and polyurethane (PU) membranes for the purpose of preparing NO-releasing potentiometric ion-selective sensors. Indeed, Espadas-Torre et al. reported that pH and K^+ sensors prepared with the NO-releasing polymer membranes (doped also with the appropriate ion-selective ionophores [tridodecylamine (TDDA) or valinomycin] for sensing purposes) exhibit similar potentiometric response sensitivities and selectivities towards H^+ and K^+ as control sensors without NO release [60]. The NO-releasing ion-selective polymer films also exhibit greatly reduced platelet adhesion and activation compared to control films without NO release when tested *in vitro* using platelet-rich sheep plasma. Mowery et al. further demonstrated that two other NO donors, diazeniumdiolated linear polyethylenimine and diazeniumdiolated methoxymethylpiperazine PVC, can also be used to prepare potentiometric sensing

membranes [61]. They also extended the application of (DMHD/N_2O_2) to a Clark-style amperometric oxygen sensor and proved that NO release does not affect the sensor's amperometric response [61]. Frost et al. utilized the diazeniumdiolated diaminoalkyltrimethoxylsilane (DACA/N_2O_2) crosslinked polydimethylsiloxane (PDMS) to coat the outer walls of a potentiometric CO_2-sensing catheter [62]. The NO-releasing CO_2 sensors exhibited comparable Nernstian response slopes as the control sensors without NO-release chemistry. Apparently, the low fluxes of NO released from such coatings do not have a significant impact on the analytical performance of such devices.

Nitric oxide release has also been employed to enhance the biocompatibility of optical sensors. Schoenfisch et al. reported a dual-layer fluorescence-based oxygen sensor configuration with the underlying NO-releasing layer made from DACA/N_2O_2 crosslinked silicone rubber (SR) covered by a second polymeric layer containing the pyrene/perylene fluorescent indicators [63]. The NO-releasing sensors yielded identical responses to oxygen as conventional sensors without NO release. Further, Schoenfisch and coworkers developed a NO-releasing xerogel-based optical pH sensor and demonstrated its improved blood compatibility through an *in vitro* platelet adhesion study [64].

The initial proof-of-concept that NO release can improve the biocompatibility of devices implanted intravascularly was performed by implanting sham catheters coated with diazeniumdiolated methoxymethylpiperazine PVC into canine carotid arteries for 6 h [61]. The catheters coated with NO-releasing polymer showed greatly reduced platelet activation and adhesion compared to conventional PVC implanted in the same animal. These experiments indicated that low levels of NO release did in fact inhibit

thrombus formation on the surface of implanted intravascular devices within the complex and dynamic environment of flowing blood.

The first *in vivo* evaluation of NO-releasing intravascular chemical sensors was reported by Schoenfisch et al. [7]. In this study, DMHD/N_2O_2 dispersed in cross-linked silicone rubber (SR) was coated over the outer SR gas-permeable tubing of a Clark-style amperometric oxygen-sensing catheter to impart NO release. These sensors were implanted in canine arteries for up to 23 h without systemic anticoagulation. During the course of the experiments, the oxygen levels monitored by the NO-releasing sensors tracked more closely with *in vitro* blood gas analysis of PO_2 levels performed on discrete blood samples drawn from the animal, as compared to non-NO release control oxygen sensors implanted within the same animal (i.e., more accurate results). At the end of each animal study, the sensors were carefully explanted from the arteries and examined by scanning electron microscopy (SEM). The NO-releasing catheters consistently showed a marked decrease in platelet adhesion under SEM, with no gross thrombus formation. On the other hand, gross thrombus formation was routinely observed on the control catheters which were covered by adhered platelets, fibrin and entrapped red cells.

These encouraging results suggested the potential of using NO-releasing polymers to enhance the biocompatibility and concomitant analytical performance of intravascular chemical sensors. However, it was found that the small molecule NO donor (DMHD/N_2O_2) could leach out of the polymer coating and a significant amount of NO was released from the decomposition of the donor outside of the polymer coating matrix [65]. This poses potential risks as the decomposition product, free dimethylhexane diamine, could react with reactive nitrogen oxide species and form a *N*-nitrosamine,

which is carcinogenic. In addition, the leaching of NO donor into the aqueous phase would reduce the effectiveness of locally released NO to inhibit platelet adhesion/activation at the polymer/blood interface (i.e., less NO being locally released at sensor/blood interface).

To address the leaching problem, Zhang et al. developed the DACA-SR/N_2O_2 material where the diazeniumdiolate groups are anchored on a diamine silane crosslinker and thus the leaching of the parent diamine from the polymer matrix is eliminated [66]. Frost et al. applied this covalently attached diazeniumdiolated DACA-SR/N_2O_2 coating (~ 100 μm thickness) on the surface of Clark-style oxygen-sensing catheters and evaluated the performance of these devices in porcine carotid and femoral arteries for 16 h [6]. The blood oxygen levels determined by the NO-releasing sensors (N = 9) were statistically identical to the standard *in vitro* blood gas measurements, while the control sensors (N = 9) implanted in the same animals showed statistically significant deviations (negative values) at 95% confidence interval in oxygen measurements after 10 h of implantation. Furthermore, the NO-releasing catheters were found to be relatively thrombus-free after explantation, while the control catheters without NO-release exhibited largely varied degrees of biological response, ranging from very few adhered platelets to a complete coverage of the surface by blood clots. Such variation in biological response is typically observed with implanted sensors, and it is precisely this variability that makes measurements with conventional sensors so unreliable.

As mentioned above, another approach to the creation of NO release polymeric coatings is to use a more lipophilic parent diamine compound with longer alkyl side-chains so that extraction into the aqueous phase is minimized [55]. Replacing the

methyl side groups in DMHD with butyl groups enhances the partition coefficient of the diamine into the organic polymer phase by 10^4. In another study, the resulting diazeniumdiolated dibutylhexyldiamine (DBHD/N_2O_2) was dispersed into SR, together with potassium tetrakis(4-chlorophenyl) borate (KTpClPB) which buffers the pH in the organic phase to maintain a more constant longer term NO release. Biocompatibility evaluations of NO-releasing catheters with outer SR coatings containing DBHD/N_2O_2 in the porcine artery model yielded similar results to other NO-releasing sensor studies, with more accurate blood oxygen measurements and less platelet adhesion and activation observed [62].

NO-releasing polymers containing DBHD/N_2O_2 have also shown improved biocompatibility when used as outer coatings for preparation of needle-type subcutaneous glucose sensors. Gifford et al. prepared glucose sensors with a thin PU/PDMS coating (~ 10 μm thick) doped with the DBHD/N_2O_2 NO donor and implanted them in rats together with control sensors [8]. Histological evaluation of neutrophil infiltration revealed that inflammatory response was greatly reduced during the first 24 h at implant sites where the NO release sensors were placed vs. control sites in the same animals. However, the NO release from the polymer coating could only last ca. 16 h, owing to the very thin coating necessary to prevent a dramatic decrease in the flux of glucose to the underlying glucose oxidase enzyme layer of the sensor. Therefore, although the sensors remained functional *in vivo* for several days, the reduction of inflammatory response was not maintained for an extended implant period (3 d). Increasing the coating thickness is not an option as it would change the membrane permeability and adversely affect the sensitivity and response time of the glucose sensor. To circumvent the limitation of NO

donor reservoir in the NO-releasing coating, alternative NO-generating approaches have been pursued to immobilize catalysts onto the polymer surface that can decompose endogenous RSNOs, an NO carrier, to generate NO *in situ* at the polymer/blood interface.

1.4.2. NO-Generating Materials

As discussed above, polymer coatings containing NO donors on the surfaces of implantable sensors will eventually be depleted, and thus these sensors are likely to eventually lose the biocompatibility advantage offered by NO release. The concept of "NO generation" coatings is to utilize the endogenous RSNO species that exist in the physiological fluids as a continuously replenishing NO donor to generate enhanced NO levels at the blood/polymer interface. RSNOs are regarded as a reservoir and carrier of NO in the body [39, 67]. The most abundant endogenous RSNOs are *S*-nitrosoalbumin (AlbSNO) and GSNO. Transnitrosylation reactions occur *in vivo* so that the nitroso-group can be transferred from one thiol to another [40, 42]. The cleavage of the S-NO bond in RSNOs to release NO can occur by three well-established mechanisms [68]. First, copper ion mediated catalytic decomposition requires Cu^{2+} to first be reduced to Cu^{+}. Copper(I) reacts with RSNO to release NO by transferring an electron, and thus forms a thiolate anion and regenerates Cu^{2+}. Under physiological conditions, ascorbate and thiolate anions are sufficient reducing agents to convert Cu^{2+} to Cu^{+}. The second RSNO decomposition pathway is through the reaction with high concentrations (> 1 mM) of ascorbate to release NO and produce thiolate and dehydroascorbate [69]. The third decomposition mechanism of RSNOs is the homolytic cleavage of the S-NO bond by light at characteristic absorbance bands of 330-350 nm or 550-600 nm, yielding

NO and the disulfide of the parent thiols [70]. Further, Hou et al. reported that glutathione peroxidase (GPx) and other seleno compounds (e.g., selenocystamine) can also catalyze RSNO decomposition [71]. Recent research using organotellurium compounds indicate that they also possess similar catalytic activities towards RSNO decomposition [72].

The potential advantage of the NO-generation approach *in vivo* is the utilization of circulating RSNO as an unlimited supply of NO at the polymer/blood interface. Duan et al. explored the possibility of generating NO by transnitrosation from endogenous RSNOs to L-cysteine immobilized on polymer surfaces [73]. They covalently attached L-cysteine to PU and polyethylene terephthalate (PET) and these L-cysteine modified polymers reduce *in vitro* platelet adhesion by more than 50% when tested in plasma, but not with platelet suspension in phosphate buffer. The suggested mechanism was through the transnitrosation of NO^+ from endogenous RSNOs (e.g., AlbSNO) to the cysteine moiety on the polymer surface to yield immobilized CysNO. CysNO is relatively unstable and can thus decompose to release NO locally at the polymer interface.

Oh et al. developed a lipophilic Cu(II)-cyclen type complex to generate NO from RSNO and nitrite under physiological conditions [74, 75]. PVC and PU films doped with this Cu(II) complex generated NO in the presence of reducing agents (e.g., ascorbate, cysteine, glutathione). It was demonstrated such polymers can generated NO with an apparent surface flux as high as 8×10^{-10} mol cm^{-2} min^{-1} from physiological levels (1 μM) of GSNO. The same polymer was also shown to generate NO from nitrite under physiological conditions in the presence of ascorbate. A material that is capable of

locally and continuously generating NO from endogenous RSNOs and nitrite could be used to tackle the biocompatibility problems for not only implantable sensors, but even long-term implants, such as stents and vascular grafts.

Besides the Cu-cyclen complex, any other form of Cu that can provide Cu^{2+} or Cu^{+} cation could also serve as the catalyst to generate NO at the polymer/blood interface. Further, it was recently discovered that organoselenium compounds and selenium containing proteins (e.g., glutathione peroxidase) are also capable of generating NO from RSNOs [71]. In Chapter 3 of this thesis, metallic copper particles (micron- or nano-sized) are loaded into the polymer coatings on the Clark-style intravascular oxygen-sensing catheters as a proof-of-concept study on NO-generating coatings for implantable sensors with enhanced biocompatibility.

1.5. Determining Endogenous RSNO Levels

The successful biomedical application of the NO-generation approach depends largely on the knowledge and control over the endogenous levels of RSNOs in blood. Indeed, the question of actual blood RSNO levels is still the center of considerable debate [76] and the reported normal values in the literature range from 15 nM to 7 μM [39, 77] for a number of reasons. The labile nature of the RSNO compounds, which can be easily decomposed by light, heat or trace metal ions [68], the difference in sample handling and analytical procedure employed, and the ease with which RSNOs, NO and their metabolites (e.g., nitrite and iron-nitrosyl) can react with blood components to give either false positives or false negatives [78-80], all add to the complexity of the accurate

determination of RSNOs in blood. Most of the methodologies that detect RSNOs in blood require complicated sample treatment which may introduce artifacts in subsequent measurements [76]. Therefore, a method to quickly measure RSNO with minimal sample preparation is surely needed.

Recently, Cha et al. reported electrochemical RSNO sensors with Cu- or Se-based catalysts immobilized at the distal tip of an NO electrode [81, 82]. A schematic of the Se-based RSNO sensor and the Se-functionalized poly(ethylenimine) (Se-PEI) is shown in Figure 1.3. When used with a control NO sensor (without Se-PEI), such RSNO sensors enable the rapid detection of RSNOs in whole blood at the bedside. Moreover, the Se-based RSNO sensor possesses almost equal sensitivity towards all low molecular weight RSNO species tested, rendering it potentially suitable to assess the 'global' RSNO concentrations in whole blood. Even within the same species, a substantial variation in endogenous RSNO concentrations may exist between individual subjects, giving rise to the difference in biological response to the NO-generating medical devices. To overcome the limitation of basal RSNO levels, it might be necessary to provide a bolus of a naturally occurring RSNO at certain intervals, or better yet to continuously infuse RSNOs intravenously to maintain blood RSNO levels that are sufficient to generate desired levels of NO at the sensor/blood interface.

(a)

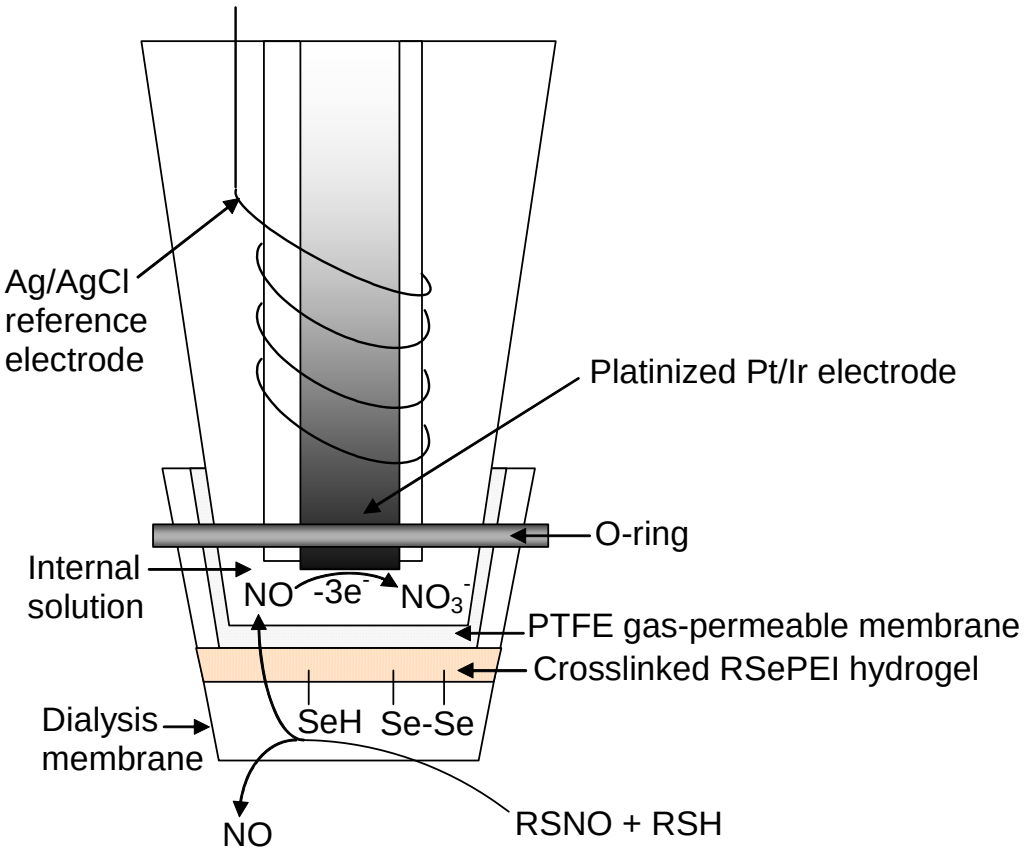

(b)

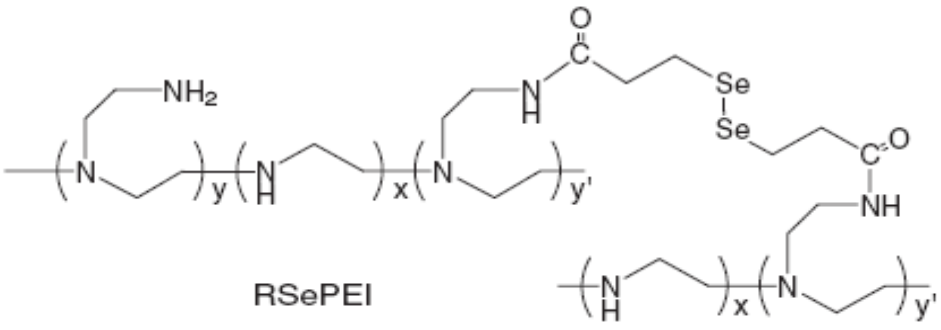

Figure 1.3. (a) Schematic of the RSe-PEI based RSNO sensor; (b) structure of the RSe-PEI catalyst.

1.6. Statement of Dissertation Research

The primary goal of this dissertation research is to develop evaluation techniques to determine the biocompatibility of the novel NO-releasing/generating polymeric materials that can ultimately be employed to prepare more biocompatible *in vivo* chemical sensors. Further, as the endogenous RSNO species play a pivotal role in the biocompatibility of new NO-generating materials, efforts are dedicated herein to examine the interaction between NO-generating materials and the blood RSNO levels by means of an electrochemical RSNO sensor based on organoselenium catalyst.

For *in vitro* biocompatibility evaluation of polymeric materials, platelet adhesion studies via scanning electron microscopy (SEM) or radioactive labeling of platelets, have traditionally been employed [60, 65, 83]. However, the SEM approach only examines a tiny fraction of the entire surface and therefore is unable to provide quantitative information about adhered platelets. The radio-labeled platelet method, on the other hand, suffers from the possible activation of platelet during the labeling step and thus might not indicate the true thrombogenicity of the material being tested. To assess the biocompatibility of NO-releasing polymers and determine the optimal NO flux for biomedical applications, a quantitative and reliable *in vitro* platelet adhesion assay is desirable. In Chapter 2, a new *in vitro* platelet adhesion assay for NO-releasing/generating polymers is described based on quantification of the lactate dehydrogenase (LDH) content of adhered platelets. Reduced platelet adhesion was found to correlate with the increase in NO fluxes emanated from NO-releasing polymers.

Platelet adhesion was effectively reduced from 14.0±2.1 $\times 10^5$ cells cm^{-2} on the control polymer to 2.96±0.18 $\times 10^5$ cells cm^{-2} on polymers with an NO flux of 7.05±0.25 $\times 10^{-10}$ mol cm^{-2} min^{-1}.

The first *in vivo* biocompatibility evaluation of NO-generating materials will be presented in Chapter 3. In this study, metallic Cu^0 particles (3 μm or 80 nm) are incorporated into the polymeric coatings on the surface of a Clark-style intravascular oxygen-sensing catheter to serve as the NO-generating catalyst. Such NO-generating sensors were implanted into porcine arteries together with control sensors without the NO-generating capability for up to 20 h. Overall, the NO-generating sensors (N=12 for the 3-μm group and N=6 for the 80-nm group) showed improved biocompatibility along with more accurate PO_2 measurements when compared to control sensors without Cu^0 particles.

The successful function of the NO-generating materials requires the knowledge and control of endogenous RSNO concentrations. The study of baseline blood RSNO levels and their changes in the presence of NO-generating materials, by means of the electrochemical RSNO sensor, will be described in Chapter 4. This includes the fundamental aspects of the sensing mechanism, as well as the applications of RSNO measurements in a number of rabbits, pigs and human subjects. A key discovery in this study is that proper sampling of blood is critical to avoid photolytic decomposition of endogenous RSNO species.

Chapter 5 provides a summary of the results obtained and offers suggestions for future research directions based on the findings of this dissertation research.

Finally, it should be noted that this dissertation is prepared on the basis of multiple

manuscripts. All the chapters, except Chapter 5, are adapted from either published articles or manuscripts to be submitted for publication. The majority of the content of this Chapter 1 is in press for the 'Special Issue on Remote Chemo/Bio-Sensing' in *Talanta*. The LDH assay on NO-releasing polymers described in Chapter 2 has been published as a full paper in *the Journal of Biomedical Materials Research, A* (2007) [84]. Chapter 3 is converted from a full paper published in the 25th Anniversary Issue of *Sensors and Actuators B, Chemical* (2007) [85]. The results of endogenous RSNO measurements in rabbit blood from Chapter 4 will be prepared into a manuscript intended for publication in *Analytical Chemistry*. The photo-instability of RSNOs discussed in Chapter 4 will be addressed separately in a letter to the editor of *Clinical Chemistry*.

1.7. References

[1] M. E. Meyerhoff, *Trends Anal. Chem.*, 12 (1993) 257-266

[2] C. K. Mahutte, *Clin. Biochem.*, 31 (1998) 119-130

[3] J. P. Wallis, *Transfus. Med.*, 15 (2005) 1-11

[4] T. J. Guzik, R. Korbut and T. Adamek-Guzik, *J. Physiol. Pharmacol.*, 54 (2003) 469-487

[5] J. P. Cooke, *Atheroscler. Suppl.*, 4 (2003) 53-60

[6] M. C. Frost, S. M. Rudich, H. P. Zhang, M. A. Maraschio and M. E. Meyerhoff, *Anal. Chem.*, 74 (2002) 5942-5947

[7] M. H. Schoenfisch, K. A. Mowery, M. V. Rader, N. Baliga, J. A. Wahr and M. E. Meyerhoff, *Anal. Chem.*, 72 (2000) 1119-1126

[8] R. Gifford, M. M. Batchelor, Y. Lee, G. Gokulrangan, M. E. Meyerhoff and G. S. Wilson, *J. Biomed. Mater. Res.*, 75A (2005) 755-766

[9] D. Giustarini, A. Milzani, I. Dalle-Donne and R. Rossi, *J. Chromatogr. B*, 851 (2007) 124-139

[10] E. Fogt, *Clin. Chem.*, 36 (1990) 1573-1580

[11] M. C. Frost and M. E. Meyerhoff, *Curr. Opin. Chem. Biol.*, 6 (2002) 633-641

[12] N. Wisniewski, F. Moussy and W. M. Reichert, *Fresenius J. Anal. Chem.*, 366 (2000) 611-621

[13] M. Frost and M. E. Meyerhoff, *Anal. Chem.*, 78 (2006) 7370-7377

[14] D. Williams, *Med. Device Technol.*, 14 (2003) 10(4)

[15] J. D. Andrade and V. Hlady, *Adv. Polym. Sci.*, 79 (1986) 1-63

[16] R. W. Colman, *Cardiovasc. Pathol.*, 2 (1993) 23-31

[17] N. Wisniewski and M. Reichert, *Colloids Surf. B Biointerfaces*, 18 (2000) 197-219

[18] G. S. Wilson and R. Gifford, *Biosens. Bioelectron.*, 20 (2005) 2388-2403

[19] J. M. Anderson, *Cardiovasc. Pathol.*, 2 (1993) 33-41

[20] R. Ballerstadt, C. Evans, A. Gowda and R. McNichols, *Diabetes Technol. Ther.*, 8 (2006) 296-311

[21] P. W. Barone, R. S. Parker and M. S. Strano, *Anal. Chem.*, 77 (2005) 7556-7562

[22] M. Gerritsen, J. A. Jansen and J. A. Lutterman, *Neth. J. Med.*, 54 (1999) 167-179

[23] U. Klueh, D. I. Dorsky and D. L. Kreutzer, *Biomaterials*, 26 (2005) 1155-1163

[24] R. A. Latour, *J. Biomed. Mater. Res.*, 78A (2006) 843-854

[25] Y. Marois, N. Chakfe, R. Guidoin, R. C. Duhamel, R. Roy, M. Marois, M. W. King and Y. Douville, *Biomaterials*, 17 (1996) 3-14

[26] V. L. Gott, J. D. Whiffen and R. C. Dutton, *Science*, 142 (1963) 1297-1298

[27] A. Kishida, Y. Akatsuka, M. Yanagi, T. Aikou, I. Maruyama and M. Akashi, *ASAIO Journal*, 41 (1995) M369-M374

[28] C. D. Ebert, E. S. Lee and S. W. Kim, *J. Biomed. Mater. Res*, 16 (1982) 629-638

[29] R. Barbucci, A. Magnani, R. Rappuoli, S. Lamponi and M. Consumi, *J. Inorg. Biochem.*, 79 (2000) 119-125

[30] P. L. Feldman, O. W. Griffith and D. J. Stuehr, *Chem. Eng. News*, 71 (1993) 26-38

[31] L. J. Ignarro, G. M. Buga, K. S. Wood, R. E. Byrns and G. Chaudhuri, *Proc. Natl. Acad. Sci. USA*, 84 (1987) 9265-9269

[32] J. G. Diodati, A. A. Quyyumi, N. Hussain and L. K. Keefer, *Thromb. Haemost.*, 70 (1993) 654-658

[33] C. M. Maragos, D. Morley, D. A. Wink, T. M. Dunams, J. E. Saavedra, A. Hoffman, A. A. Bove, L. Isaac, J. A. Hrabie and L. K. Keefer, *J. Med. Chem.*, 34 (1991) 3242-3247

[34] K. Wong and X. B. Li, *Transfus. Apheresis Sci.*, 30 (2004) 29-39

[35] J. MacMicking, Q.-w. Xie and C. Nathan, *Annu. Rev. Immunol.*, 15 (1997) 323-350

[36] B. J. Nablo, H. L. Prichard, R. D. Butler, B. Klitzman and M. H. Schoenfisch, *Biomaterials*, 26 (2005) 6984-6990

[37] W. K. C. Alderton, Chris E.; Knowles, Richard G., *Biochem. J.*, 357 (2001) 593-615

[38] L. J. Ignarro, *J. Card. Surg.*, 17 (2002) 301-306

[39] J. S. Stamler, O. Jaraki, J. Osborne, D. I. Simon, J. Keaney, J. Vita, D. Singel, C. R. Valeri and J. Loscalzo, *Proc. Natl. Acad. Sci. USA*, 89 (1992) 7674-7677

40] N. Hogg, *Free Radic. Biol. Med.*, 28 (2000) 1478-1486

[41] J. Stamler, D. Singel and J. Loscalzo, *Science*, 258 (1992) 1898-1902

[42] D. Jourd'heuil, K. Hallen, M. Feelisch and M. B. Grisham, *Free Radic. Biol. Med.*, 28 (2000) 409-417

[43] A. Schober and C. Weber, *Antioxid. Redox Signal.*, 7 (2005) 1249-1257

[44] C. A. Gruetter, B. K. Barry, D. B. McNamara, D. Y. Gruetter, P. J. Kadowitz and L. J. Ignarro, *J. Cyclic Nucleotide Res.*, 5 (1979) 211-224

[45] P. Massini, R. Kaserglanzmann and E. F. Luscher, *Thromb. Haemost.*, 40 (1978) 212-218

[46] A. Ramamurthi and R. S. Lewis, *Ann. Biomed. Eng.*, 26 (1998) 1036-1043

[47] M. W. Vaughn, L. Kuo and J. C. Liao, *Am. J. Physiol. (Heart Circ. Physiol.)*, 43 (1998) H2163-H2176

[48] P. G. Wang, M. Xian, X. P. Tang, X. J. Wu, Z. Wen, T. W. Cai and A. J. Janczuk, *Chem. Rev.*, 102 (2002) 1091-1134

[49] S. M. Shishido and M. G. de Oliveira, *Photochem. Photobiol.*, 71 (2000) 273-280

[50] A. B. Seabra, L. L. Da Rocha, M. N. Eberlin and M. G. De Oliveira, *J. Pharm. Sci.*, 94 (2005) 994-1003

[51] S. M. Shishido, A. B. Seabra, W. Loh and M. G. de Oliveira, *Biomaterials*, 24 (2003) 3543-3553

[52] K. S. Bohl and J. L. West, *Biomaterials*, 21 (2000) 2273-2278

[53] R. S. Drago and Karstett.Br, *J. Am. Chem. Soc.*, 83 (1961) 1819-&

[54] K. M. Davies, D. A. Wink, J. E. Saavedra and L. K. Keefer, *J. Am. Chem. Soc.*, 123 (2001) 5473-5481

[55] M. M. Batchelor, S. L. Reoma, P. S. Fleser, V. K. Nuthakki, R. E. Callahan, C. J. Shanley, J. K. Politis, J. Elmore, S. I. Merz and M. E. Meyerhoff, *J. Med. Chem.*, 46 (2003) 5153-5161

[56] D. J. Smith, D. Chakravarthy, S. Pulfer, M. L. Simmons, J. A. Hrabie, M. L. Citro, J. E. Saavedra, K. M. Davies, T. C. Hutsell, D. L. Mooradian, S. R. Hanson and L. K. Keefer, *J. Med. Chem.*, 39 (1996) 1148-1156

[57] M. C. Frost, M. M. Reynolds and M. E. Meyerhoff, *Biomaterials*, 26 (2005) 1685-1693

[58] H. P. Zhang, G. M. Annich, J. Miskulin, K. Stankiewicz, K. Osterholzer, S. I. Merz, R. H. Bartlett and M. E. Meyerhoff, *J. Am. Chem. Soc.*, 125 (2003) 5015-5024

[59] J. A. Hrabie and L. K. Keefer, *Chem. Rev.*, 102 (2002) 1135-1154

[60] C. Espadas-Torre, V. Oklejas, K. Mowery and M. E. Meyerhoff, *J. Am. Chem. Soc.*, 119 (1997) 2321-2322

[61] K. A. Mowery, M. H. Schoenfisch, N. Baliga, J. A. Wahr and M. E. Meyerhoff, *Electroanalysis*, 11 (1999) 681-686

[62] M. C. Frost, M. M. Batchelor, Y. M. Lee, H. P. Zhang, Y. J. Kang, B. K. Oh, G. S. Wilson, R. Gifford, S. M. Rudich and M. E. Meyerhoff, *Microchem. J.*, 74 (2003) 277-288

[63] M. H. Schoenfisch, H. P. Zhang, M. C. Frost and M. E. Meyerhoff, *Anal. Chem.*, 74 (2002) 5937-5941

[64] K. P. Dobmeier, G. W. Charville and M. H. Schoenfisch, *Anal. Chem.*, 78 (2006) 7461-7466

[65] K. A. Mowery, M. H. Schoenfisch, J. E. Saavedra, L. K. Keefer and M. E. Meyerhoff, *Biomaterials*, 21 (2000) 9-21

[66] H. P. Zhang, G. M. Annich, J. Miskulin, K. Osterholzer, S. I. Merz, R. H. Bartlett and M. E.

Meyerhoff, *Biomaterials*, 23 (2002) 1485-1494

[67] T. Rassaf, P. Kleinbongard, M. Preik, A. Dejam, P. Gharini, T. Lauer, J. Erckenbrecht, A. Duschin, R. Schulz, G. Heusch, M. Feelisch and M. Kelm, *Circ. Res.*, 91 (2002) 470-477

[68] D. L. H. Williams, *Acc. Chem. Res.*, 32 (1999) 869-876

[69] A. J. Holmes and D. L. H. Williams, *J. Chem. Soc. Perkin Trans. 2*, (2000) 1639-1644

[70] R. J. Singh, N. Hogg, J. Joseph and B. Kalyanaraman, *J. Biol. Chem.*, 271 (1996) 18596-18603

[71] Y. C. Hou, Z. M. Guo, J. Li and P. G. Wang, *Biochem. Biophys. Res. Commun.*, 228 (1996) 88-93

[72] S. Hwang and M. E. Meyerhoff, *J. Mater. Chem.*, 17 (2007) 1462-1465

[73] X. B. Duan and R. S. Lewis, *Biomaterials*, 23 (2002) 1197-1203

[74] B. K. Oh and M. E. Meyerhoff, *J. Am. Chem. Soc.*, 125 (2003) 9552-9553

[75] B. K. Oh and M. E. Meyerhoff, *Biomaterials*, 25 (2004) 283-293

[76] D. Tsikas and J. C. Frolich, *Circ. Res.*, 90 (2002) E39-E39

[77] D. Giustarini, A. Milzani, R. Colombo, I. Dalle-Donne and R. Rossi, *Clin. Chim. Acta*, 330 (2003) 85-98

[78] S. C. Rogers, A. Khalatbari, P. W. Gapper, M. P. Frenneaux and P. E. James, *J. Biol. Chem.*, 280 (2005) 26720-26728

[79] S. Basu, J. D. Hill, H. Shields, J. Huang, S. Bruce King and D. B. Kim-Shapiro, *Nitric Oxide*, 15 (2006) 1-4

[80] A. Hausladen, R. Rafikov, M. Angelo, D. J. Singel, E. Nudler and J. S. Stamler, *Proc. Natl. Acad. Sci. USA*, 104 (2007) 2157-2162

[81] W. Cha and M. E. Meyerhoff, *Langmuir*, 22 (2006) 10830-10836

[82] W. Cha, Y. Lee, B. K. Oh and M. E. Meyerhoff, *Anal. Chem.*, 77 (2005) 3516-3524

[83] M. Rodrigues and H. Sinzinger, *Thromb. Res.*, 76 (1994) 399-432

[84] Y. Wu, Z. R. Zhou and M. E. Meyerhoff, *J. Biomed. Mater. Res.*, 81A (2007) 956-963

[85] Y. Wu, A. P. Rojas, G. W. Griffith, A. M. Skrzypchak, R. H. Bartlett and M. E. Meyerhoff, *Sens. Actuators B*, 121 (2007) 36-46

CHAPTER 2

IN VITRO PLATELET ADHESION ASSAY FOR NITRIC OXIDE-RELEASING/GENERATING POLYMERS VIA LACTATE DEHYDROGENASE (LDH) QUANTIFICATION

2.1. Introduction

Nitric oxide (NO) is now widely recognized as a potent inhibitor of platelet adhesion and activation [1, 2], as well as a naturally occurring vasodilator [3]. In fact, the extraordinarily thromboresistant nature of the inner walls of blood vessels is, in part, due to the continuous production of NO by the endothelial cells that line such vessels [4, 5]. The NO flux from the endothelium is estimated to be in the range of 0.5 - 4.0 $\times 10^{-10}$ mol cm^{-2} min^{-1} [4]. Previous studies based on the discrete infusions of NO donors into blood suggested that higher NO levels produced from such donors exert greater antiplatelet activities [6-8]. However, these experiments failed to simulate the function of a healthy endothelium, which produces a low but continuous flux of NO from its surface. Another report by Ramamurthi and Lewis using flowing platelets in a membrane-based diffusion device demonstrated that platelet adhesion to a collagen-coated membrane (using radiolabelled platelets) was inhibited by very low fluxes of NO but leveled off as higher NO concentrations were used [9].

Research in this lab [10-20] and elsewhere [21, 22] has been aimed at preparing more biocompatible polymeric coatings that continuously produce NO at physiological levels to mimic the function of the healthy endothelium, thus creating non-thrombogenic surfaces. The continuous production of NO at polymer/blood interfaces can be achieved by two methods—either by doping the polymer with NO donors that can spontaneous release NO (i.e., NO-releasing polymers), or by impregnating the polymer with catalysts that react with endogenous NO precursors (e.g., *S*-nitrosothiols) to generate NO *in situ* at the polymer/blood interface (i.e., NO-generating polymers). Indeed, a growing number of reports have already demonstrated the improved blood compatibility of NO-releasing/generating polymeric materials using *in vivo* animal model studies [10-15, 23]. It has also been reported that discrete additions of NO or its donor species (e.g., diazeniumdiolates, nitrosothiols, etc.) can inhibit platelet adhesion and activation *in vitro* [6-8, 24-26]. However, there is a lack of a simple and reliable *in vitro* method to assay the platelet adhesion on polymers that continuously release or generate NO, and to assess how varying levels of NO release effect platelet adhesion. Such a method would be attractive to carry out preliminary biocompatibility studies of any new NO-releasing/generating polymers, such as determining the required NO flux and donor/catalyst amounts, before undertaking more expensive *in vivo* testing.

The two most commonly used *in vitro* platelet adhesion assays are scanning electron microscopy (SEM) [27] and radioisotope-labeled platelet counting [28]. However, both methods have their own drawbacks that render them unsuitable for quantitative assay. SEM only studies a very small fraction of the total surface that had been in contact with platelets, of which the ‘representativeness’ of the selected viewing

areas is always questionable. Radio-labeling, on the other hand, suffers from the potential for pre-activation of platelet as a result of the labeling step.

In recent years, the assay of lactate dehydrogenase (LDH) present in platelets has been reported to provide a useful approach to study *in vitro* platelet adhesion on chemically and/or physically modified surfaces [29-33]. LDH is normally stored within intact platelets and other blood cells. Elevated serum LDH levels are usually associated with cytolytic events [34]. When platelets adhered to polymer surfaces are lysed using a surfactant solution, the amount of LDH released into the bulk solution is proportional to the number of cells adhered. The activity of LDH can be measured by a simple colorimetric assay and used to quantify platelet adhesion. In this chapter, the use of an LDH assay is reported to study the efficacy of varying levels of NO, a bioactive species, released from poly(vinyl chloride) (PVC) films doped with a lipophilic diazeniumdiolate type NO donor, in reducing platelet adhesion onto the surface of such polymeric materials. It will be shown that increasing fluxes of NO release decrease the observed platelet adhesion. Such an LDH assay is also utilized to study platelet adhesion on NO-generating polymers with a lipophilic Cu(II)-cyclen type catalyst, where no statistically significant differences were found between the NO-generating and control polymers. Possible reasons for this observation will be discussed in Section **2.3.5.**

2.2. Materials and Methods

2.2.1. Preparation of NO-Releasing Polymer Coatings

Poly(vinyl chloride) (average M_W = 106,000, Aldrich, Milwaukee, WI) was mixed with sebacic acid di(2-ethylhexyl) ester (DOS, Sigma, St. Louis, MO) in dry tetrahydrofuran (THF, Fisher Scientific, Pittsburgh, PA) to make a solution containing 2% (w/v) PVC and 2% (w/v) DOS. For control films, *N*,*N*'-dibutyl-1,6-hexanediamine (DBHD, Aldrich) was mixed with potassium tetrakis(4-chlorophenyl)-borate (KTpClPB, Fluka, Buchs, Switzerland) in a 1 : 1 molar ratio and dispersed in the polymer solution to yield 4 wt% of DBHD in the final cured polymer film. The NO adduct, DBHD/N_2O_2 (diazeniumdiolated DBHD) was synthesized as previously reported [10]. DBHD/N_2O_2 and equal molar KTpClPB were dispersed into the polymer casting solution in a similar manner as the control film to yield 0.50, 1.0, 2.0 and 4.0 wt% of final DBHD/N_2O_2 loading. The coating cocktails were sonicated for 15 min and then 0.25 mL aliquots were placed in a well of 96-well round-bottom polypropylene microtiterplates (Evergreen Scientific, Los Angles, CA). The polymer film was allowed to cure under ambient condition over night before a 3 μm layer of plain PVC/DOS (1:1) was applied as a topcoat. The resulting polymer films were allowed to cure for another 24 h before use.

2.2.2. NO-Release Measurement

Nitric oxide released from the different polymer-coated wells was measured via a chemiluminescence NO Analyzer™ (NOA), Model 280 (Sievers Instruments, Boulder, CO), to assess the NO-release profile and to determine the optimal time window for

platelet adhesion studies. The entire polymer-coated well was immersed in phosphate buffered saline (PBS, 137 mM NaCl, 2.7 mM KCl, 10 mM sodium phosphate, pH 7.4) at 37 ºC and the solution was bubbled with N_2. NO released from the polymer coating within the well was purged from the buffer, carried by the N_2 gas into the chemiluminescence reaction chamber of the instrument, and monitored in real-time.

2.2.3. Platelet Adhesion Studies

Arterial blood from New Zealand white rabbits, weighing 2.5 - 3 kg, was drawn into 9:1 volume of blood : anticoagulant citrate/phosphate/dextrose solution (Abbott Labs, North Chicago, IL) containing 15.6 mM citric acid, 89.5 mM tribasic sodium citrate, 16.1 mM NaH_2PO_4 and 128 mM dextrose. NIH guidelines for the care and use of laboratory animals (NIH Publication #85-23 Rev. 1985) were observed throughout. The citrated whole blood was centrifuged at 110 ×g for 15 min at 22ºC. Platelet-rich plasma (PRP) was collected from the supernatant. To re-establish platelet activity, $CaCl_2$ was added to the PRP to raise [Ca^{2+}] by 2 mM. Before PRP incubation, the polymer-coated microtiter plate wells were pre-hydrated by incubating with 200 μL PBS for 3 h at 37 ºC to achieve the optimal NO fluxes. The PBS solution was removed after this pre-incubation period. Then, 100 μL of re-calcified PRP was added to each polymer-coated well and incubated for 1 h at 37 ºC under static conditions. The PRP was then decanted and the wells were washed once with 200 μL PBS. The entire duration from blood collection to the conclusion of the platelet adhesion step was less than 3 h.

2.2.4. LDH Assay

Adhered platelets were lysed using a lysing buffer which was PBS plus 1% (w/v) Triton X-100 (Sigma) and 0.75% (w/v) bovine serum albumin (Sigma). One hundred and fifty μL of lysing buffer was incubated in each well for 1 h at 37 ºC with occasional agitation to completely disrupt the platelet membranes. Then, 100 μL of each lysate solution was pipetted into wells of a second 96-well polystyrene microtiter plate (Fisher) that contained 100 μL of reagent from an LDH assay kit (Roche Applied Sciences, Indianapolis, IN). Absorbance of each well at 490 nm was monitored for 1 h by a Labsystems Multiskan RC microplate reader (Fisher). The slopes derived from the initial linear portion of the absorbance vs. time curves were used for LDH quantification.

Blank experiments were performed in a similar manner. Briefly, free LDH from rabbit muscle (Roche Molecular Biochemicals, Mannheim, Germany) was dissolved in the same lysing buffer at 3 mU/mL. Then, 150 μL of this free LDH solution was placed in polymer-coated wells that had been previously hydrated with PBS buffer for 3 h to establish relatively stable NO release fluxes. The wells were further incubated with the LDH solution for 1 h at 37 ºC. In this way, the free LDH would have the same duration of exposure to the same NO flux as the LDH originating from adhered platelets. The activity of the free LDH was assayed in an identical manner as the LDH in the lysate solutions.

2.2.5. Platelet Counting and LDH Calibration

Platelet rich plasma, obtained as described above, was further centrifuged at 1500 ×g for 15 min to produce platelet-poor plasma (PPP) and a platelet pellet. The supernatant PPP was carefully removed and the pellet of platelets was gently resuspended

in Tyrode's buffer (137 mM NaCl, 95 mM $NaHCO_3$, 1.8 mM $CaCl_2$, 1.0 mM $MgCl_2$, 2.7 mM KCl, 0.4 mM NaH_2PO_4 and 5 mM D-glucose). The platelet number in this suspension was counted by a Z1 Coulter particle counter (Beckman-Coulter, Miami, FL). Varying volumes of the platelet suspension derived from the pellet were also placed in the lysing buffer and incubated at 37 ºC for 1 h to completely release the LDH content of the platelets. Then, 100 μL of each sample was mixed with equal volume of the LDH assay kit reagent in polystyrene microplate wells and assayed for LDH activity. The slopes obtained were used to construct the calibration curve of LDH activity versus platelet number, based on the Coulter counter measurement of the original stock platelet suspension in cells/ml.

2.2.6. SEM Analysis

Scanning electron microscopy (SEM) images for surfaces of the various polymeric films were obtained in addition to the LDH assays. After PRP incubation, adhered platelets in some wells were fixed with 4% glutaraldehyde (Sigma) for 1 h and then dehydrated in a series of ethanol solutions and dried overnight [13]. The bottom hemisphere was cut, sputter-coated with gold and examined by a Hitachi S-3200N scanning electron microscope.

2.2.7. Preparation, Characterization and Platelet Adhesion Studies of NO-Generating Polymers

A lipophilic Cu(II)-cyclen analog, Cu(II)-dibenzo-[e,k]-2,3,8,9-tetraphenyl-1,4,7,10-tetraaza-cyclododeca-1,3,7,9-tetraene (Cu-DTTCT), was prepared by a

previously reported method [35]. Cu-DTTCT was dissolved in dry THF and mixed with THF solutions of PVC, 2-nitrophenyl octyl ether (NPOE, Fluka) and/or DOS to yield polymer solutions of 2% (w/v) PVC and 2% (w/v) plasticizer (i.e., NPOE or DOS) containing various amounts of Cu-DTTCT (2 or 5 wt% in the final cured polymer). Two hundred and fifty μL of the polymer solution was loaded into each well of a 96-well polypropylene microtiter plate and allowed to cure over night before vacuum drying for 24 h. The control polymer film was prepared by substituting Cu-DTTCT with unmetallated DTTCT ligand and cured in the same way as described above.

To determine the NO-generation, the polymers were dip-coated onto glass-slides, dried in the same manner and then placed in the NOA cell containing 2 mL PBS, 5 μM S-nitrosoglutathione (GSNO, prepared fresh via a reported method [36]), 30 μM reduced glutathione (GSH, Sigma) and 10 μM EDTA at 37 ºC.

For the platelet adhesion study, rabbit blood was drawn into a syringe with 5 U/cc sodium heparin (Baxter, Deerfield, IL) and centrifuged as in Section **2.2.3.** to obtain PRP. The platelet number was counted by the method described in Section **2.2.5.** One hundred μL of PRP was incubated at 37 ºC for 30 min in either NO-generating or control wells. Five μM GSNO was supplemented to one half of the NO-generating and control wells. The PRP was later removed and the wells were washed once with 200 μL PBS. The assay for LDH content followed the same procedure outlined in Section **2.2.4.**

2.3. Results and Discussion

2.3.1. NO-Releasing Polymer Coatings

By using a microtiter plate with rounded well bottoms, a polymer coating of relatively consistent thickness can be achieved. The coating method described in the Experimental Section yields a 1.74 cm^2 polymer film with ca. 60 μm thickness as determined by an optical microscope. Addition of KTpClPB to the underlying layer of the plasticized PVC film helps to achieve a more stable NO flux by maintaining charge neutrality and a constant pH within the polymer phase as the DBHD/N_2O_2 species releases NO and creates excess amine sites in the form of DBHD [10]. The NO release from DBHD/N_2O_2 decomposition can occur via two mechanisms, proton-driven [37] or thermal dissociation [10]. In this experiment, temperature was maintained at 37 ºC, except for the final assay of LDH on the microplate reader. Further, the pH of all solutions, including the anticoagulated PRP, was kept at pH 7.4 for the precise manipulation of NO fluxes.

All of the DBHD/N_2O_2 doped polymer films exhibited continuous NO release for over 24 h. However, maximum NO fluxes were typically observed between 2 - 5 h after wetting and the overall magnitude of NO fluxes for the films was proportional to the amount of DBHD/N_2O_2 doped within the underlying polymer layer. The typical NO release profiles for the coatings over the first 8 h are shown in Figure 2.1(A) for films doped with 0 - 4 wt% DBHD/N_2O_2 (and equal moles of KTpClPB). It is obvious that the NO flux decays significantly for the film with the highest NO donor loading (4 wt%), while the others remain relatively stable. Thus, to ensure that all platelet adhesion studies

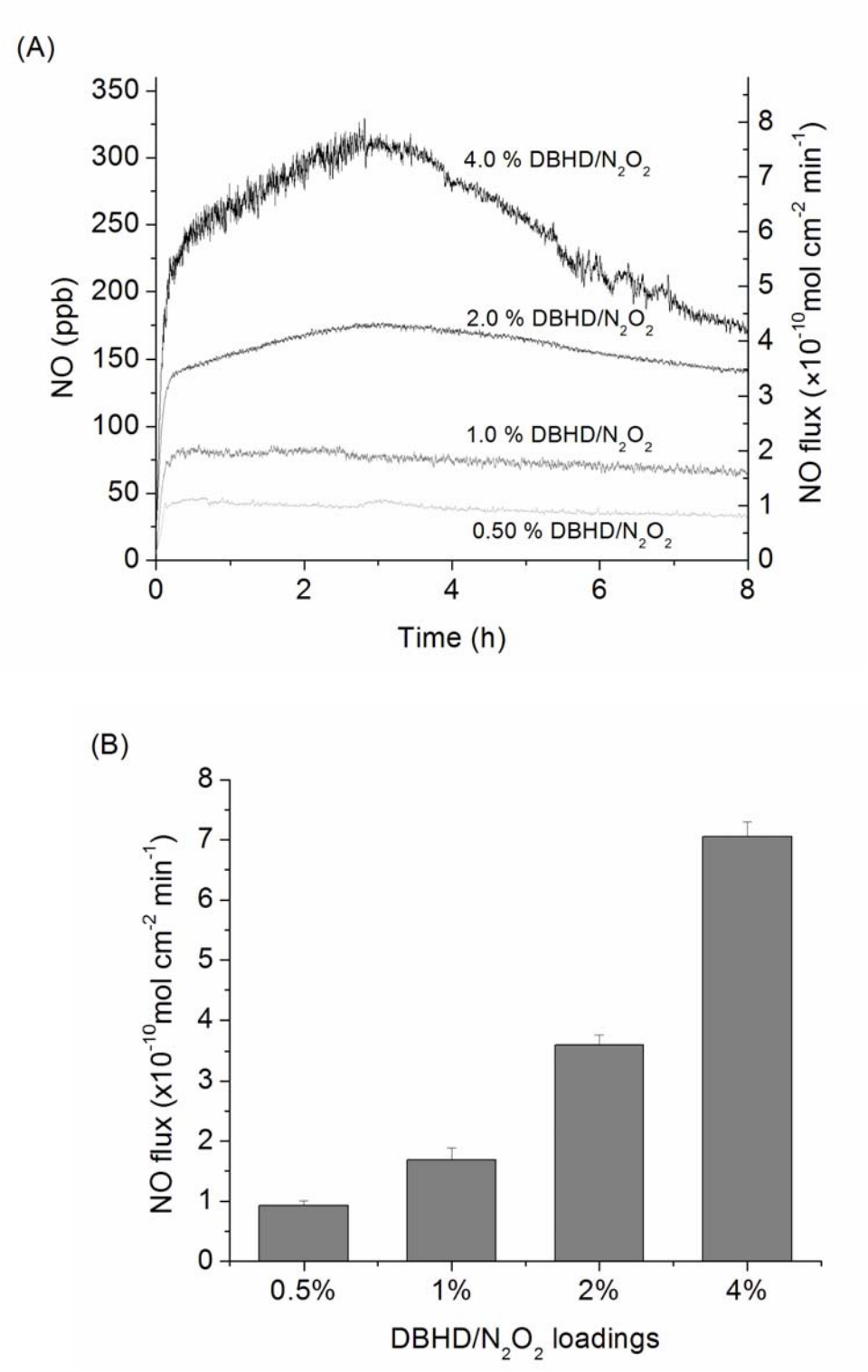

Figure 2.1. (A) NO flux profiles for polymer-coated wells doped with 0.50, 1.0, 2.0 and 4.0 wt% DBHD/N_2O_2 and equimolar KTpClPB. (B)Average NO fluxes and S.D. during the 3-4 h time window for each DBHD/N_2O_2 loading. N = 4 for each loading.

are conducted during a period of relatively constant NO flux, the time window between 3 - 4 h was selected for the platelet studies for all polymer film compositions examined. Figure 2.1(B) shows the statistics for the average flux levels at each DBHD/N_2O_2 concentration (N = 4 films). Average fluxes during this period for the four different loadings were 0.93(± 0.07), 1.69(± 0.19), 3.59(± 0.17), and 7.05(± 0.25) $\times 10^{-10}$ mol cm^{-2} min^{-1}, respectively. Higher DBHD/N_2O_2 loadings (e.g., 8 wt%) were also tested. They yielded fluxes of over 10×10^{-10} mol cm^{-2} min^{-1}. However, the polymer surfaces become much rougher in this case, as determined by SEM. This is likely due to the poor solubility of DBHD/N_2O_2 in the polymer matrix and therefore the surface roughness becomes more pronounced as the DBHD/N_2O_2 concentration goes above 4 wt%.

2.3.2. Platelet Adhesion

Unlike radioactive labeling of platelet, the major advantage of the LDH assay is its simplicity, which minimizes possible activation of resting platelets. Hence it has the potential to be more reproducible. This attribute is critical for the evaluation of potentially more biocompatible materials. Platelet adhesion experiments were repeated using three different lots of blood (from different animals) and the results were found to be quite reproducible. During the initial incubation step, PRP was in contact with 0.834 cm^2 of polymer surface in each well. This surface area was thus used to calculate the average platelet density on the films after determining LDH activity. However, it should be noted that the platelet coverage was not even over the entire surface of the polymer films (as determined by SEM), likely owing to the hemispherical shape of the wells. No fixation was used after platelet adhesion since platelets fixed with the common fixative,

glutaraldehyde, exhibited no LDH activity in the subsequent assay. Therefore, the unfixed platelets were loosely adhered to the polymer surfaces. Rinsing the wells three times yielded near-baseline LDH activities across all polymers tested, probably because of the removal of adhered platelets. In the final protocol, the wells were washed only once after platelet incubation, which was found to be sufficient to distinguish the extent of platelet adhesion as a function of NO flux.

2.3.3. LDH Assay

Prior to testing the effect of NO with respect to platelet adhesion, it was necessary to establish that NO has no effect on LDH activity. As a free radical, NO is known to react with various enzymes, which could possibly change their function and efficacy in catalysis [38, 39]. Previous studies using the LDH assay to assess the biocompatibility of polymers involved evaluating only physically [31, 33] or chemically [30, 32] modified surfaces, not a material that releases a reactive species such as NO. Consequently, it was crucial to verify that any 'observed' reduction in LDH activity derived from experiments using PRP was indeed the results of less adhered platelets rather than any inhibition of LDH function in the presence of continuous NO production.

An appropriate blank experiment was performed to evaluate the influence of continuous NO release on LDH activity. The enzyme concentration was set at 3 mU/mL since this was the level typically seen for the control experiments (after cell lysis) with platelets. Table 2.1 lists the free LDH activity in the control and DBHD/N_2O_2 load wells, as well as the blank with only plain 1:1 PVC/DOS films and no other additives. Interestingly, the control wells have slightly lower apparent LDH activities. LDH

Composition	Blank	Control	0.5%	1%	2%	4%
% LDH	100.0	89.7	103.6	98.1	98.9	93.3
S.D.	0.2	3.3	2.4	2.7	2.0	0.9

Table 2.1. Free LDH activity after 1 h incubation in blank (plain PVC/DOS), control and various NO-releasing polymer-coated wells, as determined by colorimetric reaction rate. LDH activity was set to 100% in blank polymer wells and others were plotted as the relative percentage. N = 3 for each polymer composition.

activity also decreases with higher NO donor loading in the polymer films. Since LDH has an iso-electric pH value (pI) of 4.6, it will be negatively charged in the PBS buffer. Thus, electrostatic interaction with the positively-charged surface of the polymers is a possible explanation for the data shown in Table 2.1. The control polymer has the highest concentration (4 wt%) of free amine (DBHD) which will gradually become protonated to create a positively charged surface (as it diffuses into the top coat layer of plain PVC polymer). Once LDH is attracted to polymer surface, less free LDH will be measured in the bulk solution, hence giving a false-negative result.

In the case of the NO-releasing polymers, the amine will also be formed upon hydrolysis of the diazeniumdiolate [37]. However, at the time of assay, the diazeniumdiolate is not 100% hydrolyzed and therefore amine sites in NO-releasing polymers will be fewer compared to those in the control. Because of this difference in amine site density between the diazeniumdiolated and non-diazeniumdiolated DBHD, the false negatives cannot be simply corrected by simultaneously collecting the LDH activities from same wt% control and DBHD/N_2O_2 loaded polymer films. Even though a top coat was applied and bovine serum albumin was added to the lysing buffer to minimize nonspecific adsorption of LDH to the surface of the polymers, it cannot be completely eliminated. This false-negative result from the control polymers suggested that the actual LDH levels in control polymer coated wells could be ~ 10% higher than that measured from this LDH assay (see below).

Basal LDH present in plasma could also adsorb onto the polymers and contribute to a common baseline across all polymers tested. It has been reported that PRP contains significant LDH activity and that LDH activity can be detected on polymer surfaces

incubated with PPP [29]. This adsorbed LDH may later be desorbed during the cell lysing stage and contribute to total LDH activity in this assay. To prove this, PRP was replaced by PPP in the platelet adhesion step, followed by identical washing, lysis and assay procedures. The baseline LDH level in PPP was found to be equivalent to a platelet density of ca. 1.00 (±0.25) $\times 10^5$ cm^{-2} on all polymers. This baseline was not subtracted from the platelet adhesion results, since there could be more cytolysis in a given preparation of PPP (as it was prepared by centrifugation at a much higher RCF than PRP) that can give rise to a higher serum LDH level. However, the presence of this background LDH activity derived from the plasma suggests an even greater reduction, percentage-wise, of adhered platelets on NO-releasing polymers for the experiments described below.

As shown in Figure 2.2, progressively fewer platelets adhered on polymer surfaces as the NO flux increases. The control polymer has an apparent platelet density of 14.0 (±2.5) $\times 10^5$ cm^{-2}, while the 0.5%, 1%, 2% and 4% DBHD/N_2O_2 doped films reduced the platelet density to 7.06 (±1.0) $\times 10^5$ cm^{-2}, 4.82 (±0.79) $\times 10^5$ cm^{-2}, 4.16 (±0.68) $\times 10^5$ cm^{-2} and 2.96 (±0.21) $\times 10^5$ cm^{-2}, respectively (N = 12 for all experiments, using at least 3 different blood lots as the source for the PRP). In all cases, platelet adhesion on the NO-releasing polymers is statistically different from the control ($p < 0.0001$). The influence of LDH adsorption via the mechanisms discussed above is insignificant as compared to the great reduction of LDH activities on NO-releasing polymer surfaces.

Polymers with higher DBHD/N_2O_2 loadings (i.e., 8, 12 and 16 wt%) have also been tested in the above manner. Bearing in mind DBHD/N_2O_2's poor solubility in these polymer matrices, it is not surprising that more platelet adhesion occurs on these rougher

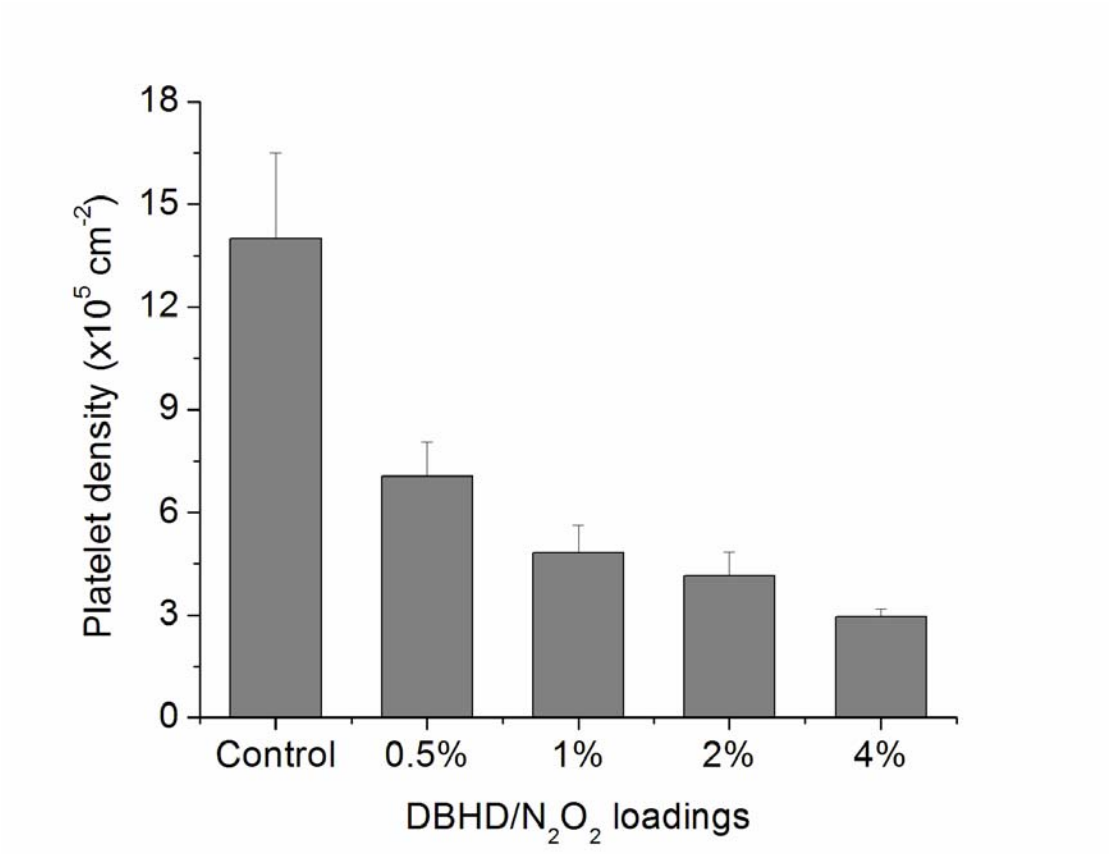

Figure 2.2. Platelet adhesion density on control and various DBHD/N_2O_2 loaded polymer coatings as determined by LDH assay. N = 12 for each polymer composition.

surfaces despite the fact that the NO fluxes are even higher. Indeed, another *in vivo* model with DBHD/N_2O_2 coated on the inner walls of rabbit extracorporeal circuits provided similar results – with an intermediate level of DBHD/N_2O_2 loading yielding the best biocompatibility [40]. However, such results do not necessarily suggest the inability of NO as an inhibitor of platelet adhesion and activation at those higher fluxes. Should a new lipophilic NO donor be developed in the future than can provide smoother surfaces while still maintaining the desirable properties of DBHD/N_2O_2, such as minimal donor leaching and a wide range of attainable NO fluxes, the effect of platelet inhibition by NO fluxes higher than those tested herein could be explored.

2.3.4. SEM Analysis

To verify the results obtained from the LDH assay, SEM images were taken from the control and 4% DBHD/N_2O_2 doped films. The SEM micrographs shown in Figure 2.3 were taken at the center of the well bottoms. It is obvious that platelets on NO-releasing surfaces were much less activated compared with those on the control surface. Also, there were far fewer platelets per viewing area on NO-releasing surfaces. However, SEM does not serve as a quantitative measure since the surface it examines constitutes only a tiny portion of the total surface in contact with platelet-rich plasma. This is the reason why the LDH assay was used to evaluate average platelet adhesion over the entire surfaces.

2.3.5. LDH Assay of NO-Generating Polymers

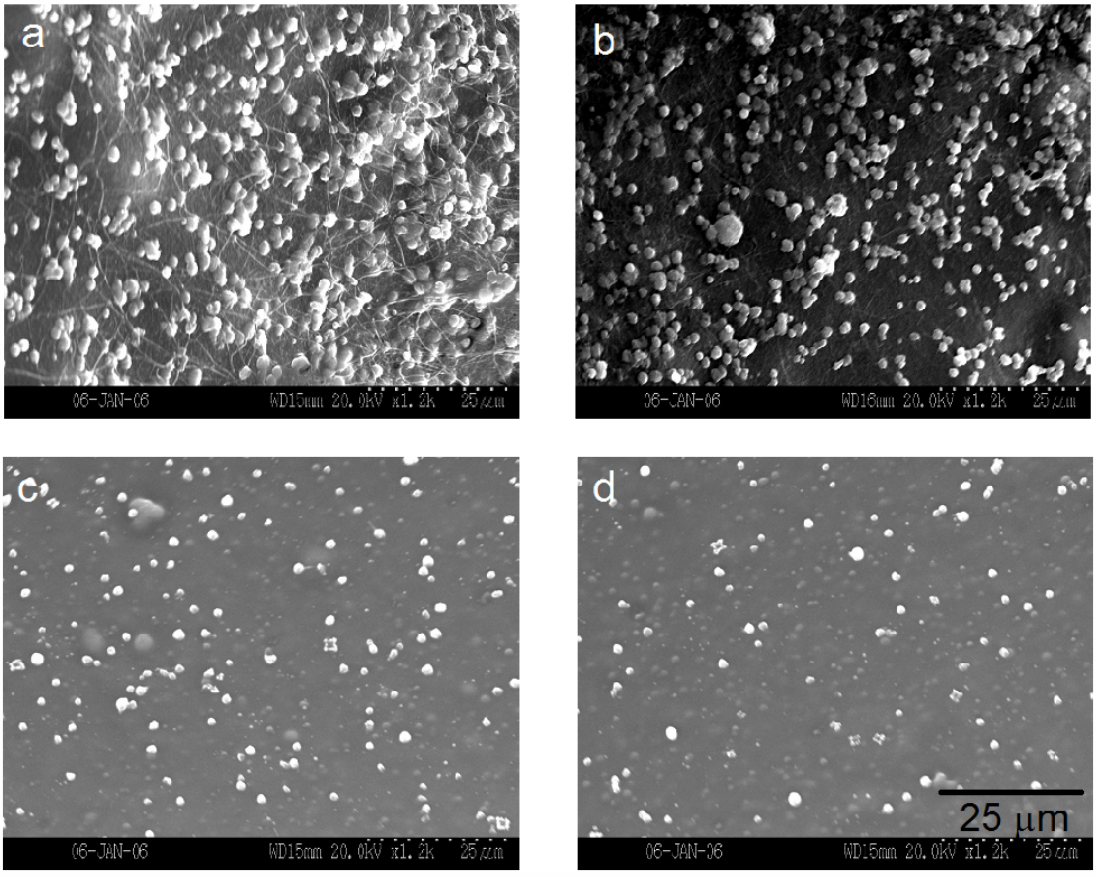

Figure 2.3. SEM micrographs of adhered platelets on control polymers (**a**, **b**) and 4 wt% DBHD/N_2O_2 loaded polymers (**c**, **d**) after 1 h PRP incubation.

Heparin was used instead of citrate as the anticoagulant in experiments involving Cu-DTTCT polymers because citrate ions act as chelator for metal cations and thus poison the catalyst. In contrast to the NO-releasing polymers, NO-generating polymers based on the Cu-DTTCT catalyst cannot produce NO spontaneously. Rather, they require the presence of RSNO species in the aqueous phase to serve as the substrate, and therefore the level of NO produced depends not only on the amount of catalyst in the polymer phase but also on the concentration of RSNO substrate in the solution phase. RSNO compounds are labile and can be decomposed by a number of stimuli [41]. As a result, a steady level of NO-generation at the interface requires a relatively constant level of RSNO species being present, such as the scenario *in vivo*. However, the requirement of stable RSNO level presents a significant challenge to the current design of the *in vitro* platelet adhesion experiment. This is because the RSNOs will decompose during the incubation period as NO is being generated at the polymer/plasma interface.

Due to its chemical instability, little endogenous RSNO can be preserved in the final PRP as determined by NOA. Therefore, GSNO was added to some of the wells to compensate for the possible loss of endogenous RSNO during PRP preparation. The wells without added GSNO serve as controls. The NO- generation profile of polymers with different wt% of Cu-DTTCT is illustrated in Figure 2.4.

However, it is important to realize that the NO-generation kinetics depicted in Figure 2.4 might be different from the actual rate of NO-generation in the microtiter plate wells. In the measurement of NO-generation, a polymer film of 1.5 cm^2 was placed in 2 mL of PBS containing 5 μM GSNO (i.e., the surface/volume ratio is 0.75 cm^{-1}). When 0.1 mL PRP was incubated in polymer-coated wells, it was in contact with 0.834 cm^2 of

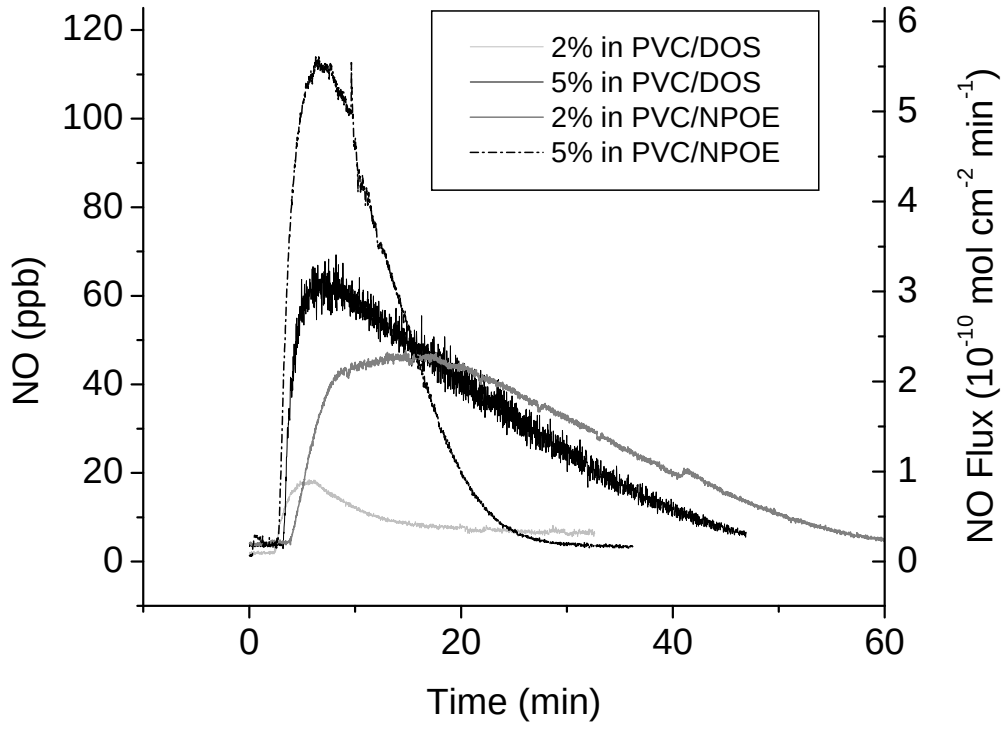

Figure 2.4. NO generation from Cu-DTTCT doped PVC polymers in the presence of 5 μM GSNO, 30 μM GSH and 10 μM EDTA in 2 mL PBS.

the polymer coating (surface/volume ratio of 8.34 cm^{-1}). The depletion of RSNO might occur much faster in the microwells, as a much larger NO-generating surface was exposed to a given volume of aqueous RSNO solution. Despite the higher surface-to-volume ratio, the NO flux does not increase in the case of microwells. This is because the flux depends only on the concentration of RSNO in solution and that of catalyst in the polymer phase, and will be normalized on the basis of surface area.

To achieve the sustained NO-generation above 1×10^{-10} mol cm^{-2} min^{-1} for at least 30 min, 2% Cu-DTTCT in PVC/NPOE was finally chosen as the NO-generating polymer film to coat the microtiter plate wells. A control polymer coating was prepared with the same wt% of DTTCT ligand in PVC/NPOE. The LDH assay result of platelet adhesion on NO-generating and control polymers, either in the presence or absence of added GSNO, is summarized in Figure 2.5. It is obvious that additional GSNO can inhibit platelet adhesion, even in the case of control polymer. Unfortunately, the NO-generating polymer does not further inhibit platelet adhesion.

One possible reason for the inability of NO-generating polymers to inhibit platelet adhesion is the rapid decomposition of RSNO in the NO-generating microwells, as discussed above. The NOA experiment using a much smaller NO-generating polymer piece per unit volume showed that NO-generation could last ~ 30 min, which is the typical time window for the platelet adhesion experiment. It can be speculated that the duration of NO-generation will be much shorter in the microwells where the surface/volume ratio is more than 10 times larger. However, due to the practical limitation in the NOA cell design, it is difficult to simulate the situation that exists in the microplate wells. Raising the RSNO concentration in order to prolong the NO generation

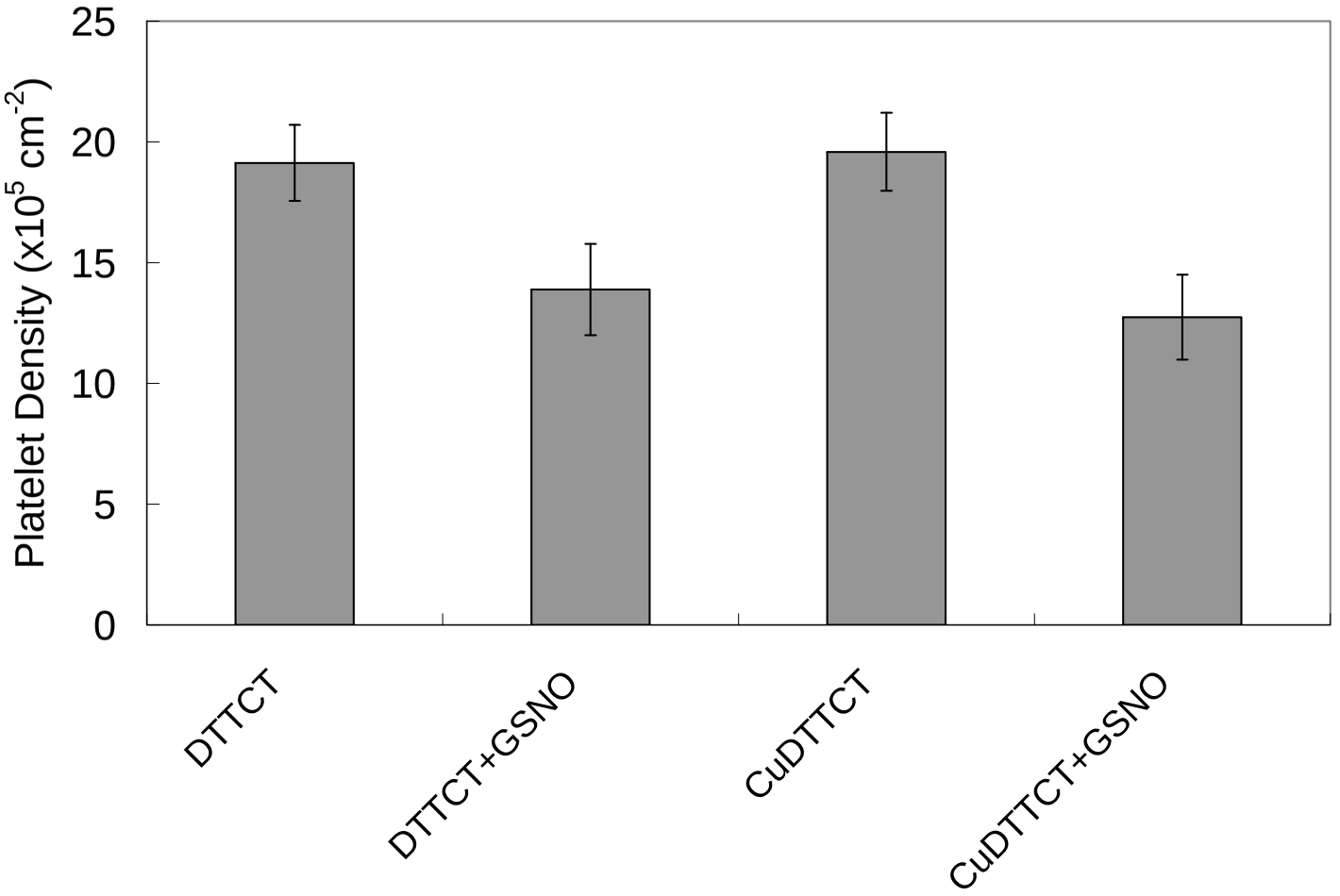

Figure 2.5. Platelet adhesion on NO-generating and control polymers assessed by LDH assay (N=16 each).

is not an option, as 5 μM is by far the upper limit of physiological RSNO levels. Lowering the concentration of Cu-DTTCT catalyst in the polymer film is not a practical choice either, because it is desirable to maintain the NO flux above 1×10^{-10} mol cm^{-2} min^{-1}. Lower catalyst amount is accompanied by lowered NO flux, as discussed earlier.

Another variable is the photo-instability of GSNO. Results indicate that GSNO at μM concentrations can be easily decomposed by light. Exposure to light cannot be completely eliminated in the handling of plasma. Therefore, it is likely that the added GSNO decomposes and provides a bolus of NO at the beginning of PRP incubation. This may explain why NO-generating polymer cannot further inhibit platelet adhesion, since the added GSNO might have already been depleted by light. This also explains why the control polymer, which cannot decompose RSNO, results in decreased platelet adhesion as well.

The last question is the choice of RSNO species. Besides the role of NO carrier, RSNO may also act directly as a platelet inhibitor [42] and the ability to inhibit platelets is a function of the RSNO structure. It has been reported that GSNO is a more potent platelet inhibitor than some other RSNOs such as *S*-nitroso-*N*-acetyl-penicillamine (SNAP) [43]. Further investigation in this direction may require a search for alternative RSNOs that are more photo-stable and less anti-platelet in nature.

2.4. Summary

NO-Releasing Polymers: The thromboresistance of a healthy endothelium involves a complex, synergistic mechanism in which NO plays a very important role. In this chapter, an *in vitro* platelet adhesion assay via platelet LDH release is presented to study the hemocompatibility of polymer films that are capable of either continuously releasing small fluxes of NO or catalytically generating NO from endogenous substrates, to mimic the function of the human endothelium. Using this assay, it was found that continuous NO release from 1:1 PVC/DOS polymer film matrix at close to physiological fluxes (0.93 - 7.05 $\times 10^{-10}$ mol cm^{-2} min^{-1}) helps to reduce platelet adhesion from 14.0 ($\pm$2.1) $\times 10^5$ cells cm^{-2} to 2.96 ($\pm$0.18) $\times 10^5$ cells cm^{-2} on such polymer surfaces. SEM micrographs support the findings of the LDH assay by showing that the platelets were fewer in number and less activated on the NO-releasing surfaces. The precision of this assay is affected slightly by the adsorption of LDH on polymer surfaces. Due to electrostatic interactions between the positively-charged polymer surface and the negatively-charged LDH, the actual adhered platelets on polymers with the highest NO flux could be ~ 7% more than that measured in this assay. However, this false-negative is more significant (~ 10%) with control polymers which have the highest positive charge. The basal LDH level present in plasma is likely to contribute to a common baseline for all polymers tested, which is difficult to precisely determine. Nevertheless, taking such background levels into consideration only strengthens our finding that the LDH assay scheme can be employed to study, *in vitro,* the effect of NO release on platelet adhesion.

It should be noted that the fluxes determined to reduce platelet adhesion for the *in vitro* studies described above may be different than the fluxes required to obtain a similar decrease in platelet adhesion when polymer surfaces are in contact with flowing whole blood. This is because the surface concentrations of NO gas will vary depending on the composition of the flowing blood, including scavenging reactions with hemoglobin in red blood cells, thiol groups and normal oxidation of NO by blood oxygen. In addition, platelet adhesion will also be influenced by the hemodynamics [44]. Clearly, the methodology reported here using microtiter plate wells coated with polymer that releases NO only provides a preliminary assessment as to the potential capability of such coatings to prevent thrombosis when used *in vivo*. Ultimately, the LDH assay methodology described herein can also be used to assess platelet adhesion on NO-releasing materials that are tested intravascularly. Such studies are currently in progress in this laboratory.

NO-Generating Polymers: The catalytic NO generation requires the concerted action between the RSNO species in aqueous phase and the catalyst in the polymer phase. Therefore, it is much more complicated to simulate in an *in vitro* test setting. The experiment described in this chapter is the first attempt to study the biocompatibility of NO-generating polymers *in vitro*. However, a number of serious challenges were encountered as discussed in Section **2.3.5**. As is the case for any biomaterial, the most desirable biocompatibility evaluation of NO-generating polymers would be via *in vivo* study. An example of this is the focus of Chapter 3.

2.5. References

[1] P. L. Feldman, O. W. Griffith and D. J. Stuehr, *Chem. Eng. News*, 71 (1993) 26-38

[2] J. G. Diodati, A. A. Quyyumi, N. Hussain and L. K. Keefer, *Thromb.Haemost.*, 70 (1993) 654-658

[3] C. M. Maragos, D. Morley, D. A. Wink, T. M. Dunams, J. E. Saavedra, A. Hoffman, A. A. Bove, L. Isaac, J. A. Hrabie and L. K. Keefer, *J. Med. Chem.*, 34 (1991) 3242-3247

[4] M. W. Vaughn, L. Kuo and J. C. Liao, *Am. J. Physiol. (Heart Circ. Physiol.)*, 43 (1998) H2163-H2176

[5] C. Michiels, *J. Cell. Physiol.*, 196 (2003) 430-443

[6] M. R. Hernandez, R. Tonda, G. Arderiu, M. Pino, M. Serradell and G. Escolar, *Eur. J. Clin. Invest.*, 35 (2005) 337-342

[7] K. S. B. Masters, E. A. Lipke, E. E. H. Rice, M. S. Liel, H. A. Myler, C. Zygourakis, D. A. Tulis and J. L. West, *J. Biomater. Sci. Polym. Ed.*, 16 (2005) 659-672

[8] M. R. Rossiello, S. Momi, R. Caracchini, S. Giannini, G. Guglielmini, A. Monopoli, E. Ongini, N. Semeraro, M. Colucci and P. Gresele, *J. Thromb. Haemost.*, 3 (2005) 2554-2562

[9] A. Ramamurthi and R. S. Lewis, *Ann. Biomed. Eng.*, 26 (1998) 1036-1043

[10] M. M. Batchelor, S. L. Reoma, P. S. Fleser, V. K. Nuthakki, R. E. Callahan, C. J. Shanley, J. K. Politis, J. Elmore, S. I. Merz and M. E. Meyerhoff, *J. Med. Chem.*, 46 (2003) 5153-5161

[11] H. P. Zhang, G. M. Annich, J. Miskulin, K. Osterholzer, S. I. Merz, R. H. Bartlett and M. E. Meyerhoff, *Biomaterials*, 23 (2002) 1485-1494

[12] P. G. Parzuchowski, M. C. Frost and M. E. Meyerhoff, *J. Am. Chem. Soc.*, 124 (2002) 12182-12191

[13] M. C. Frost, S. M. Rudich, H. P. Zhang, M. A. Maraschio and M. E. Meyerhoff, *Anal. Chem.*, 75 (2003) 1037-1037

[14] M. H. Schoenfisch, K. A. Mowery, M. V. Rader, N. Baliga, J. A. Wahr and M. E. Meyerhoff, *Anal. Chem.*, 72 (2000) 1119-1126

[15] K. A. Mowery, M. H. Schoenfisch, J. E. Saavedra, L. K. Keefer and M. E. Meyerhoff, *Biomaterials*, 21 (2000) 9-21

[16] C. Espadas-Torre, V. Oklejas, K. Mowery and M. E. Meyerhoff, *J. Am. Chem. Soc.*, 119 (1997) 2321-2322

[17] H. P. Zhang, G. M. Annich, J. Miskulin, K. Stankiewicz, K. Osterholzer, S. I. Merz, R. H. Bartlett and M. E. Meyerhoff, *J. Am. Chem. Soc.*, 125 (2003) 5015-5024

[18] Z. R. Zhou and M. E. Meyerhoff, *Biomacromolecules*, 6 (2005) 780-789

[19] Z. R. Zhou and M. E. Meyerhoff, *Biomaterials*, 26 (2005) 6506-6517

[20] M. M. Reynolds, Z. R. Zhou, B. K. Oh and M. E. Meyerhoff, *Org. Lett.*, 7 (2005) 2813-2816

[21] K. S. Bohl and J. L. West, *Biomaterials*, 21 (2000) 2273-2278

[22] D. J. Smith, D. Chakravarthy, S. Pulfer, M. L. Simmons, J. A. Hrabie, M. L. Citro, J. E. Saavedra, K. M. Davies, T. C. Hutsell, D. L. Mooradian, S. R. Hanson and L. K. Keefer, *J.Med. Chem.*, 39 (1996) 1148-1156

[23] Y. Wu, A. P. Rojas, G. W. Griffith, A. M. Skrzypchak, R. H. Bartlett and M. E. Meyerhoff, *Sens. Actuators B,* 121 (2007) 36-46

[24] K. Wong and X. B. Li, *Transfus. Apheresis Sci.*, 30 (2004) 29-39

[25] T. Shahbazi, N. Jones, M. W. Radomski, M. A. Moro and D. Gingell, *Thromb. Res.*, 75 (1994) 631-642

[26] P. A. Whiss, R. G. G. Andersson and U. Srinivas, *J. Immunol. Methods*, 200 (1997) 135-143

[27] J. G. White, In: J. M. Gibbins, M. P. Mahaut-Smith, Eds. *Methods in Molecular Biology (Platelets and Megakaryocytes)*, Totowa, NJ: Humana Press, 2004. p. 47-63

[28] M. Rodrigues and H. Sinzinger, *Thromb. Res.*, 76 (1994) 399-432

[29] Y. Tamada, E. A. Kulik and Y. Ikada, *Biomaterials*, 16 (1995) 259-261

[30] W. B. Tsai, J. M. Grunkemeier and T. A. Horbett, *J. Biomed. Mater. Res.*, 44 (1999) 130-139

[31] J. Y. Park, C. H. Gemmell and J. E. Davies, *Biomaterials*, 22 (2001) 2671-2682

[32] L. J. Suggs, J. L. West and A. G. Mikos, *Biomaterials*, 20 (1999) 683-690

[33] L. Kikuchi, J. Y. Park, C. Victor and J. E. Davies, *Biomaterials*, 26 (2005) 5285-5295

[34] J. Rivera, M. L. Lozano, V. Vicente, In: J. M. Gibbins, M. P. Mahaut-Smith, Eds. *Methods in Molecular Biology (Platelets and Megakaryocytes)*. Totowa, NJ: Humana Press; 2004. p 57-72.

[35] B. K. Oh and M. E. Meyerhoff, *Biomaterials*, 25 (2004) 283-293

[36] J. S. Stamler and J. Loscalzo, *Anal. Chem.*, 64 (1992) 779-785

[37] K. M. Davies, D. A. Wink, J. E. Saavedra and L. K. Keefer, *J. Am. Chem. Soc.*, 123 (2001) 5473-5481

[38] S. Wassmann, K. Wassmann and G. Nickenig, *Hypertension*, 44 (2004) 381-386

[39] I. Kwiecien, M. Sokolowska, E. Luchter-Wasylewska and L. Wlodek, *Int. J. Biochem. Cell Biol.*, 35 (2003) 1645-1657

[40] A. M. Skrzypchak, N. G. Lafayette, R. H. Bartlett, Zhengrong Zhou, M. C. Frost, M. E. Meyerhoff, M. M. Reynolds and G. M. Annich, *Perfusion*, 22 (2007) 193-200

[41] D. L. H. Williams, *Acc. Chem. Res.*, 32 (1999) 869-876

[42] N. Hogg, *Free Radic. Biol. Med.*, 28 (2000) 1478-1486

[43] S. C. Askew, A. R. Butler, F. W. Flitney, G. D. Kemp and I. L. Megson, *Bioorg. Med. Chem.*, 3 (1995) 1-9

[44] E. Dejana, A. Remuzzi, L. R. Languino, V. Costantini, D. Lauri, A. Zanetti and G. Degaetano, *Methods Find. Exp. Clin. Pharmacol.*, 7 (1985) 153-159

CHAPTER 3

MORE BIOCOMPATIBLE INTRAVASCULAR OXYGEN SENSORS VIA CATALYTIC DECOMPOSITION OF *S*-NITROSOTHIOLS TO GENERATE NITRIC OXIDE *IN SITU*

3.1. Introduction

As introduced in Chapter 1, monitoring the cardiopulmonary function of critically ill patients mandates the continuous measurements of blood gases and electrolytes. The development of implantable sensors (electrochemical and/or optical) capable of reliably measuring important physiological species, such as PO_2 , PCO_2, pH, electrolytes, glucose and lactate *in vivo,* has remained a great challenge for several decades [1, 2]. A variety of prototype catheter-style commercial devices have been developed for intravascular blood gas sensing purposes [3, 4]. However, these devices have not found widespread use in the clinical arena, primarily due to the erratic results obtained when used for continuous *in vivo* measurements. Such errant results arise from the biological responses of living systems to foreign devices implanted in the blood stream. Proteins, such as collagen, fibrinogen and von Willebrand factor, adsorb onto the polymer surfaces of the implanted sensors within seconds [5, 6]. The adsorbed protein layer mediates the adhesion and activation of metabolically active cells, e.g., platelets, that later arrive [7, 8]. Platelets

play a key role in blood coagulation since activated platelets keep recruiting circulating cells to the polymer surfaces, which ultimately leads to the formation of blood clots [9]. The presence of active cells on the surface of such devices causes localized changes in pH, PO_2 and PCO_2 values due to cellular respiration compared to the bulk blood [1], yielding significant errors when results are compared to values obtained from *in vitro* measurements on discrete samples of blood.

Nitric oxide has been widely recognized as a potent vasodilator and inhibitor of platelet adhesion and activation [10-13]. It is produced from L-arginine by a class of enzymes known as nitric oxide synthases (NOS). The perfect thromboresistance of the human endothelium has been attributed in part to the low but continuous production of NO in this layer [14, 15]. Endothelial cells that line the inner walls of healthy blood vessels produce NO with an estimated surface flux level of 0.5-4.0 $\times 10^{-10}$ mol cm^{-2} min^{-1} [16]. Therefore, one approach to potentially resolve the hemocompatibility problem is to release or generate NO locally at the blood/sensor interface at or above the flux of normal endothelial cells in order to inhibit platelet adhesion and activation, and thus prevent gross thrombus formation. Biomedical devices (i.e., intravascular sensors, vascular grafts, extracorporeal circuits, etc.) coated with polymers containing diazeniumdiolate-type NO donors have already been shown to exhibit improved biocompatibility via various *in vivo* evaluations (in animal models) [17-19]. However, due to the limited reservoir of the NO donors in the polymer coatings, the NO-release approach is only suitable for biomedical devices that require short-term blood contact times, such as hemodialysis and extracorporeal circulation, but not for long-term (i.e., weeks or months) implantation. To maintain NO production for extended periods of time it may be possible to take

advantage of endogenous species such as nitrosothiols (RSNOs) that are constantly produced in the body (from NO generated by NOS) to generate NO *in situ* at the polymer/blood interface.

Nitric oxide has very short lifetime in blood [20] due to its reactivity with various blood components [21]. In contrast, more abundant (i.e., micromolar concentrations) and stable forms of NO in blood are *S*-nitroso adducts with thiol groups (RSNOs) [22], such as *S*-nitrosoalbumin (AlbSNO), *S*-nitrosocysteine (CysNO) and *S*-nitrosoglutathione (GSNO) [22-24]. One well-known mechanism of RSNO decomposition to yield NO is catalyzed by Cu^{+} [25], in which Cu^{+} is produced from the reduction of Cu^{2+} by thiolates or other reducing equivalents that exist in the physiological environment (e.g., ascorbate). It has already been demonstrated that polymer films doped with lipophilic cyclen-type Cu(II) complexes [26] and Cu(II)-cylen complex covalently linked to poly(2-hydroxyethyl methacrylate) hydrogels [27] are capable of generating significant NO fluxes ($>1\times10^{-10}$ mol cm^{-2} min^{-1}) in the presence of physiologically relevant concentrations of GSNO and appropriate reducing agents. However, our preliminary studies indicate that such polymer films based on these Cu(II)-cylen complexes are not ideally suited for long-term NO-generation *in vivo* due to the loss of NO-generating functionality after extended storage in plasma. In this chapter, the use of polymer films doped with small metallic copper particles as the catalytic coatings on the surface of intravascular electrochemical oxygen sensing catheters is examined. Such coatings can generate NO *in situ* at the sensor/blood interface via a slow corrosion of the copper particles to produce copper ions. When placed in porcine arteries, the oxygen sensing catheters with NO-generating capability are shown to exhibit improved blood

compatibility and more accurate PO_2 measurements when compared to corresponding control oxygen sensing catheters implanted within the same animals.

3.2. Materials and Methods

3.2.1. Materials

Sodium chloride, potassium chloride, sodium nitrite, reduced L-glutathione (GSH), sulfuric acid (95-98%), bicinchoninic acid (disodium salt), dibutyltin dilaurate (95%), Triton X-100, bovine serum albumin and 3-μm copper powder were purchased from Sigma-Aldrich (St. Louis, MO). Copper nanoparticles (80 nm size) were from Inframat Advanced Materials (Farmington, CT). Ethylenediaminetetraacetic acid (EDTA) was obtained from Mallinckrodt (Paris, KY). Methocel 90 HG and 3-aminopropyltrimethoxy-silane were from Fluka (Milwaukee, WI). The silicone rubber tubing (0.51 mm i.d. × 0.94 mm o.d.) used to construct catheters was obtained from Helix Medial, Inc. (Carpinteria, CA), and Silastic medical grade tubing (0.94 mm i.d. × 1.29 mm o.d.) was received as a gift from Medtronic (Minneapolis, MN). Silicone rubber (RTV-3140) was the product of Dow Corning (Midland, MI). Tecophilic SP-60D-60 and Tecoflex SG-80A polyurethanes were from Noveon (Cleveland, OH). A quick-setting two-part epoxy was the product of Super Glue Corp. (Rancho Cucamonga, CA). The PTFE-coated Pt/Ir and Ag wires employed to fabricate the oxygen sensing catheters were products of MedwireCorp. (Mt. Vernon, NY). Ultra 4-way stopcocks and Angiocath catheter guides (16g × 1.16 in) used for catheter implantation in the arteries of pigs were from Medex (Hillard, OH) and Becton Dickinson (Sandy, UT), respectively.

3.2.2. Fabrication of NO-Generating Oxygen Sensors

The Clark-type amperometric oxygen sensing catheters employed in this work were fabricated as previously reported [17, 19]. However, instead of applying an NO-release polymer coating on the surface of the silicone rubber catheter, a thin layer of a polymer doped with Cu^0 catalyst (in the form of either micron- or nano-sized Cu^0 particles) was coated on the surface of the silicone rubber tubing (see Figure 3.1). Briefly, the sensor sleeves were made by cutting the thinner silicone rubber tubing (from Helix Medical) into 25 mm pieces and filling ~ 2 mm length on one end with RTV-3140. The sensor sleeves were cured under ambient conditions for 24 h. Two different sizes of copper particles (3 μm and 80 nm) were evaluated for *in vivo* biocompatibility, together with their respective controls (polymer coating without Cu^0 particles). In the case of 3-μm Cu^0 particle coatings, 3% (w/v) of Cu^0 particles were suspended in a THF solution of 5% (w/v) RTV-3140 and 2.5% (w/v) SP-60D-60 hydrophilic polyurethane (HPPU). This mixture was sonicated for 30 min before the catheter sleeves were dip-coated once in this suspension. Thirty minutes later, one top-coat of 1% RTV-3140 and 0.5% HPPU (w/v) was applied to the sensor sleeves by dip-coating. The coatings were first cured overnight at ambient moisture, and then further dried under vacuum for 24 h. Coatings on control sensors were prepared in the same manner except that no copper particles were added to the polymer solution used for the underlying coating.

To apply the polymer coating doped with the copper nanoparticles to the sensors, an adhesion-promoting layer was added between the silicone rubber sensor sleeve and the Tecoflex SG-80A polyurethane layer which contained the copper nanoparticles. This

adhesion layer was made from 10% RTV-3140, 1% 3-aminopropyltrimethoxy-silane and 0.1% dibutyltin dilaurate catalyst (all w/v) in THF. This adhesion layer was cured under ambient moisture for 24 h before the catalyst layer was dip-coated on the sensor. The catalytic layer was prepared using a THF solution with 3 w/v% of Tecoflex SG-80A and 1 w/v% Cu^0 nanoparticle catalyst and sonicated for 20 min. The sensor sleeves with the adhesion promoter layer were dip-coated once in this polymer mixture and dried under ambient conditions overnight and then dried again under vacuum for 24 h. Control sensor sleeves were coated in the same manner with the only difference being the absence of copper particles in the outer polymer layer. No additional topcoat was applied to prepare the sensors with the nanoparticle-based coating.

To construct the functional electrochemical oxygen-sensing catheter, the sensor sleeves were filled with 0.15 M KCl and 1.5 wt% Methocel internal electrolyte solution (see Figure 3.1). The entire sensor sleeve was sealed and glued to the sensor body by epoxy. The Teflon coated Pt/Ir working electrode was polarized at -0.7 V vs. the Ag/AgCl reference electrode. Current output was recorded via a DATAQ Instruments DA-700 USB data acquisition card (Akron, OH) by WinDAQ/Lite software. The sensor's response to oxygen was evaluated via bench experiments by using different tonometered solutions of oxygen (0, 5, 10, 21 and 30% of O_2, balanced with N_2). Sensors were placed in each solution for 10 min and the output current was recorded by the aforementioned protocol.

3.2.3. *In Vitro* Nitric Oxide Generation

The NO-generating ability of sensor sleeves was examined before and after the *in*

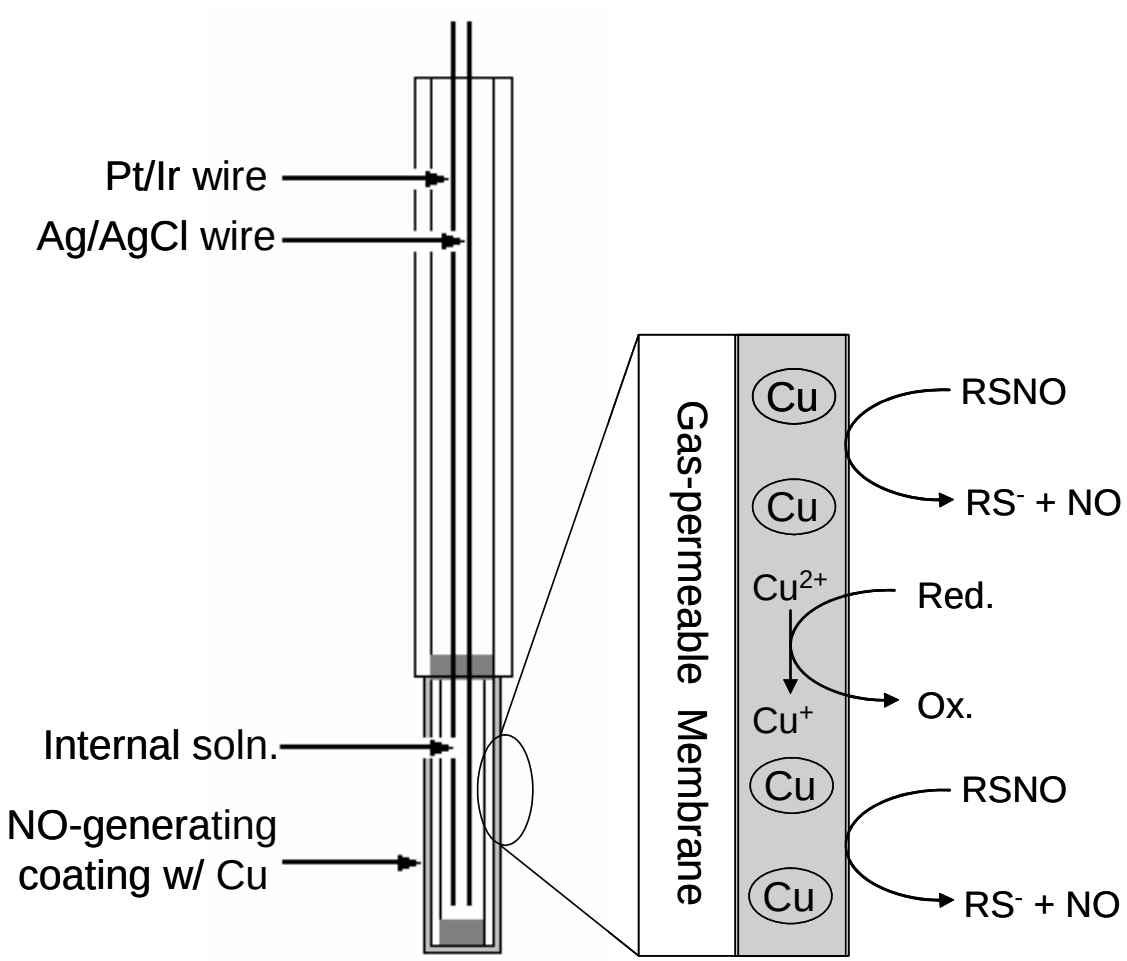

Figure 3.1. Schematic of intravascular oxygen sensor design and the NO generation mechanism

vivo studies using a chemiluminescence NO analyzer. Nitrosoglutathione (GSNO) was prepared by the reaction of equal-molar glutathione (GSH) and $NaNO_2$ in 0.06 M H_2SO_4. To an amber glass reaction cell containing 2 mL PBS (138 mM NaCl, 2.7 mM KCl and 10 mM sodium phosphate, pH 7.4) was added 1 μM GSNO, 30 μM GSH and 5 μM EDTA (to chelate metal ion contaminates that might otherwise decompose GSNO). The solution was bathed at 37 ºC and continuously bubbled withN_2. Any NO produced in the test solution was purged from the buffer, carried by the N_2 gas into the chemiluminescence reaction chamber and monitored in real-time. The baseline NO level was recorded for ~ 5 min before the Cu^0-containing sensor sleeves were placed in the substrate solution.

3.2.4. *In Vitro* Copper Corrosion

The copper-containing sensor sleeves were bathed in 5 mL PBS (pH 7.4) for 1 d at 37 ºC under constant shaking. The bathing solution was then tested for copper content using a bicinchoninic acid (BCA) assay as previously reported [28]. The calibration standards were prepared via serial dilution from a stock 1000 ppm $Cu(NO_3)_2$ (Fisher) solution into PBS. The absorbance at 357 nm was used for quantification.

3.2.5. *In Vivo* Biocompatibility Evaluation

Assessment of the *in vivo* biocompatibility and analytical performance of the NO-generating oxygen sensing catheters was performed by implanting sensors in nine female juvenile swine, weighing 25 - 30 kg. Six of the nine animals were used for the evaluation of the 3-μm Cu^0 particle based coating and the remaining three animals were used to

assess the sensors with polymer coatings containing the Cu^0 nanoparticles. Mechanical gas anesthesia was maintained during the experiment with a mix of 1-3% liquid for inhalation isofluorane (Hospira, Inc., Lake Forest, IL) and 21% oxygen. The depth of anesthesia was monitored following the University of Michigan's University Committee on Use and Care of Animals protocol that was pre- approved for these experiments.

Cut-downs of the animals were made on both groins as well as the bilateral sides of the neck for isolation of the femoral and carotid arteries, respectively. An arterial 14-gauge catheter was advanced into the right thyrocervical trunk to monitor systemic hemodynamics (blood pressure and heart rate) and to acquire blood samples for activated coagulation time (ACT) and *in vitro* arterial blood gas (ABG) values using a Radiometer Medical ABL-505 standard blood gas analyzer (Copenhagen, Denmark). The right internal jugular vein was exposed and dissected from surrounding tissues and a 9 Fr Arrow® catheter was advanced to monitor central venous pressure (CVP), and to further administer i.v. fluids (lactated ringers) and medications. The arterial and CVP lines were attached to fluid pressure transducers (Abbott Critical Care Systems. North Chicago, IL) and monitored continuously on a Series 7000 Pressure Monitor (Marquette Electronics, Milwaukee, WI). The bladder of each animal was surgically drained by placing a Foley catheter directly into the bladder.

For each swine, four sensors were implanted: two NO-generating sensors and two control sensors. One NO-generating sensor and one control sensor were placed in the carotid arteries, while the second pair was placed in the femoral arteries via 16-gauge Angiocath 1.16 inch cannulae. The cannula tips were trimmed off by ~ 1 cm to make an angle that allows for the ease of intravascular implantation. Sensors were slid into the

cannulae and fixed to the 4-way stopcock by epoxy. Approximately a 1 cm length of the sensing catheter extended past the end of the cannula and was exposed to flowing blood in the animal. The artery distal to the cannula insertion was not ligated. Slow saline drips (0.1-0.2 mL/min) containing 1 U/mL of heparin were supplied to each sensor site via pressure bags to prevent back-flow of blood into the cannulae. Sensors were implanted such that the sensor tip was exposed to oncoming blood flow and the small amount of heparin present in the saline drips was washed distally from the sensor, never flowing over the sensor surface.

No systemic anticoagulation agent was administered during each animal study. Activated coagulation times (ACT) were measured before sensor implantation and was checked every 4 h during the experiment to ensure that the slow heparin infusion does not lead to any significant systemic anticoagulation. One hour after implantation, sensors were calibrated *in situ* via a one point calibration (assuming zero current for zero oxygen level and that the observed current corresponds to the blood oxygen PO_2 level measured *in vitro* by the ABL-505 blood gas monitor at the point of calibration). Continuous amperometric sensor output was recorded, and discrete blood samples were drawn periodically and analyzed by the ABL-505 to evaluate the accuracy of the implanted sensors' performance. During the first 2 h, blood samples were drawn every 15 min, and during hours 3-4, samples were drawn every 30 min. During the remainder of the experiment, samples were drawn every hour for comparison purposes. In total, 24 oxygen sensing catheters were evaluated (12 NO-generating sensors and 12 controls) in the 3-μm particle group and a total of 12 (6 NO-generating and 6 controls) were studied in the nanoparticle group.

Upon termination of every animal preparation, the femoral and carotid arteries were excised distal to the implanted sensor. The animal was then euthanized with a bolus injection of Fatal-Plus (Vortech Pharmaceutical, Dearborn, MI). To prevent scraping off of the surface bio-layer, the sensors were carefully dissected from the arteries without pulling them out of the vessels or through the cannula, and rinsed in PBS to remove loosely adsorbed blood elements.

3.2.6. Surface Clot Evaluation

Digital images of the oxygen sensing catheters were taken immediately after the removal of sensors from the blood vessels. A lactate dehydrogenase (LDH) assay has been reported previously (see Chapter 2) as a useful approach for quantifying platelet adhesion to surfaces [29]. In this chapter, this LDH assay was used to assess the degree of gross thrombus and cell adhesion on the sensor surfaces after the *in vivo* experiments. The portion of catheter tips that had been exposed to the blood stream was cut off and stored in 1.5 mL lysis buffer solution (PBS buffer with 1 wt% Triton X-100 and 0.75 wt% bovine serum albumin) for 1 h to lyse any cells that were adhered on the catheter surfaces. The copper-loaded catheter tips were then saved and later tested for the NO generation *in vitro* to assess whether exposure to flowing blood significantly changes the ability to catalyze the RSNO decomposition. The lysate solution was then further diluted 1:5 with the lysing buffer. One hundred μL of the final lysate was mixed, in triplicate samples, with 100 μL of reagent from an LDH assay kit (Roche Applied Sciences, Indianapolis, IN) into wells of a 96-well polystyrene microplate (Fisher) and the absorbance at 490 nm was monitored by a Labsystems Multiskan RC microplate reader

(Fisher). The linear portion of absorbance vs. time curve was used for quantitating LDH activity.

3.3. Results and Discussion

3.3.1. NO-Generating Polymer Coatings

In preliminary experiments, a variety of polymer matrices containing 3-μm Cu^0 particles were tested, among which the 2:1 blend of RTV-3140 silicone rubber and Tecophilic SP-60D-60 HPPU yielded the optimal balance of adhesiveness to the SR tubing of the catheter and adequate hydrophilicity to allow diffusion of RSNO species into the polymeric layer containing the Cu^0 particles. The optimal particle:polymer ratio (40 w/w% for 3-μm and 33 w/w% for 80-nm particles) was determined by the peak fluxes of NO generation from GSNO for each formulation. Another goal was to use the least possible amount of copper so as to minimize any potential toxic effects [30] that may be caused by continuous copper corrosion. Previous *in vivo* experiments [17, 19] that employed NO-releasing polymer films required thick polymer coatings (~100 μm) in order to achieve the desired flux and duration of NO release. Since the NO-generation strategy suggested here only requires a very thin layer of Cu^0 catalyst to be immobilized at the sensor surface, the thickness of the sensor coating with 3-μm particles could be reduced to as little as ~ 7 μm, while coatings can be even thinner for films containing the Cu^0 nanoparticles. At the same time, using the 3-μm Cu^0 particles produces slightly rougher sensor surfaces than the controls (based on scanning electron micrographs (SEM), not shown here). This may put the NO-generating sensors at a disadvantage since rougher

surfaces are prone to induce more thrombus formation [31]. However, it was found that much smoother surfaces can be readily achieved using the polymer films containing the Cu^0 nanoparticles as the catalytic layer, with negligible change of surface roughness as determined by SEM. The utilization of an adhesion promoter layer allows for the use of polyurethanes as the coating material to load the copper nanoparticles on the silicone rubber surfaces of the catheters. Tecoflex SG-80A was found to offer the best combination of NO flux and adhesive properties in this case.

In preliminary *in vitro* experiments to assess NO generation capability of the different coatings, the GSNO and GSH concentrations were set at 1 μM and 30 μM, respectively, which is close to their physiological levels [23]. As shown in Figure 3.2, the NO-generating polymer coatings on sensor sleeves, either made from 3-μm (Figure 3.2-1) or 80-nm Cu^0 particles (Fig. 3.2-2), were capable of generating physiologically relevant ($>1\times10^{-10}$ mol cm^{-2} min^{-1}) levels of NO both before and after implantation within a porcine artery for 20 h. The levels of generated NO detected by chemiluminescence decrease over time as the GSNO substrate in the test solution is consumed. The sensor sleeves tested were different in length before (25 mm) and after (10 mm) the *in vivo* study, as only the exposed portion was taken after the implantation. Thus, the NO flux data were normalized to reflect this change in surface area. Interestingly, the sensors coated with polymer containing the 3-μm Cu^0 particles actually generated higher fluxes after the *in vivo* experiment. This might be due to the hydrophilic moiety in the polymer becoming more completely hydrated allowing for faster GSNO diffusion into the film. Although there is no method currently available to directly measure the NO fluxes at the sensor surfaces *in vivo*, it is anticipated that the oxygen

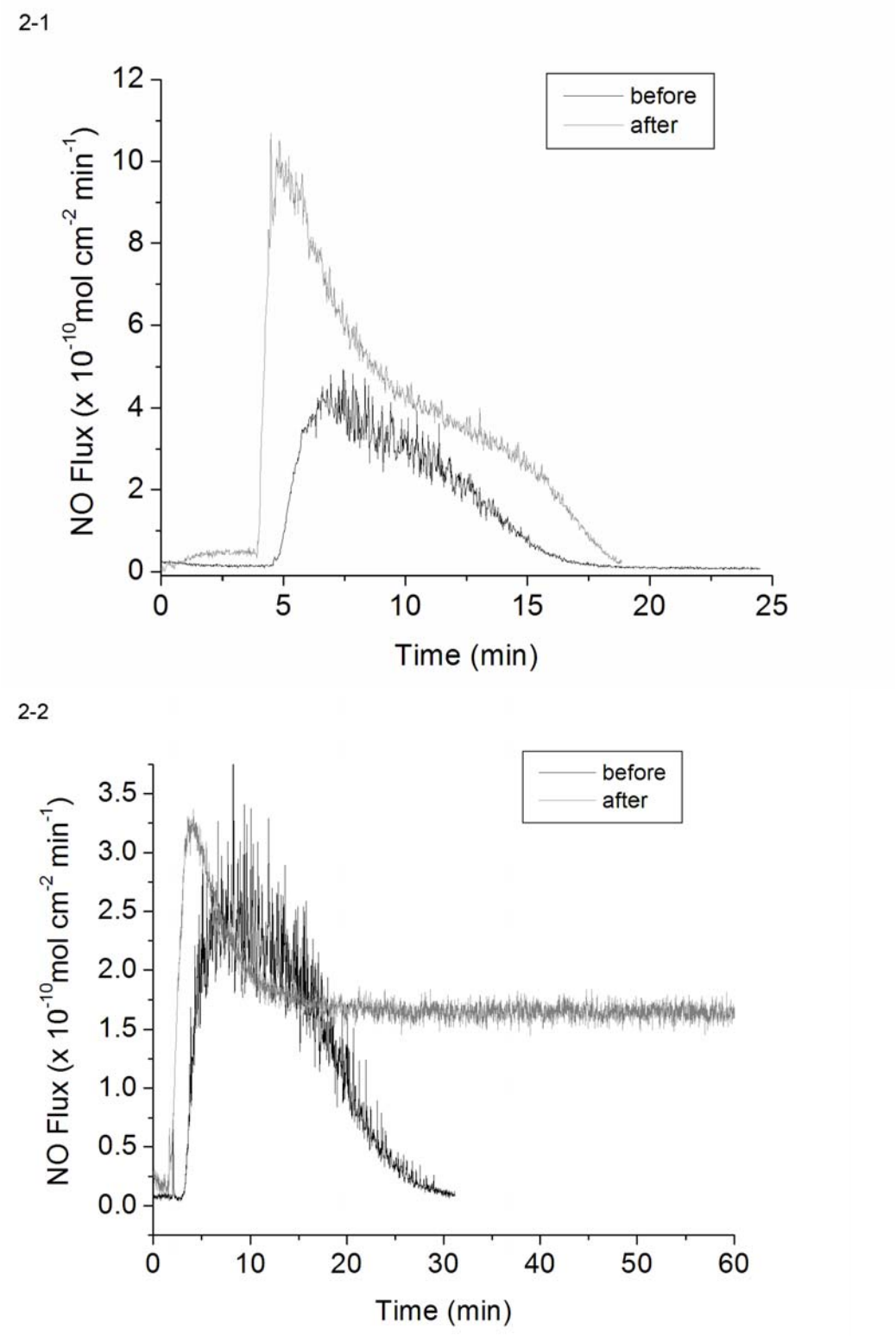

Figure 3.2. *In vitro* generation of NO from 1 μM GSNO, 30 μM GSH and 5 μM EDTA in 2 mL PBS at 37ºC by the catalysis of (1) 3 μm and (2) 80 nm Cu^0 particle coated sensor sleeves before and after animal studies.

sensors coated with the films containing the Cu^0 particles are, in fact, able to continuously generate NO *in vivo* from endogenous RSNO substrates.

Our previous results with NO-releasing polymers showed that NO released from the sensor surface does not interfere with its oxygen measurements during the time frame of the *in vivo* experiments [17]. In this study, the possible effects of adding the copper particles to the outer layer of the sensor on the amperometric oxygen sensitivity and response times of the devices were also examined. Figure 3.3 illustrates the typical current responses to different levels of PO_2 displayed by the NO-generating sensors based on the 3-μm and nano-Cu^0 particles embedded in the outer polymer coatings. As shown, the introduction of the Cu^0 catalysts does not significantly impact the electrochemical oxygen response of the sensors, with responses linear to at least 227 mmHg (30% O_2 balanced by N_2) and no dramatic change in response time (compared to control sensors without the coatings). As shown in Figure 3.3, the output currents of given sensors do vary as the result of different working electrode areas exposed in the fabrication step. This is the reason why *in vivo* calibration needs to be performed at the beginning of each experiment.

3.3.2. *In Vitro* Copper Corrosion

Since it is known that the catalytic species required to decompose RSNO species to NO is either Cu(I) or Cu(II) ions, the NO generation process observed must be due to a slow corrosion of the metallic copper particles in the polymeric matrix. Further, copper is an essential trace element in biological systems. The average intake of copper by human adults ranges from 0.6 – 1.6 mg/d [32]. While trace amounts of copper are vital for the

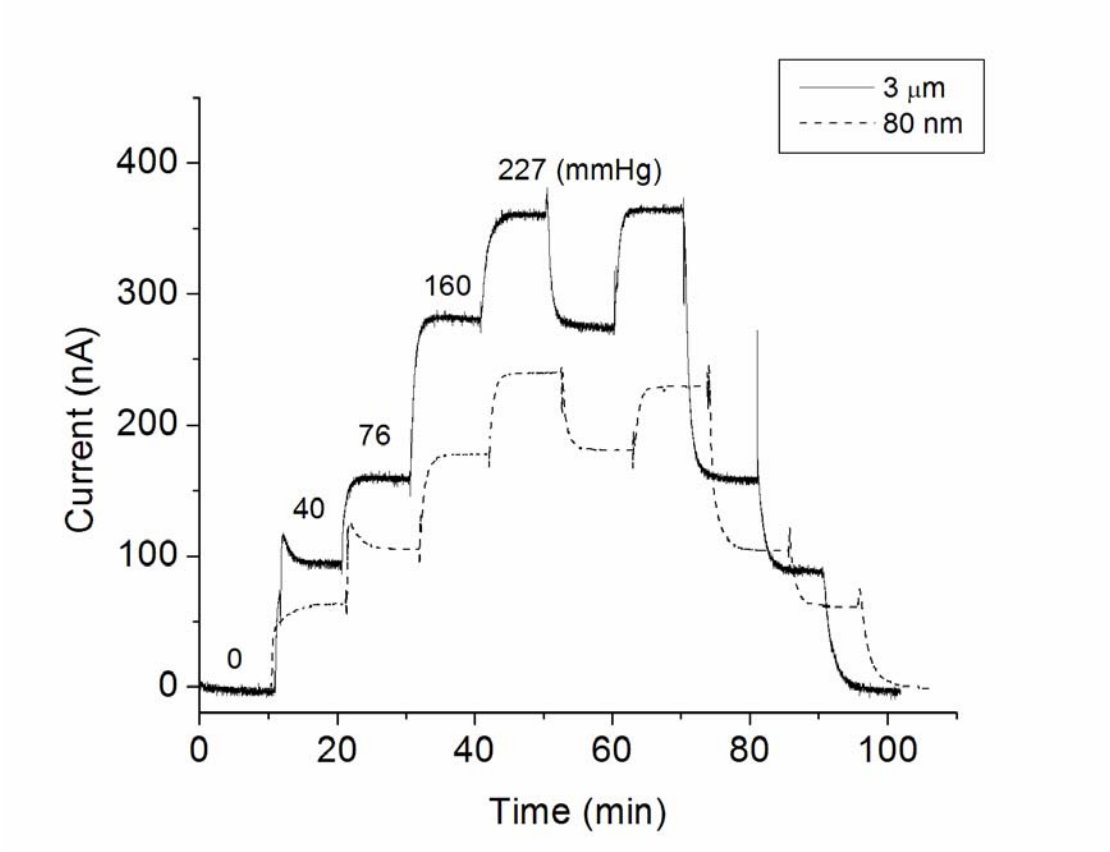

Figure 3.3. Amperometric responses of NO-generating oxygen sensors prepared with 3 μm and 80 nm Cu^0 particle coatings to 0, 5, 10, 21 and 30% oxygen balanced with nitrogen. The actual oxygen partial pressures are indicated for each oxygen level.

healthy functioning of organisms, excess copper build-up in the body could cause Wilson's disease which may lead to impaired liver function [30]. Given that NO-generation of the outer polymeric layers of the oxygen sensing catheters relies on the corrosion of metallic copper particles to provide reactive surface ions, it is critical to establish that copper corrosion is well below the level required for safe use under physiological conditions. Copper analysis via the colorimetric BCA assay has excellent sensitivity and selectivity, and the results have been reported to correlate very well with a conventional atomic absorption method [28]. Using this assay, the levels of copper ions present in PBS solutions in which a Cu^0 particle based coatings were soaked in for at least 24 h were measured. The corrosion rate for copper was determined to be 4.84 ± 0.37 μg/d (N = 4) per catheter sleeve for coatings that contain the 3-μm Cu^0 particles and 0.78 ± 0.17 μg/d (N = 3) for the Cu^0 nanoparticle-based coating. In both cases, this is less than 1% of the recommended daily intake for human adults [32]. Therefore, with only 4 relatively small sensors implanted in each animal, it is unlikely that copper leaching from the surface of the sensors will have any toxic effects. Moreover, the sensors were implanted in a dynamic flow environment so that there would not be any locally accumulated copper levels to be concerned about. In fact, no unusual inflammation was observed at any of the sensor implant sites that were used to carry out the animal experiments reported in this study.

3.3.3. Blood-Compatibility and Surface Thrombus Evaluation

3.3.3.1. 3-μm Cu^0 particle coated sensors

Without administration of a systemic anticoagulation agent, 12 pairs of control and NO-generating sensors were implanted in porcine carotid and femoral arteries for at least 20 h. The animals' ACTs remained within the normal range of 75-120 s throughout, suggesting no systemic effects of the heparin drips at each sensor site. Any gross thrombi on the surfaces of the implanted sensors were determined by observing formation of mature blood clot with a dark color and fibrin networks after the sensors were excised from the arteries. For all the oxygen sensors implanted, 9 of 12 control sensors showed visible thrombus formation after being explanted and rinsed in PBS; in contrast, only 3 of 12 NO generating sensors had visible clots on them. In all cases where one or two NO-generating sensors developed observable blood clots, both control sensors in the same animal had significant clots over them as well. This might imply that lower than normal RSNO levels existed in these test animals. In such cases the NO-generating functionality of the Cu^0 particle coatings would not provide adequate surface levels of NO to improve thromboresistancy.

Two representative pairs of sensors in the 3-μm Cu^0 particle group after explantation are shown in Figure 3.4-1 and Figure 3.4-2, each pair from the same animal. In each panel (A) represents NO-generating sensors and (B) represents the control sensors. To the right of the dashed lines is the portion of the sensors that have been exposed to blood flow. In general, NO-generating sensors are darker in color than the controls due to the copper particles in the outer polymeric coating. Both NO- generating sensors (i.e., A1 and A2) appear clean. However, a mature blood clot has developed over control sensor B1. Control sensor B2 appears to be free of clot. Only 3 of 12 control sensors exhibited such thrombus-free surfaces after being explanted.

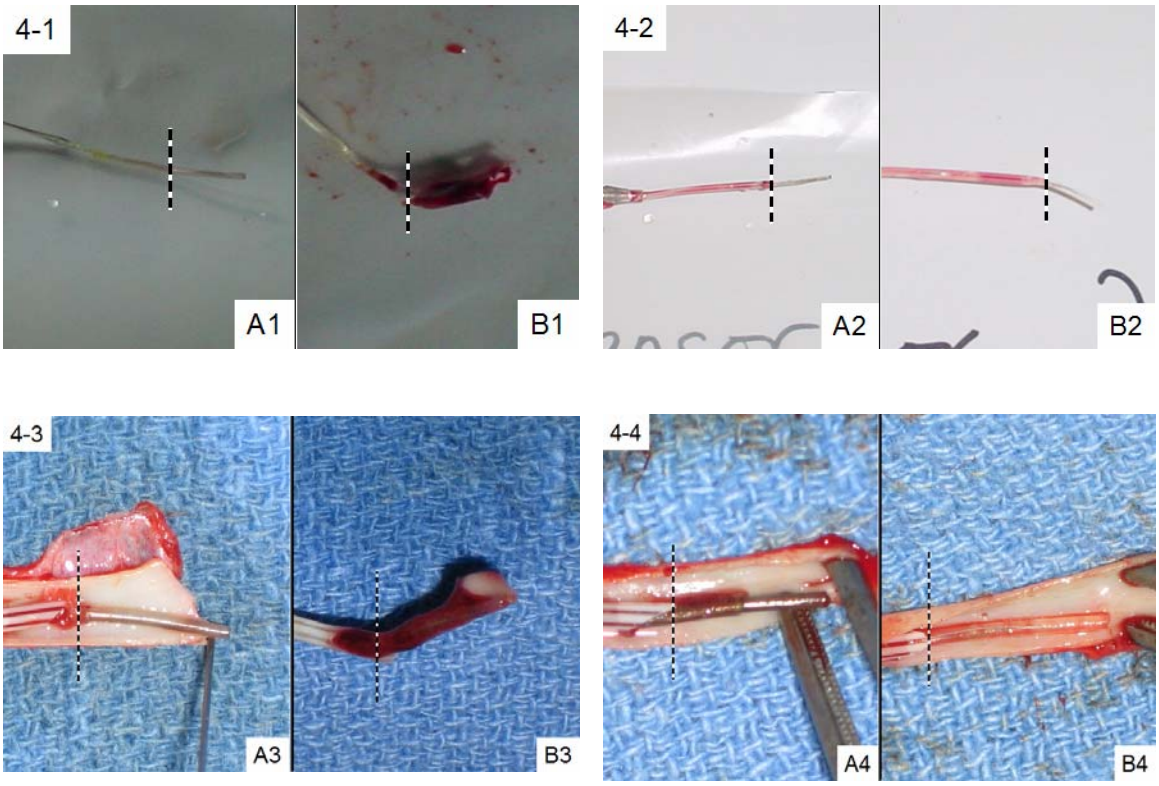

Figure 3.4. Images of four representative pairs of NO-generating (Panel A) and control (Panel B) sensors after in vivo studies. The portion to the right of the dotted lines had been exposed to blood. Sensors A1, B1, A2 and B2 are from the 3-μm particle group while Sensors A3, B3, A4 and B4 are from nanoparticle group.

SEM is normally used for the surface analysis of blood-contacting materials [33]. It is ideal in providing detailed image at a very small region of the surface but fails to give quantitative information on a macroscopic scale. In this study, an LDH assay was used to better quantify platelet and other cell adhesion to surfaces of the implanted oxygen sensing catheters. LDH is a very important metabolic enzyme commonly found in blood cells and an LDH assay has already been used in determining the degree of platelet adhesion to surfaces *in vitro* [29, 34, 35]. The LDH content of a given cell is normally proportional to its size [29]. Table 3.1 lists the corresponding LDH assay results of the two specific pairs of sensors examined above. Not surprisingly, sensor B1 exhibited substantial LDH activity in the resulting lysate solution (37.4 mU) whereas sensor A1 showed significantly less LDH activity. Overall, a summary of LDH assay data for all 3-μm Cu^0 particle coated sensors (N=12) and their corresponding controls is provided in Table 3.1. As can be seen, the average amount of LDH activity on control sensors is nearly 10 times the levels found on the sensors fabricated with the polymer coating containing the 3-μm copper particles. These two data sets are statistically different at the 95% confidence interval (p = 0.022 with 22 degrees of freedom).

3.3.3.2. Cu^0 Nanoparticle Coated Sensors

Coatings with Cu^0 nanoparticles yielded similar results as those with 3-μm Cu^0 particles. Overall, three out of six control sensors developed mature blood clots on the surface while only one NO-generating sensor had surface clot. Figures 3.4-3 and 3.4-4 also show two typical pairs of nanoparticle-coated sensors. Sensors A3 and A4, the two NO-generating devices, both turned out to be relatively clean after 19 h of implantation.

Sensor Group	NO-generating (A)	Control (B)
A1 & B1	0.14	37.4
A2 & B2	1.67	0.11
3-μm particle (N=12)	2.97 ± 2.05	24.1 ± 20.9
A3 & B3	5.18	38.8
A4 & B4	5.32	4.07
Nanoparticle (N=6)	3.22 ± 2.54	25.3 ± 22.2

Table 3.1. LDH assay of surface clots for the 4 pairs of sensors examined in Figure 3.4, and the statistical results of LDH levels in the two groups.

Control sensor B4 was also free of blood clot. However, a mature clot that developed around control sensor B3 had completely engulfed the sensing tip. The LDH assay results for these two pairs of sensors, as well as the statistical analysis of the entire Cu^0 nanoparticle test group (N=6), are summarized in Table 3.1. Again, on average, the sensors coated with the polymer film containing the Cu^0 nanoparticles tend to have much lower LDH activity originating from their surfaces, suggesting that much less cell adhesion occurs for this group. The difference in LDH activities between NO-generating and control sensors in this category is also statistically significant ($p = 0.013$). The LDH assay results are not affected by the small amount of corroded copper that is present in the lysate solution. A control experiment with free LDH in the presence and absence of 1 μg/mL Cu^{2+} ions (much higher than the possible amount of leached copper during the 1 h incubation period, see **3.2**) showed the same LDH enzyme activities.

3.3.4. *In Vivo* O_2 Sensor Performance

3.3.4.1. 3-μm Cu^0 Particle Coated Sensors

The corresponding PO_2 levels determined by the two pairs of sensors from Figures 3.4-1 and 3.4-2, as well as the 'true values' obtained from *in vitro* blood gas analyzer measurements over 20 h of implantation, are shown in Figures 3.5-1 and 3.5-2. Implanted sensors are able to track closely with the PO_2 values measured by benchtop blood gas analyzer when their surfaces are not covered by blood clots, as were the cases for both NO-generating sensors in Figures 3.5-1 and 3.5-2, and the control sensor in Figure 3.5-2 (sensor B2). However, when blood clots develop over the sensor surfaces, the metabolism of cells within the clot consumes oxygen, rendering false-negative in the

PO_2 measured by such sensors. The extent of surface clot dictates the deviation from true values. As seen in Figure 3.5-1, sensor B1, which had a complete coverage of clot over the sensing tip started to show false-negative oxygen values 5 h into the experiment and eventually provided readings that were ~ 20% of the true PO_2 values. On the other hand, control sensor B2 in Figure 3.5-2, and both NO-generating sensors (A1 and A2) in Figures 3.5-1 and 3.5-2, which had clean surfaces, traced PO_2 levels quite accurately. Such variations in the analytical performance of control sensors reflect the biocompatibility issues usually encountered with intravascular sensors, with some sensors completely covered by blood clot while others remain relatively clean.

Figure 3.6-1 summarizes the *in vivo* analytical results for both NO-generating and control sensors (N = 12 each) in the 3-μm copper particle coated group. The average percent deviations (from the true values derived from benchtop blood gas machine) of O_2 levels determined by each set of implanted sensors, as well as their standard deviations, are plotted as a function of time. It is clear that the NO-generating sensors yield more accurate PO_2 results overall, with the percentage deviation ranging only from -12% to + 9% and the average values of PO_2 nicely straddling the true values throughout the experiment. The control sensors, however, consistently exhibited negative deviations greater than -20% from the 6 h point forward, with the largest average error being -42% at the 12 h time point.

Such lowered responses to O_2 correlated very well with the observed surface thrombosis on these control sensors. The standard deviations of the control set were also significantly larger than those in the NO-generating set. Table 3.2 lists the average percent deviation of NO-generating and control sensors at 5, 10, 15 and 20 h time points

as well as their 95% confidence intervals. The difference between the measurements made by NO-generating sensors and those derived from benchtop blood gas machine (considered 100% accurate) was not statistically significant at any time point during the experiment. In contrast, the control sensors showed statistically significant differences (at 95% confidence) at the 15 and 20 h time points when compared to *in vitro* blood gas results. Indeed, the control sensor results were statistically different from blood gas values from 11 h onwards. Moreover, the PO_2 values measured by control sensors were statistically different from that measured via NO-generating sensor at 95% confidence level ($t = 2.31$, $p = 0.031$ with 22 degrees of freedom) at the final 20 h time point.

Although the majority of NO-generating sensors remained thrombus-free after explantation and most control sensors were covered with blood clots, the small fraction of clotted NO-generating sensors and thrombus-free control sensors significantly impacted the PO_2 measurements made within the respective category. For the sake of clarity, such 'abnormal' sensors were excluded from the 3-μm group and the PO_2 outputs from the remaining truly thrombus-free NO-generating sensors and clotted control sensors (N=9 each) are plotted in Figure 3.7. It can be seen that the standard deviations of each type of sensors were narrowed and the average PO_2 values reported by the control sensors were even lower. Indeed, at each hour after the 5 h time point, the average PO_2 levels reported by the NO-generating sensors vs. controls were statistically different at 99% confidence interval ($t \geq 3.67$, $p \leq 0.0021$ with 16 degrees of freedom).

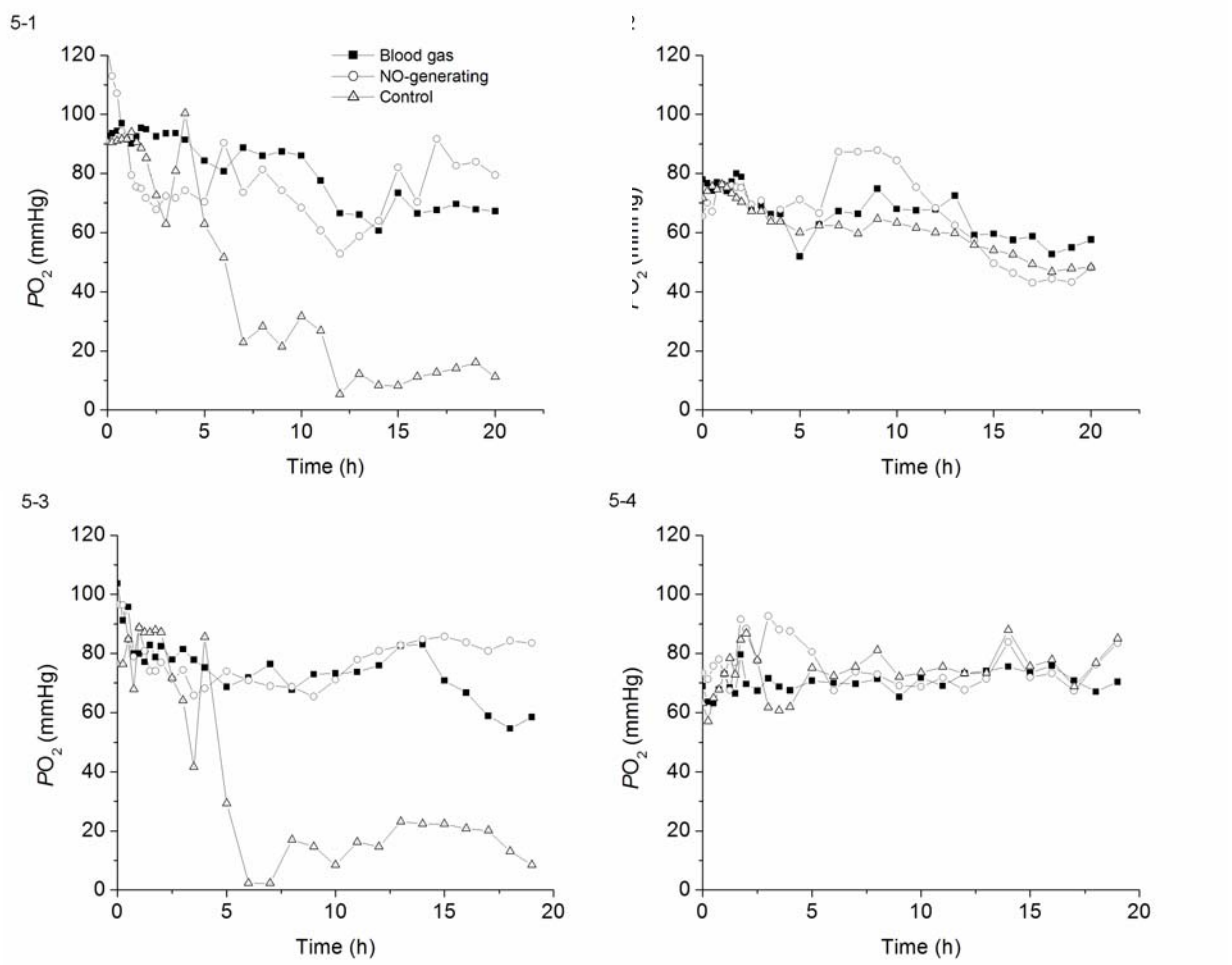

Figure 3.5. The PO_2 values measured by the same four pairs of NO-generating and control sensor shown in Fig. 3.4 as compared to the standard blood gas analyzer results for each experiment. (5-1) sensors A1 & B1; (5-2) sensors A2 & B2; (5-3) sensors A3 & B3, and (5-4) sensors A4 & B4

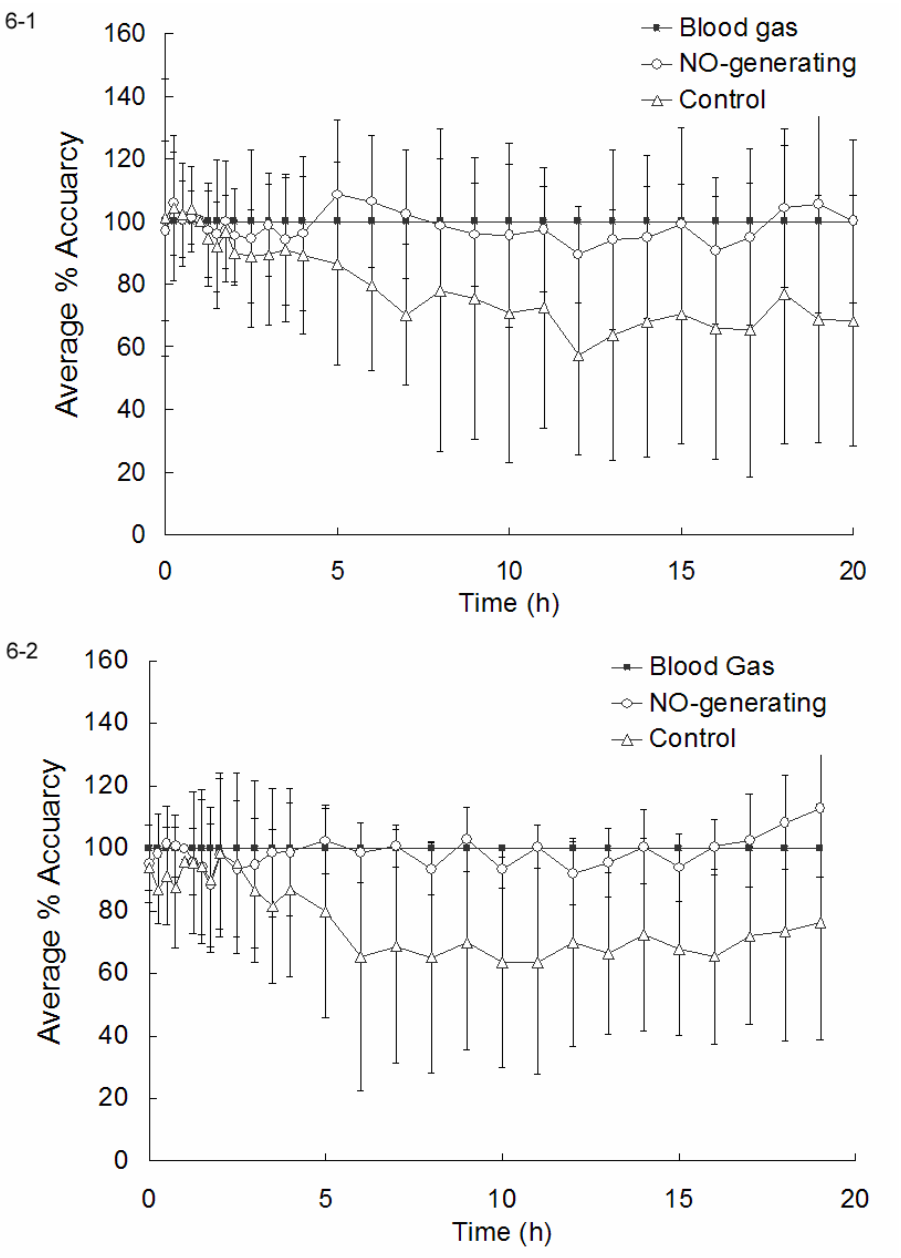

Figure 3.6. Plots of the average percent accuracy of: (1) NO-generating sensors based on 3-μm Cu^0 particles and control sensors (N = 12 each), and (2) NO-generating sensors based on 80 nm Cu^0 particles and control sensors (N = 6 each), as compared to *in vitro* blood gas analyzer results, which were considered 100% accurate.

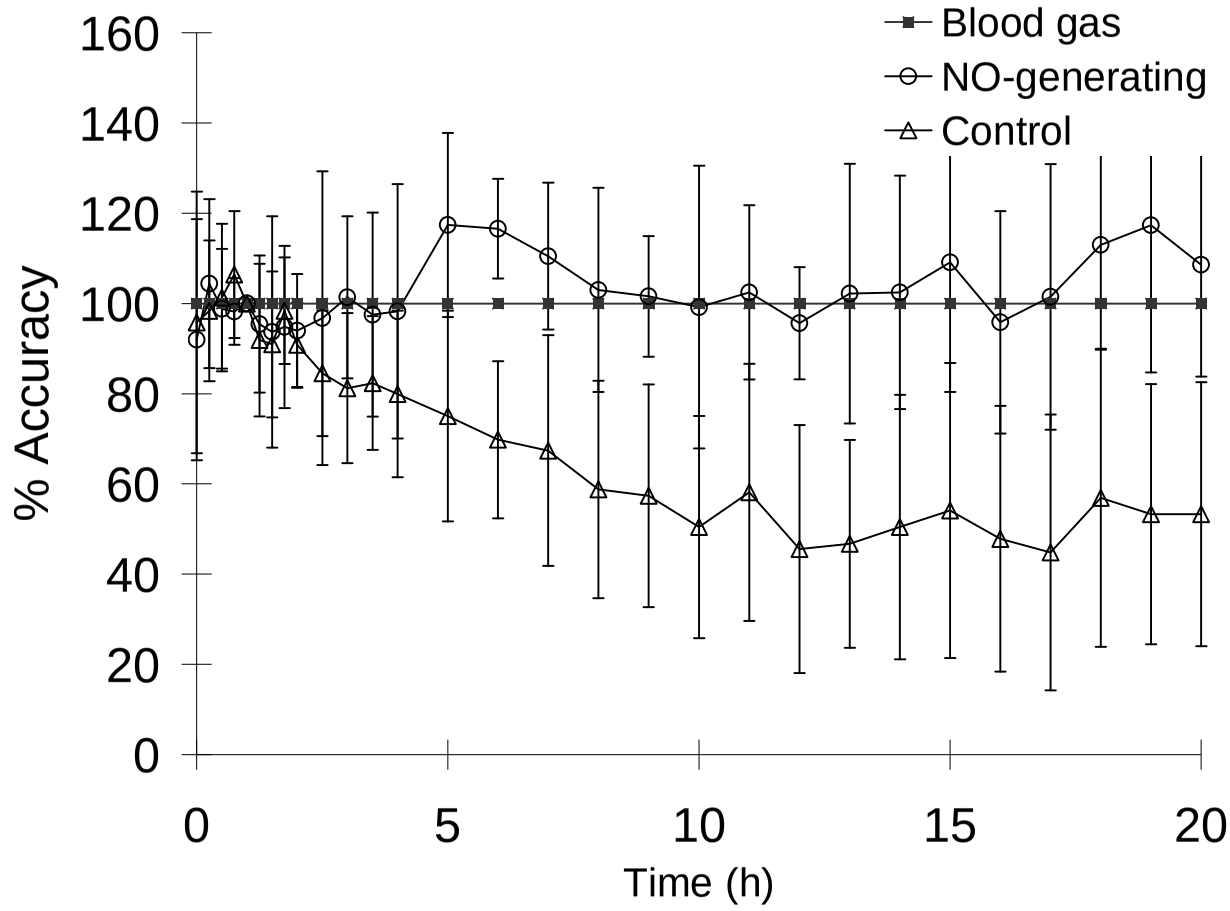

Figure 3.7. Plot of the average percent accuracy of thrombus-free NO–γενερατινγ σενσορσ ανδ χλοττεδ χοντρολ σενσορσ ιν τηε 3–μm Cu^0 particles group (N = 9 each),

Time (h)	NO-generating sensors		Control sensors	
	Avg. % deviation	95% Conf. interval	Avg. % deviation	95% conf. interval
5	+ 8.6	± 15.1%	-13.6	± 20.6%
10	- 4.4	± 18.6%	-29.3	± 30.3%
15	- 0.8	± 19.5%	-29.6	± 26.4%
20	+ 0.2	± 16.6%	-31.7	± 25.4%

Table 3.2. Average percent deviation and the 95% confidence intervals for PO_2 measurements made by sensors in the 3 μm particle group.

3.3.4.2. Cu^0 Nanoparticle Coated Sensors

PO_2 values recorded from the same two pairs of Cu^0 nanoparticle coated sensors shown in Figures 3.4-3 and 3.4-4 are illustrated in Figures 3.5-3 and 3.5-4. The results are quite similar to those observed with the 3-μm Cu^0 particle coatings. Sensors with little or no blood clots (i.e., sensors A3, A4 and B4) traced well with corresponding *in vitro* blood gas measurements. In contrast, sensor B3, a control sensor, which was completely covered by clot, yielded significantly lower PO_2 values from the 5 h point forward and actually reported values of oxygen that were near zero.

Figure 3.6-2 provides a summary of the *in vivo* oxygen sensing data obtained from the six pairs of sensors coated with the copper nanoparticle layer. Again, NO-generation via the presence of the Cu^0 nanoparticle catalyst provides more accurate *in vivo* measurements of PO_2 throughout the 19 h implantation period. The average percent deviation from *in vitro* blood gas readings ranged from -11% to +12%. Control sensors show considerable (> 20%) false negatives after 5 h into the experiment, with average PO_2 values deviating up to -36% at 10 h. Like the control group of 3-μm Cu^0 particles, greater standard deviations were also observed in the nanoparticle control sensor group. The average percent deviation at 5, 10, 15 h and the 95% confidence interval of measurements derived from each group are listed in Table 3.3. Statistical analysis of the data shown in Table 3.3 for the nanoparticle coated sensors indicates that the NO-generating sensors accurately traced PO_2 levels at the 95% confidence interval level (no statistically significant deviations from *in vitro* values), but the control sensor measurements did not agree with the true values at the same confidence interval from the 10 h point forward.

Time (h)	NO-generating sensors		Control sensors	
	Avg. % deviation	95% Conf. interval	Avg. % deviation	95% conf. Interval
5	+ 2.4	± 10.9%	-20.2	± 35.6%
10	- 6.5	± 6.6%	-36.5	± 35.3%
15	- 6.1	± 11.4%	-32.2	± 28.8%

Table 3.3. Average percent deviation and the 95% confidence intervals for PO_2 measurements made by sensors in the nanoparticle group.

3.4. Summary

Copper particle-based polymer coatings capable of generating physiological levels of NO in the presence of endogenous RSNO species have been applied to the surface of intravascular electrochemical oxygen sensing catheters. These sensors, when tested *in vivo* via a porcine artery model, exhibit improved blood-compatibility over the control sensors as evidenced by less propensity toward surface thrombus formation and more accurate analytical results. Three out of 12 NO-generating sensors in the 3-μm particle group, and 1 out of 6 NO-generating sensors in the nanoparticle group showed some degree of blood clot on the surfaces. This might be the result of low RSNO levels in these animals and hence NO levels generated were not sufficient to completely suppress thrombus formation. It should also be noted that the surfaces of NO-generating sensors were not as smooth as those of the control sensors, especially for the larger copper particles, which is a disadvantage in terms of preventing clot formation. However, there is still a statistical difference between the two groups of sensors. At 95% confidence level, the NO-generating sensors agreed very well with *in vitro* blood gas measurements with no statistically significant differences throughout the experiment. On the other hand, control sensors results were statistically different from *in vitro* blood gas measurements after about 10 h implantation.

The control sensor behavior found in this work is representative of intravascular sensing devices developed thus far, which explains their limited use in real clinical applications. The NO-generation strategy offers a potential solution to this problem and may find use in other blood-contacting devices as well. Ongoing research in this group is

focusing on covalently linking various species to polymers that can provide the same NO-generation capability as the copper particles used here. New polymers containing immobilized organoselenium species [36] appear most promising as new NO generating materials for such implantable sensor applications.

3.5. References

[1] M. C. Frost and M. E. Meyerhoff, *Curr. Opin. Chem. Biol.*, 6 (2002) 633-641.

[2] C. K. Mahutte, *Clin. Biochem.*, 31 (1998) 119-130.

[3] M. E. Meyerhoff, *Trends Anal. Chem.,* 12 (1993) 257-266.

[4] E. Fogt, *Clin. Chem.*, 36 (1990) 1573-1580.

[5] J. D. Andrade and V. Hlady, *Adv. Polym. Sci.*, 79 (1986) 1-63.

[6] T. A. Horbett, in *Biomaterials Science - An Introduction to Materials in Medicine*, B. D. Ratner, A. S. Hoffman, F. J. Schoen, and J. E. Lemons, Eds., 2nd ed. San Diego, CA: Elsevier Academic Press, 2004, pp. 237-246.

[7] S. R. Hanson, in *Biomaterials Science - An Introduction to Materials in Medicine.*, B. D. Ratner, A. S. Hoffman, F. J. Schoen, and J. E. Lemons, Eds., 2nd ed. San Diego, CA: Elsevier Academic Press, 2004, pp. 332-338.

[8] T. Lisman, C. Weeterings, and P. G. de Groot, *Front. Biosci.,* 10 2005) 2504-2517.

[9] J. W. M. Heemskerk, E. M. Bevers, and T. Lindhout, *Thromb. Haemost.,* 88 (2002) 186-193.

[10] J. G. Diodati, A. A. Quyyumi, N. Hussain, and L. K. Keefer, *Thromb. Haemost.*, 70 (1993) 654-658.

[11] L. J. Ignarro, G. M. Buga, K. S. Wood, R. E. Byrns, and G. Chaudhuri, *Proc. Natl. Acad. Sci. USA,* 84 (1987) 9265-9269.

[12] M. Radomski, R. Palmer, and S. Moncada, *Proc. Natl. Acad. Sci. USA,* 87 (1990) 5193-5197.

[13] P. L. Feldman, O. W. Griffith, and D. J. Stuehr, *Chem. Eng. News*, 71 (1993) 26-38.

[14] M. W. Radomski, P. Vallance, G. Whitley, N. Foxwell, and S. Moncada, *Cardiovasc. Res.,* 27 (1993) 1380-1382.

[15] C. Michiels, *J. Cell. Physiol.*, 196 (2003) 430-443.

[16] M. W. Vaughn, L. Kuo, and J. C. Liao, *Am. J. Physiol. (Heart Circ. Physiol.),* 43 (1998) H2163-H2176.

[17] M. H. Schoenfisch, K. A. Mowery, M. V. Rader, N. Baliga, J. A. Wahr, and M. E. Meyerhoff, *Anal. Chem.,* 72 (2000) 1119-1126.

[18] H. P. Zhang, G. M. Annich, J. Miskulin, K. Osterholzer, S. I. Merz, R. H. Bartlett, and M. E. Meyerhoff, *Biomaterials*, 23 (2002) 1485-1494.

[19] M. C. Frost, S. M. Rudich, H. P. Zhang, M. A. Maraschio, and M. E. Meyerhoff, *Anal. Chem.*, 74 (2002) 5942-5947.

[20] K. Wong and X. B. Li, *Transfus. Apheresis Sci.,* 30 (2004) 29-39.

[21] J. P. Wallis, *Transfus. Med.,* 15 (2005) 1-11.

[22] J. S. Stamler, O. Jaraki, J. Osborne, D. I. Simon, J. Keaney, J. Vita, D. Singel, C. R. Valeri, and J. Loscalzo, *Proc. Natl. Acad. Sci.USA*, 89 (1992) 7674-7677.

[23] D. Giustarini, A. Milzani, R. Colombo, I. Dalle-Donne, and R. Rossi, "Nitric oxide and S-nitrosothiols in human blood," *Clin. Chim. Acta*, 330 (2003) 85-98.

[24] D. Jourd'heuil, K. Hallen, M. Feelisch, and M. B. Grisham, "Dynamic state of S-nitrosothiols in human plasma and whole blood," *Free Rad. Biol. Med.*, 28 (2000) 409-417.

[25] D. L. H. Williams, *Acc. Chem. Res.*, 32 (1999) 869-876.

[26] B. K. Oh and M. E. Meyerhoff, *J. Am. Chem. Soc.,* 125 (2003) 9552-9553.

[27] S. Hwang, W. Cha, and M. E. Meyerhoff, *Angew. Chem.*, 118 (2006) 2811-2814.

[28] A. J. Brenner and E. D. Harris, *Anal. Biochem.*, 226 (1995) 80-84.

[29] Y. Tamada, E. A. Kulik, and Y. Ikada, *Biomaterials*, 16 (1995) 259-261.

[30] K. G. Daniel, R. H. Harbach, W. C. Guida, and Q. P. Dou, *Front. Biosci.*, 9 (2004) 2652-2662.

[31] G. Clarotti, F. Schue, J. Sledz, A. A. B. Aoumar, K. E. Geckeler, A. Orsetti, and G. Paleirac, *Biomaterials*, 13 (1992) 832-840.

[32] H. Tapiero, D. M. Townsend, and K. D. Tew, *Biomed. Pharmacother.,* 57 (2003) 386-398.

[33] J. G. White, in *Methods in Molecular Biology (Platelets and Megakaryocytes)*, vol. 272, J. M. Gibbins and M. P. Mahaut-Smith, Eds. Totowa, NJ: Humana Press, 2004, 47-63.

[34] W. B. Tsai, J. M. Grunkemeier, and T. A. Horbett, *J. Biomed. Mater. Res.*, 44 (1999) 130-139.

[35] L. J. Suggs, J. L. West, and A. G. Mikos, *Biomaterials*, 20 (1999) 683-690.

[36] W. Cha and M. E. Meyerhoff, *Biomaterials*, 28 (2007) 19-27.

CHAPTER 4

FURTHER STUDIES AND BIOMEDICAL APPLICATIONS OF AMPEROMETRIC *S*-NITROSOTHIOL SENSORS BASED ON IMMOBILIZED ORGANOSELENIUM CATALYST

4.1. Introduction

S-Nitrosothiols (RSNOs) play important roles in the storage, transport and metabolism of nitric oxide (NO) [1]. The physiological properties of RSNOs are similar to those of NO in terms of vasodilation [2, 3] and inhibition of platelet activation and aggregation [3, 4]. Endogenous RSNO formation may occur through the reaction between cysteinyl residues on peptides/proteins and the reactive intermediates of NO (e.g., NO^+, $ONOO^-$) [5, 6]. Such oxidative intermediates of NO can also react with low molecular weight thiols (cysteine, glutathione, etc.) to form corresponding *S*-nitrosothiols (see Figure 4.1). The *S*-nitrosation of thiols *in vivo* is a reversible process. Therefore, transnitrosation can occur in which the nitroso- group is transferred from one *S*-nitrosothiol to another thiol through the nucleophillic attack of the thiolate anion on the nitrogen atom of the *S*-nitrosothiol [7, 8]. Although the biological lifetime of RSNOs is substantially longer than that of the free radical NO [9], they are still relatively labile and are subject to thermal-, photo- and trace metal ions (e.g., Cu^+, Fe^{2+}) induced decomposition [10]. Indeed, the antiplatelet and vasodilating functions of RSNO are

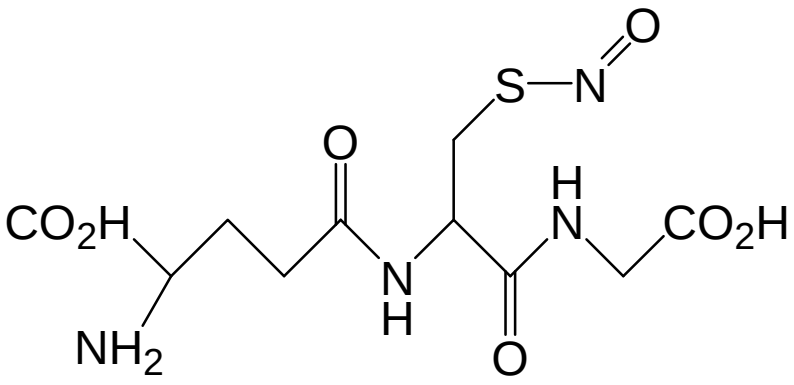

S-Nitrosoglutathione (GSNO)

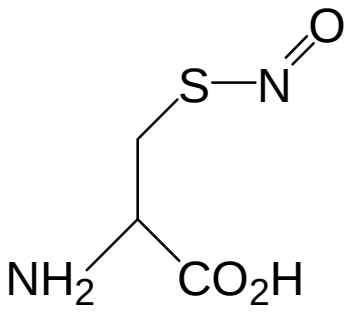

S-Nitrosocysteine (CysNO)

Figure 4.1. Structures of representative endogenous LMW RSNOs

thought to be mediated by cellular surface proteins which can decompose RSNO to yield NO *in vivo* [11-13]. Recently, it has also been discovered that organoselenium compounds and proteins that contain selenocysteine moieties, such as glutathione peroxidase (GPx), are also capable of decomposing RSNOs [14]. Not surprisingly, GPx has also been found to inhibit platelet activation [15].

In addition, RSNOs have been suggested as a potential biological marker for endothelial function [16]. Kelm and co-workers assessed the endothelial function of healthy volunteers and patients with cardiovascular risk factors (e.g., hypertension, hypercholesterolemia, smoking, or diabetes) by flow-mediated dilation and measured the concentrations of total plasma nitroso-compounds (RXNO: the sum of *S*-nitrosothiols, *N*-nitrosamines, and iron-nitrosyl species) from all human subjects [17]. It was found that endothelial dysfunction is associated with the depletion of nitroso-/nitrosyl- species in plasma, which is likely to contribute to the increased risk of major cardiovascular events such as heart attack, stroke and thrombosis.

As a result of the growing interests in the physiological and pharmacological importance of RSNOs, numerous approaches have been devised to determine the level of RSNOs in biological fluids, including colorimetric [18], fluorometric [18-20], chemiluminescent [21, 22], and 'biotin-switch' assays [23]. The coupling of the above detection techniques with high-pressure liquid chromatography has also been employed by many researchers to study biological RSNO concentrations [8, 24, 25]. However, these techniques are not capable of direct measurements of RSNOs in biological samples. Rather, complex sample pre-treatments are required and the detected signals originate from the reactions between the decomposition products of RSNO and the added

reagent(s). For example, $HgCl_2$ cleavage of RSNOs yields nitrite in the presence of oxygen, which can either be quantified colorimetrically via the Griess assay or fluorometrically after the reaction with 2,3-diaminonaphthalene [18] or 4,5-diaminofluorescein [20]. Reductive chemiluminescence, which detects NO instead of RSNO, requires the conversion of RSNO to NO by reduction (e.g., triiodide or Cu(I)/Cysteine) prior to analysis. In addition, the popular triiodide chemiluminescence assay requires three separate measurements of the plasma samples in order to obtain RSNO concentration data [26]. Due to the intrinsic instability of RSNO species and the artifacts that may be introduced during the pre-treatment steps [27, 28], such as the contribution from endogenous NO/NO_2^-, or the decomposition of RSNO before analysis by reacting with trace metal ions, these methodologies yield highly variable values of RSNO concentrations in biological fluids. A recent review by Giustarini et al. summarized the reported normal levels of RSNOs in human and animal plasma, which range from 20 nM to 7 μM [29]. Further, since blood must be spun down to remove red cells for all existing measurement techniques, even a low level of hemolysis can create free oxyhemglobin in the plasma that can scavenge NO liberated from the RSNO species prior to NO detection [30]. For these reasons, while measurement of total RSNO levels may be a good biomarker for endothelial function testing (as well as thrombotic risk assessment due to their inherent anti-platelet activity), methods must be devised to determine total RSNO levels in the plasma of whole blood samples freshly drawn from the patient without time delay or pretreatment steps.

Electrochemical sensors have already been employed to determine NO concentrations in various media, including biological fluids [31-34]. Cha et al. recently

reported an amperometric RSNO sensor based on a modified amperometric NO sensor with immobilized organoselenium catalyst (e.g., RSePEI, 3,3'-dipropionic acid diselenide (SeDPA) crosslinked onto polyethylenimine backbones) behind a dialysis membrane (see Figure 1.3) [35]. Such an RSNO sensor offers a potentially convenient approach to quantify total RSNO concentrations in blood without prior separation. Indeed, in principle, blood can be analyzed for RSNO content immediately at the bedside without any sample pretreatments. In contrast to a previously described Cu-catalyst based RSNO sensor [36], the major advantage of the Se-catalyst based sensor is the nearly equal sensitivity towards all low molecular weight (LMW) RSNO species (e.g., *S*-nitrosoglutathione (GSNO), *S*-nitrosocysteine (CysNO)), thus making it more appropriate to assess the 'global' concentration of LMW RSNO species in biological samples. In this chapter, further characterization of this new RSNO sensor with respect to response towards macromolecular RSNOs (e.g., *S*-nitrosoalbumin, AlbSNO), and effect of hemoglobin levels on samples are discussed. In addition, the first application of the sensor to assess RSNO levels in samples of whole rabbit and pig blood is described.

4.2. Materials and Methods

4.2.1 Materials

Microporous poly(tetrafluoroethylene) (PTFE) membranes (Tetratex, pore size 0.07 μm, thickness ~18 μm) were obtained from Donalson Co., Inc. (Minneapolis, MN). Dialysis membranes (Spectra/Por 7, MW cutoff = 50 kDa) were purchased from Spectrum Laboratories Inc. (Rancho Dominguez, CA). Polyethylenimine (PEI, avg. Mw

760 kDa), cysteine, glutathione (GSH), bovine serum albumin (BSA), 1,4-dithiothreitol (DTT), ethylenediamine tetraacetic acid (EDTA), glutaraldehyde (25 wt% solution), *N*-(3-dimethylaminopropyl)-*N*'-ethylcarbodiimide hydrochloride (EDC), *N*-hydroxylsuccinimide (NHS), sodium borohydride, and sodium nitrite were products of Sigma-Aldrich (St. Louis, MO) and were used as received. 3,3'-Dipropionic acid diselenide (SeDPA) was synthesized as described in the literature [37]. Phosphate-buffered saline (PBS, 138 mM sodium chloride, 2.7 mM potassium chloride, 10 mM sodium phosphate, pH 7.4), as well as all other solutions used in this work, were prepared in the laboratory from Milli-Q grade deionized water (18.2 MΩ, Millipore Corp., Billerica, MA).

4.2.2. Preparation of *S*-Nitrosothiols

Solutions of *S*-nitrosocysteine and *S*-nitrosoglutathione (5 mM of each) were prepared by reacting the corresponding thiols with acidified $NaNO_2$ according to a previously described procedure [38]. *S*-Nitrosoalbumin was synthesized by first reducing BSA with DTT before the reaction with acidified $NaNO_2$ [39]. The RSNO solutions were kept in dark and used within 4 h of preparation.

4.2.3. Fabrication of Amperometric NO/RSNO Sensors

The organoselenium-containing PEI catalyst (RSePEI) was synthesized by coupling PEI to activated SeDPA via the EDC/NHS chemistry, and the resulting RSePEI was then crosslinked onto a dialysis membrane with glutaraldehyde. The detailed procedure has been described elsewhere [39]. Sensors used in this study were the

miniaturized version of the previously reported design [35]. Briefly, Pt/Ir wire (10Ir7T, 0.18 mm diameter, Medwire, Mt. Vernon, NY) without PTFE coating was sealed in a glass capillary and further platinized to form the working electrode. The Ag/AgCl reference electrode was made from Ag wire (Ag3T, Medwire, with the Teflon coating stripped off) immersed in 100 mM phosphate buffer (pH 4.4) containing 50 mM NaCl and 0.005% Methocel 90 HG (Fluka, Buchs, Switzerland) as the internal solution. The gas-permeable microporous PTFE membrane was treated with 0.5 μLTeflon-AF (DuPont Fluoroproducts, Wilmington, DE) and mounted on the sensor body made from a 200 μL micropipette tip. To prepare the catalytic membrane, 3 wt% of the RSePEI solution was mixed at a 1:1 ratio with 1 wt% of glutaraldehyde, and 10 μL of this mixed catalyst solution was applied onto a dialysis membrane of ca. 0.5 cm^2 in size. In the RSNO sensor, the RSePEI immobilized dialysis membrane was attached to the outside of the gas-permeable membrane with an O-ring, with the RSePEI hydrogel layer trapped between the dialysis membrane and PTFE gas-permeable membrane of the NO sensor. For the NO sensor, a blank dialysis membrane without the immobilized catalyst was used to assemble the device. Both sensors were polarized at + 0.75 V vs. Ag/AgCl overnight prior to use. All subsequent calibrations and measurements were performed at the same applied potential.

4.2.4. NO and RSNO Sensor Calibrations

Amperometric measurements were performed using Diamond Electro-Tech electrochemical analyzers (Ann Arbor, MI) interfaced with a Dataq DI-158U analog/digital data acquisition device (Dataq Instruments, Akron, OH). The NO and

RSNO sensors were both placed in a home-made amber glass cell (25 mL capacity) containing 10 mL PBS with 0.5 mM EDTA. The solution was deoxygenated with N_2 and the temperature was maintained at 34 ºC throughout the experiment. During the NO calibration, small aliquots of saturated NO solution (contains 1.9 mM NO at room temperature) were injected into the buffer under a N_2 atmosphere and the responses from both sensors were simultaneously recorded by the WINDAQ software (Dataq Instruments). RSNO calibration was performed under N_2 bubbling by injecting GSNO into the same buffer with 100 μM of GSH present as the reducing agent.

4.2.5. Detection of Macromolecular RSNOs

S-Nitrosoalbumin (AlbSNO) was prepared from reduced BSA and acidified $NaNO_2$ following a reported procedure [39]. The AlbSNO concentration was determined via a chemiluminescence Cu(I)/cysteine assay [40]. In the electrochemical measurement, the same dual sensor configuration as in NO/RSNO calibration was adapted. A certain amount of AlbSNO was injected into 10 mL PBS buffer containing 0.5 mM EDTA and 100 μM reducing agent (i.e., GSH or cysteine). The amperometric responses to each injection of AlbSNO were recorded and later converted to LMW RSNO equivalents based on previous calibrations with the LMW RSNOs that correspond to the given reducing agent used in the experiment.

4.2.6. Matrix Effects in Physiological Fluids

4.2.6.1. RSNO Sensitivity in Diluted Plasma

Rabbit plasma was obtained by centrifuging heparinized rabbit whole blood at 110 ×*g*. Five mL of the plasma was diluted into 10 mL PBS with 1.5 μmole GSH and 7.5 μmole EDTA (yielding final GSH concentration of 100 μM and EDTA concentration of 0.5 mM). GSNO calibration was performed using the same protocol described in the RSNO calibration section and was compared with the results obtained from buffer only.

4.2.6.2. Free Hemoglobin Effect

The red blood cell concentrate from plasma separation was lysed in a 1:4 dilution with 10 mM EDTA as previously reported [41] and centrifuged at 1300 ×*g* to remove membrane fragments. The concentration of free oxyhemoglobin was determined from UV-Vis by the method reported by Benesh et al [42]. For GSNO calibration, 15 mg/dL oxyhemoglobin was added in addition to all other reagents used in the aforementioned GSNO calibration procedure to simulate the typical level of plasma free hemoglobin.

4.2.7. Photo-Decomposition of Blood RSNO

The dual-sensor configuration was also employed for whole blood RSNO measurements. Ten mL of deoxygenated PBS containing 1.5 μmole GSH and 7.5 μmole EDTA was equilibrated at 34 ºC under a N_2 atmosphere prior to blood injection until a steady baseline amperometric signal was achieved for both sensors. Blood samples from pigs were collected by venipuncture in the abdomen via a butterfly needle (23G, Abbott, North Chicago, IL) into a 5 mL heparinized syringe (5 U/cc final heparin) wrapped in Al foil. To evaluate the effect of light exposure on the stability of RSNO species in blood**,** another blood sample was drawn from the same animal with the 1 ft long butterfly tube

wrapped in Al foil as well. Both samples were collected fresh and injected into the PBS buffer within 3 min. Taking the blood dilution into account, the final concentrations of GSH and EDTA were equal to that previously used in the GSNO calibration (i.e., 100 μM GSH and 0.5 mM EDTA). After the amperometric responses from both sensors reached steady-state, an aliquot from the 5 mM GSNO stock solution was added to the diluted blood to raise the GSNO concentration by 1 μM. This standard addition method is used to calibrate the RSNO sensor in blood [43].

4.2.8. RSNO Determination in Rabbit Blood

New Zealand White rabbits (2.5-3.2 kg body weight) were used in this study. A 5 mL of blood sample was drawn from rabbit carotid artery into a syringe with 5 U/mL sodium heparin (Baxter, Deerfield, IL). To avoid potential loss of blood RSNO due to photo-decomposition, the blood sample was protected from light using aluminum foil covered syringe and immediately analyzed according to the procedure described above for pig blood RSNO determinations. After the amperometric responses from both sensors reached steady state, the standard GSNO addition method was used to calculate the blood RSNO concentrations.

4.2.9. Monitoring RSNO Levels in Rabbits under Extracorporeal Circulation

The above blood RSNO determination was part of a biocompatibility study involving rabbits hooked to NO-generating extracorporeal circulation (ECC) loops (i.e., loops coated with plasticized PVC containing Cu-DTTCT catalyst) in an arterial/venous shunt model connecting the rabbit's carotid artery and jugular vein. The design and

biocompatibility evaluation of the NO-releasing version of the extracorporeal circuits based on DBHD/N_2O_2 has been described in detail previously [44]. In this study, rabbits under anesthesia were randomly assigned into three different categories: rabbits in Group I were hooked to Cu-based NO-generating ECC loops; in Group II, rabbits were hooked to control ECC loops that did not generate NO; the rabbits in Group III were just placed under anesthesia without ECC loops attached. The baseline RSNO levels in all the rabbits, as well as the RSNO levels one hour after the surgical implantation of the ECC loops (or no loop as in Group III), were measured by the RSNO sensor following the procedure described above.

4.2.10. RSNO Measurements for Pig Blood

The RSNO concentrations were also measured in porcine blood. The pigs used in these experiments were implanted with NO-generating (i.e., Cu-DTTCT-containing polymer coated) or control vascular grafts. In each animal, either two NO-generating or two control grafts were implanted between the femoral artery and vein. The RSNO levels in arterial and venous blood were measured before and after the graft surgery following the same protocol used for the rabbit blood experiments described above. In a follow-up study, the blood RSNO concentration was monitored periodically for up to 3 weeks after surgery by obtaining blood samples from the jugular veins. The samples were freshly collected and measured within 3 min following the same procedure used to assess rabbit blood.

4.3. Results and Discussion

4.3.1. Sensitivity Towards NO and RSNO

The RSNO sensor shown in Figure 1.3 is actually a modified NO sensor with an additional catalytic surface layer capable of decomposing RSNO to yield NO. Therefore both, sensors exhibit amperometric responses toward the added NO standard as shown in Figure 4.2a. The NO sensor was more sensitive towards NO compared with the RSNO sensor as it lacks the extra diffusion barrier imposed by the crosslinked RSePEI hydrogel layer. However, upon addition of GSNO, only the RSNO sensor exhibits substantial amperometric response (see Figure 4.2b). The RSNO sensor's response to GSNO is totally reversible as the amperometric signal quickly returns to its original baseline when the GSNO solution is replaced by blank buffer. During the RSNO calibration, a reducing agent such as GSH is necessary to produce the surface RSeH species needed to decompose RSNO [39], and the concentration of this reducing agent has been optimized in this study for the best RSNO sensitivity. EDTA is also added to chelate any trace metal ion contaminants (e.g., Cu^{2+} or Fe^{2+}) that might otherwise decompose RSNO in the presence of GSH. As shown in Figure 4.2b, the NO sensor exhibits only slight increase in signal during the GSNO calibration. This indicates that without the RSePEI catalyst, the self-decomposition of the RSNO species in the bulk solution is minimal. The small current response from the NO sensor might come from the NO generated at the distal tip of the RSNO sensor (i.e., diffusion into the bulk solution from catalytic layer). However, such 'cross-talk' between the two sensors is eliminated in actual blood measurements as the blood sample contains oxyhemoglobin, a very efficient scavenger of NO. Such

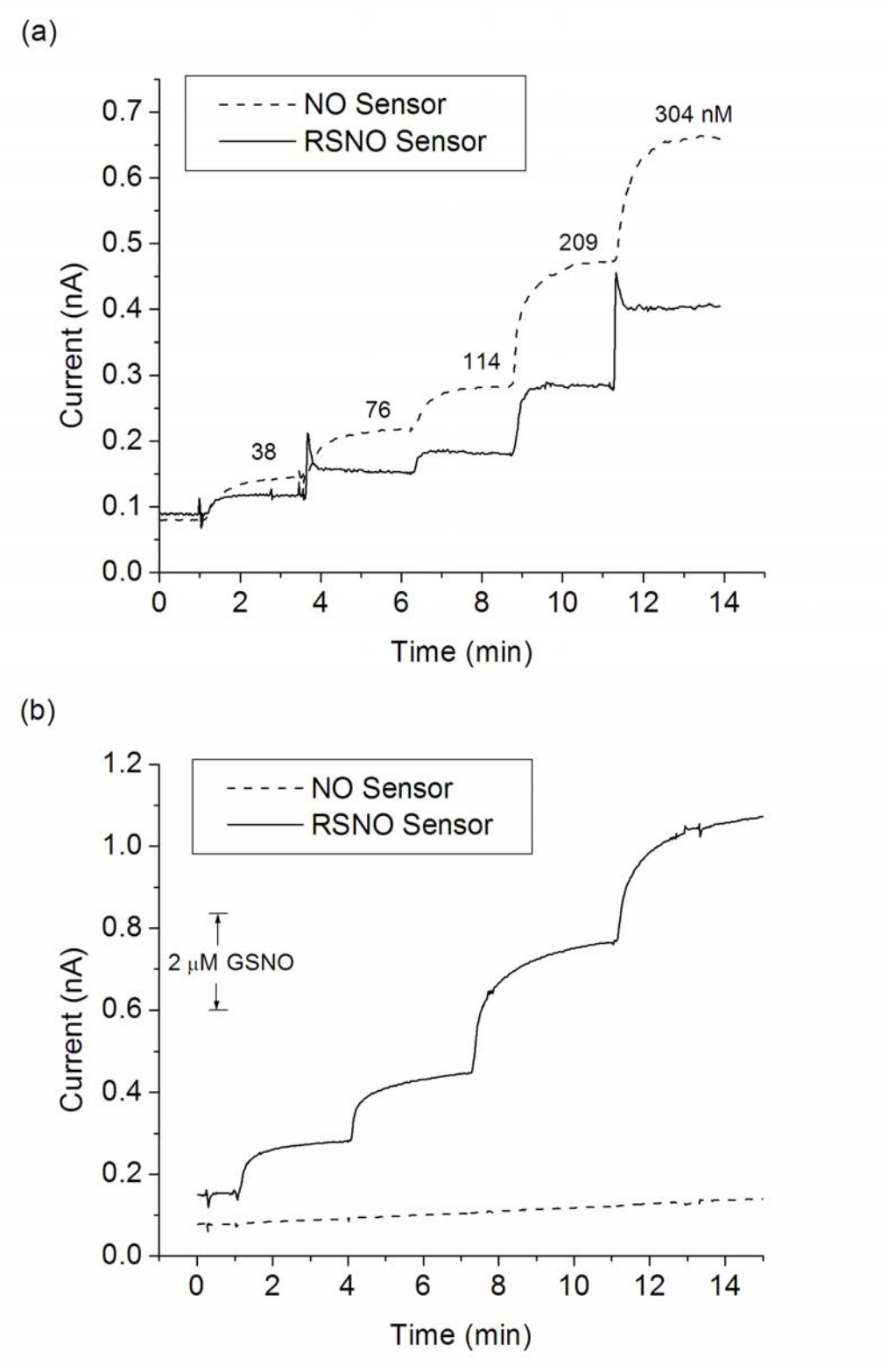

Figure 4.2. Calibration curves of the RSNO and NO sensor for (a) NO in PBS buffer, and (b) GSNO in PBS buffer containing 100 μM GSH and 0.5 mM EDTA.

attributes are essential for the dual sensor set-up to reliably detect RSNOs in biological samples. Unlike the previously reported Cu-based RSNO sensor [36], a significant improvement of the RSe-based RSNO sensor is its nearly equal sensitivity towards most LMW RSNOs encountered in blood [35], thus making it suitable to assess the overall concentration of all LMW RSNO species (e.g., GSNO, CysNO, etc.) present in blood.

The RSe-catalyzed RSNO decomposition requires the presence of a reducing agent such as GSH or cysteine. Therefore, the magnitude of RSNO sensor response to a given RSNO species depends not only on the RSNO concentration, but also on the type and concentration of reducing agent used. The amperometric response of the RSNO sensor towards a given concentration of RSNO increases as more reducing agent is present. However, results suggest (data not shown) that when the GSH concentration is > 100 μM, the RSNO sensor's sensitivity towards RSNO is not further enhanced by increasing concentrations of GSH. Therefore, 100 μM GSH is used in both sensor calibration and actual blood measurement to provide sufficient reducing equivalents for RSNO decomposition and to eliminate the dependence of RSNO sensor signal on endogenous reducing agent concentrations in blood.

It should be noted that the GSNO calibration is not used to calculate the final blood RSNO concentrations. Rather it serves as indication of the proper functionality of the RSNO sensor. The GSNO and NO calibrations of RSNO sensor in buffer reveals a ca. 10-fold sensitivity difference with the RSNO sensor being more 'sensitive' to NO than GSNO (i.e., the RSNO sensor showed similar total amperometric response to 100 nM NO and 1 μM GSNO). The reason is that for the GSNO measurement, only a fraction of the NO generated by the RSe-catalyzed GSNO decomposition can diffuse to

the electrode surface to be detected by the NO-sensitive electrode of the RSNO sensor. Nevertheless, this fraction appears to be constant within the concentration range of interest, as evidenced by the linear range of the GSNO response.

As mentioned earlier, the amperometric responses of the RSNO sensor to various LMW RSNO species are similar when the same thiol species is used as the reducing agent (e.g., GSH or cysteine). However, it should be noted that the sensor signal is dependent on the type of reducing thiol used, with cysteine usually yielding higher current response compared to GSH to detect the same RSNO concentration. This is likely due to the smaller size of the cysteine molecule (vs. GSH), which diffuses more easily into the dialysis membrane and hence produces more reduced RSeH species within the RSePEI hydrogel layer for the decomposition of RSNO. However, the choice of reducing agent is unlikely to affect the RSNO measurements in blood, since the reducing agent is expected to affect the amperometric signals from endogenous RSNOs and added GSNO standard to a similar extent.

The current output of amperometric sensors is also dependent on temperature. Therefore, temperature control is critical for the accurate measurements of RSNO by the new electrochemical RSNO sensor. To minimize delay in blood measurements, the temperature of the diluent buffer and the blood sample should be the same. Thus the entire setup was thermostated at 34 ºC, a few degrees lower than the body temperature of animals, to adjust for the small temperature drop in the blood sample after it is drawn into the syringe. For the same reason, all calibrations were performed at this temperature as well.

4.3.2. AlbSNO Detection via Transnitrosation

Due to the molecular weight cut-off of the outer dialysis membrane (50 kDa), high molecular weight (HMW) RSNO species such as *S*-nitrosoalbumin (66 kDa) or *S*-nitrosohemoglobin (64 kDa) cannot diffuse through the membrane of the sensor to reach the crosslinked RSePEI hydrogel. Therefore, the current RSNO sensor design cannot directly measure HMW RSNOs. However, another mechanism known as transnitrosation exists where the nitroso group can be exchanged between an RSNO and a free thiol [45]. Although the transnitrosation process normally favors the formation of HMW RSNOs under physiological conditions [8], it is still possible to form a substantial amount of LMW RSNO by reacting HMW RSNO with excess (e.g., 100 μM) of LMW thiols (e.g., GSH or cysteine). In this case, the added GSH or cysteine acts as both a reducing agent to produce the needed RSeH surface catalyst and a transnitrosating agent to accept the nitrosonium ion (NO^+) to form the corresponding LMW RSNO. The transnitrosation efficiency is a function of the reducing agent concentration, but increasing GSH/cysteine concentrations can only improve the yield of LMW RSNOs to a limit. For example, 100 μM cysteine is the optimal concentration to obtain the maximum detectable current from the transnitrosation of AlbSNO. Higher (e.g., 200 or 500 μM) cysteine concentrations result in lower amounts of CysNO detected by the RSNO sensor. Since CysNO is much less stable compared to most LMW RSNOs (e.g., GSNO or *S*-nitroso-*N*-acetyl-penicillamine, SNAP), this is likely due to the auto-decomposition of CysNO in high concentrations of reducing agent [10].

The detection of AlbSNO in 100 μM cysteine yielded ~ 84% equivalent to the response of the same sensor to CysNO over a much longer period of time (i.e., 20-30

min, see Figure 4.3). The transnitrosation efficiency of 100 μM GSH was lower (c.a. 60%). This is probably because of the weaker reducing power of GSH and its larger size, resulting in slower diffusion through the dialysis membrane. As discussed earlier, the RSNO sensor response depends on the thiol species. Therefore, it is worth mentioning that the percentage of AlbSNO recovery reported herein is calculated on the basis of corresponding RSNO calibration using its parent thiol as the reducing equivalent (i.e., GSNO/GSH or CysNO/Cysteine). The prolonged response time towards AlbSNO compared to LMW RSNOs also suggests the involvement of a slow transnitrosation reaction, which must occur prior to the diffusion of RSNO through the outer dialysis membrane.

Although it takes much longer to reach the steady-state current in transnitrosation measurements, it is unlikely that the amperometric signal of the RSNO sensor in the presence of AlbSNO originates from the auto-decomposition of AlbSNO in the presence of free thiols. To check the background NO signal during transnitrosation, only the NO sensor was placed in a solution containing same concentrations of AlbSNO and cysteine. Over the same time window, less than 5% of NO equivalents to the added AlbSNO were detected by the NO sensor. This is further supported by the chemiluminescence NO measurement—only a negligible amount of NO (2-4 ppb) was detected when the same concentrations of AlbSNO, EDTA and reducing agent were mixed together in the absence of RSePEI catalyst.

4.3.3. Matrix Effects in Biological Fluids

4.3.3.1. Diluted Plasma

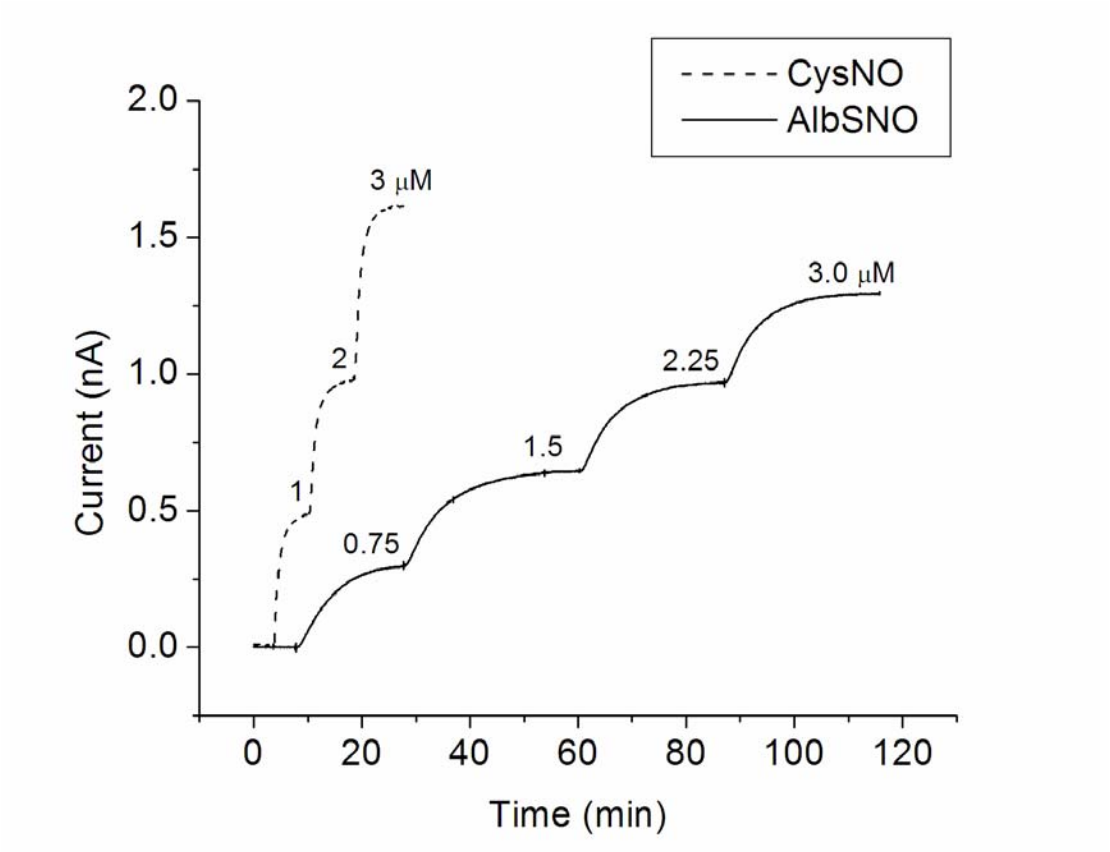

Figure 4.3. The responses of a RSNO sensor to CysNO and AlbSNO in PBS containing 100 μM cysteine and 0.5 mM EDTA.

The successful translation of calibrations performed in buffer to that in plasma is essential for the validation of RSNO measurements in blood. Towards this goal, the RSNO sensor response to GSNO was also evaluated in a 1:2 dilution of plasma into PBS (see Figure 4.4a). The presence of plasma did not affect the calibration towards LMW RSNO species. Therefore, it can be concluded that the non-specific adsorption of plasma proteins and platelets, if any, does not alter the diffusion of RSNOs and reducing agent to the RSePEI hydrogel layer behind the dialysis membrane.

4.3.3.2. Free Hemoglobin

It is well known that oxyhemoglobin is a potent scavenger of NO to yield methemoglobin and nitrate [46], and that deoxyhemoglobin acts as nitrite reductase to produce NO [47]. In the current sensor configuration, hemoglobin cannot diffuse through the dialysis membrane to directly react with the NO produced by the RSePEI-catalyzed RSNO decomposition. However, physiological levels [48] of free hemoglobin can still affect the RSNO sensor response. As shown in Figure 4.4b, the presence of free oxyhemoglobin reduces the GSNO signal, especially at low GSNO concentrations. In another experiment, ~ 20% decrease in amperometric response was observed when free hemoglobin was added after the steady-state current was reached in the presence of 4 μM GSNO. This is likely attributed to the role of oxyhemoglobin as an NO 'sink' on the outside of the dialysis membrane. The NO produced within the thin catalyst layer between the dialysis and gas permeable membrane can diffuse in all directions. Under normal conditions, the fraction of NO that diffuses to the surface of the gas-sensing electrode to yield the amperometric signal is constant. When hemoglobin is present in

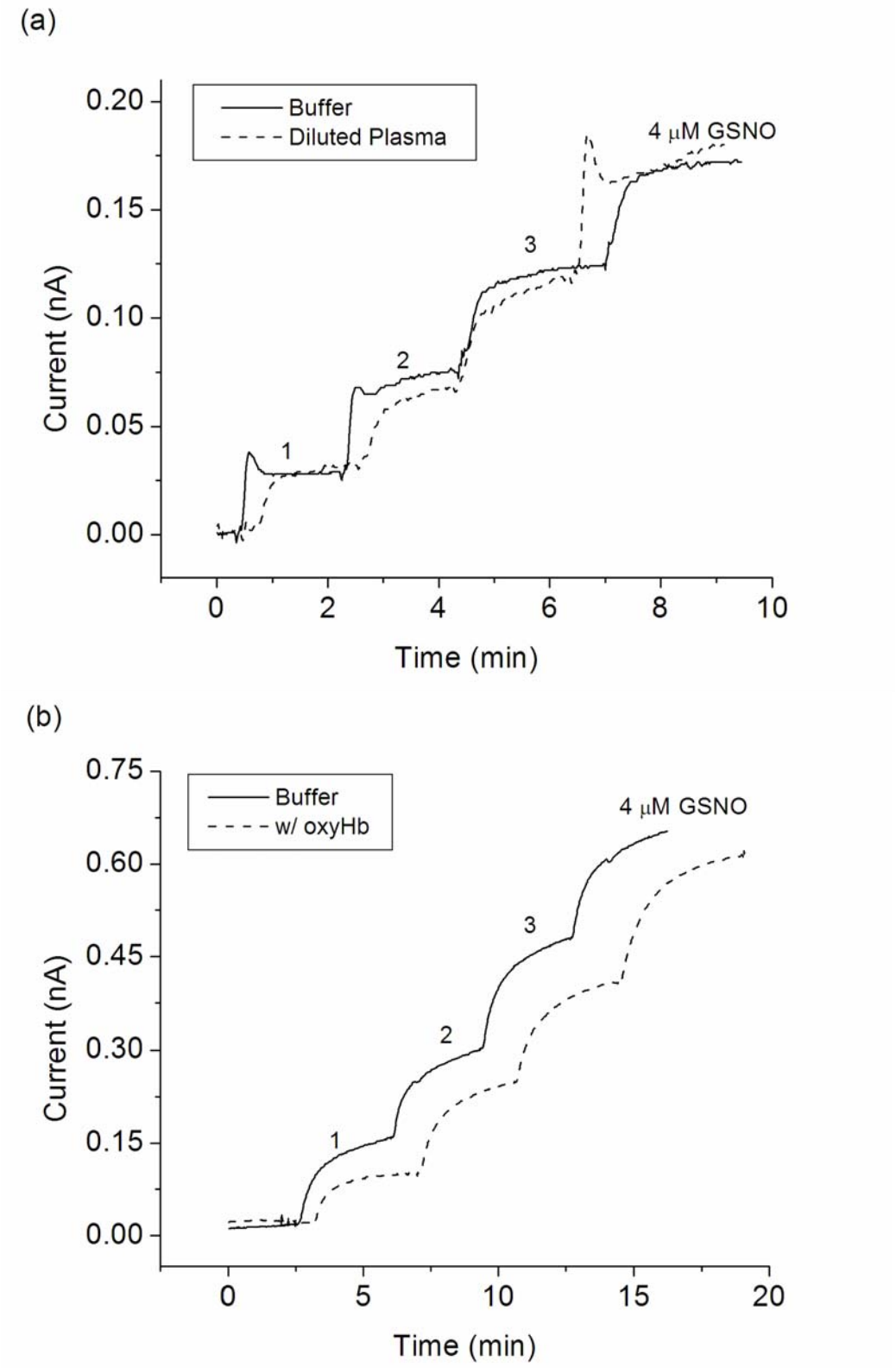

Figure 4.4. GSNO calibrations in biological matrices. (a) in PBS and 1:2 diluted rabbit plasma; (b) in PBS with and without 15 mg/dL oxyhemoglobin.

the solution outside the dialysis membrane, it scavenges NO, lowering the NO concentration outside the dialysis membrane and therefore creating a steeper concentration gradient. As a result, more NO diffuses to the outside of the dialysis membrane, creating a lower steady-state NO level within the RSePEI layer. It can be speculated that such scavenging effects would be similar to both endogenous RSNOs and the GSNO added during blood measurements. Thus, this effect of hemoglobin, as well as other possible NO scavengers in blood, should be taken into account in the final blood measurement via the proposed standard addition method. After the amperometric response from blood samples reaches a steady-state, one or more aliquots of a GSNO standard with known concentration was spiked into the diluted blood samples to correct for the scavenger and viscosity effect in blood (see below, Figure 4.5a). The calibration obtained from the standard addition is used instead of the prior GSNO calibration in buffer to calculate the final concentration of RSNO in blood samples.

4.3.4. Photo-Instability of RSNOs

The literature reported values of endogenous RSNO concentrations range from tens of nM to a few μM [29]. One important reason behind these variable values for endogenous RSNO concentrations is the labile nature of the RSNO compounds, which can easily be decomposed by heat, light and metal ions [10]. For the same reason, it is believed that sample handling is critical for proper determination of endogenous RSNO levels. However, most current techniques for blood RSNO measurements require the separation of blood by centrifugation and subsequent treatments of plasma samples with various reagents [26, 49]. During these processes, the exposure to light is difficult to

completely eliminate. The advantage of the electrochemical RSNO sensor is the minimal sample preparation: the blood RSNOs can be measured immediately in fresh whole blood without the need for any plasma separation. Therefore, the artifacts that might be introduced during the sample handling steps can be avoided. In addition, this unique advantage of the RSNO sensor also offers a chance to study in detail the effects of blood exposure to external variables, such as light, on the stability of endogenous RSNOs.

Despite the general perception that the absorbance of blood is so large that it protects the endogenous species from photodecomposition, it was discovered in this research that for fresh blood, very little amperometric response could be obtained if the samples had not been well protected from light, even over a very short period of time during the drawing of the blood sample. To study the effect of light exposure on the stability of endogenous RSNOs, an experiment was designed to draw blood through a butterfly needle tubing either with or without protection from light. The butterfly needle contains a plastic tube 12 inch in length and ca. 1 mm in i.d. It is connected to a heparinized 5 mL syringe that is always protected from light via Aluminum foil. During blood collection, it normally takes less than 20 sec for blood to pass through the butterfly tube. Figure 4.5a shows representative RSNO sensor responses to the venous blood from the same animal (pig) by both the covered and exposed sampling method. Using the standard addition method, which is discussed in more detail below, the RSNO concentration in this particular experiment was determined as 1.45 μM when the entire path of blood was protected from light. However, when the butterfly tube was not protected from light, the measured RSNO level dropped to 0.40 μM (i.e., 27.6%). It can be seen that the RSNO sensor responses to the GSNO standard were reproducible.

(a)

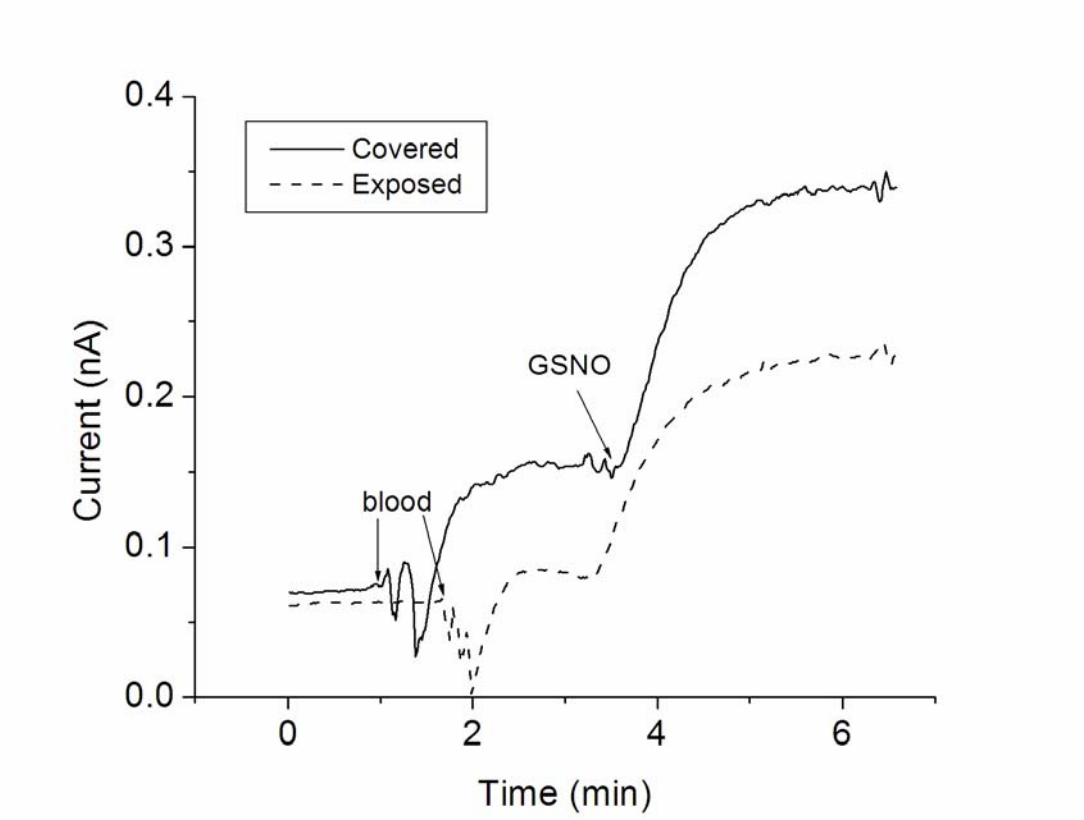

(b)

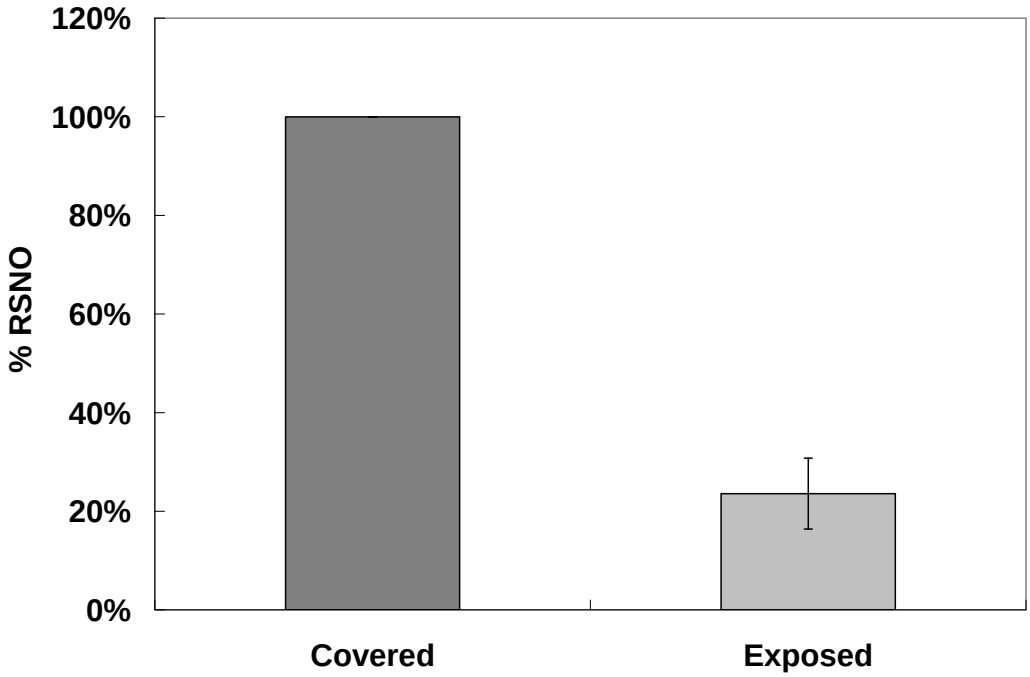

Figure 4.5. RSNO concentrations measured by exposed and covered sampling. (a) Amperometric responses from the RSNO sensors to blood followed by a standard addition of 3 μM GSNO; (b) RSNO concentrations measured in eight animals.

Therefore, the only plausible explanation for the decreased blood signal is the photodecomposition of RSNO during exposed sampling. A total of 8 sets of measurements of this type were performed in this manner with 6 pigs and a drop of RSNO level in the exposed blood samples was always observed. The results are summarized in Figure 4.5b with the RSNO levels from covered samples normalized to 100%. It can be seen that the RSNO levels dropped substantially in exposed blood samples, to only 23.6 $\pm$7.2 % of that obtained from covered samples. This suggests that exposure to light, though brief, has a significant impact on the RSNOs in blood samples. The light effect can be expected to be much more significant on plasma samples, as they lack the 'shield' from light offered by red blood cells. This might also explain why some researchers found the LMW RSNO species 'undetectable' in blood samples [16]. This research emphasizes the importance of sample handling in RSNO determination and also helps to elucidate the controversy over endogenous RSNO levels.

4.3.5. RSNO Determinations in Rabbit Whole Blood

The widely used triiodide assay method in RSNO quantification requires to centrifuge blood first and then to make three separate measurements of the obtained plasma sample in order to differentiate nitrite, RSNO and other nitroso- species such as *N*-nitrosamine and iron-nitrosyl compounds [26]. The merit of the RSNO sensor described herein is its specificity towards RSNO species, which can be harnessed to measure RSNOs directly in whole blood without the need for centrifugation or other subsequent treatments of plasma samples. Our studies have proved that the RSe-based catalyst is highly selective for RSNOs against other NO derivatives commonly

encountered in blood. No amperometric responses are observed for up to 2 mM nitrite or 300 μM *N*-nitrosamine (*N*-nitroso-*L*-proline) [50]. Therefore, the contribution to the amperometric signals from such compounds in the blood sample would be negligible.

Blood is an extremely complicated matrix containing low levels of NO as well as other volatile species (e.g., ammonia, hydrogen peroxide, etc.) that might be oxidized at the applied potential used in the RSNO sensor. This demands the use of a control NO sensor, which is almost identical to the RSNO sensor except it does not possess the RSePEI catalyst layer. The signal from the control sensor can be used to correct for the contributions from potential interfering species. Both the NO sensor and the RSNO sensor must be calibrated with NO first, thus the difference in the measured current from blood samples reflects the additional amount of NO being produced at the electrode surface due only to the Se-catalyzed decomposition of RSNOs. Based on the calibrations for NO and standard addition of GSNO into diluted blood samples, this additional NO signal can be translated into RSNO concentrations in blood.

A representative blood RSNO measurement is shown in Figure 4.6, where the amperometric responses from both sensors have been converted into the equivalent concentrations of NO. After the blood RSNO signal stabilizes, 3 μM GSNO is added to the diluted blood to implement a standard addition method for quantifying total RSNO levels. The RSNO concentrations in blood are calculated according to Equation 4.1:

$$[\mathrm{RSNO}]_{\text{whole blood}} = DF*([\mathrm{NO}]_{\text{RSNO Sensor}} - [\mathrm{NO}]_{\text{NO Sensor}})*SR_{RSNO\ Sensor} \qquad (4.1)$$

where *DF* represents the dilution factor of blood sample (i.e., *DF* = 3 in this case); [NO]

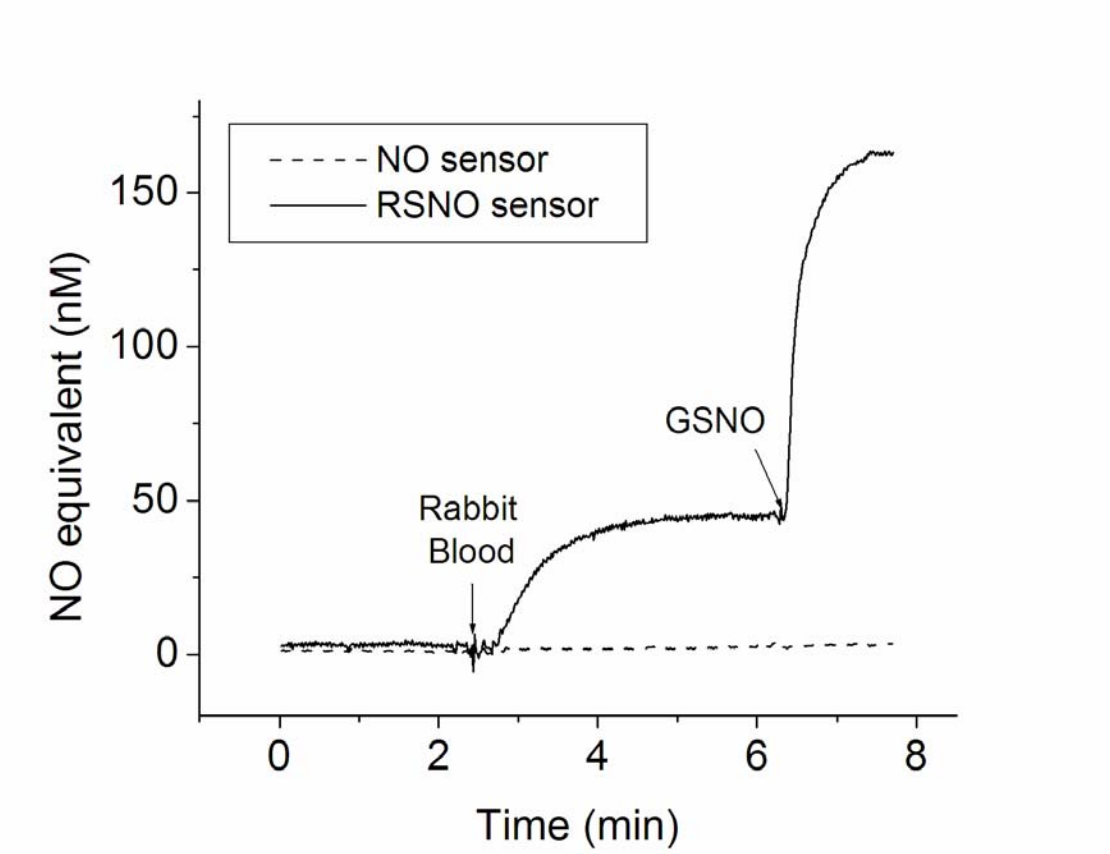

Figure 4.6. Rabbit blood RSNO measurement by the RSNO/NO sensor pair followed by a standard addition of 3 μM GSNO.

is the NO equivalent concentrations (based on previous calibration of NO) measured by the RSNO and NO sensors, respectively; $SR_{RSNO\ Sensor}$ refers to the sensitivity ratio between GSNO and NO for the RSNO sensor. This sensitivity ratio is obtained by dividing the RSNO sensor sensitivity towards GSNO in diluted blood (based on standard addition) by that towards NO in buffer.

It should be noted that hematocrit (Hct) is not taken into account in the above equation to calculate RSNO levels, since the effect of Hct on endogenous RSNOs is still unclear. Indeed, there is even a lack of consensus thus far regarding the levels of *S*-nitrosohemoglobin within red blood cells [51, 52]. Hct is an important parameter in clinical diagnostics to obtain the concentrations of analytes in plasma versus those in whole blood [53]. However, it is not yet clear whether LMW RSNOs can diffuse freely into and from the red blood cells (i.e., evenly distributed in whole blood). All the results reported herein are based on the assumption that RSNO concentrations in plasma and red blood cells are the same, which requires further experimental validation. In case this assumption is not valid, a correction for Hct needs to be made, resulting in Equation 4.2:

$$[\mathrm{RSNO}]_{\mathrm{plasma}} = (DF\text{-}\mathrm{Hct}\%)*([\mathrm{NO}]_{\mathrm{RSNO\ Sensor}} - [\mathrm{NO}]_{\mathrm{NO\ Sensor}})*SR_{RSNO\ Sensor}/(1\text{-}\mathrm{Hct}\%) \quad (4.2)$$

The effect of Hct should also be considered in obtaining $SR_{RSNO\ Sensor}$, since the added RSNO standard is distributed in the volume of diluted blood minus that occupied by the red blood cells.

Using this analytical approach (no Hct correction), the RSNO concentrations in a group of 32 rabbits were determined to be 3.04 ± 1.93 μM. The normal endogenous total

RSNO concentration has been the spotlight of controversy over the past decade [29] due to its labile nature and the various analytical methods employed in its detection. Interestingly, this study reveals that even by the same analytical method with minimal sample preparation, substantial variations of RSNO concentration still exist among individual animals of the same species. The RSNO concentrations span over a range from 0.37 μM to 7.44 μM with the majority (18 out of 32) falling between 1-3 μM. A plot of the distribution of RSNO levels is shown in Figure 4.7. It should be noted that the sensitivity of the RSNO sensor is not compromised after repeated exposure to fresh blood.

Previous reports suggested that the majority of RSNOs in circulating blood exist in the form of AlbSNO [54]. As discussed earlier, the RSNO sensor is capable of detecting HMW RSNOs such as AlbSNO at near quantitative yield through a transitrosation reaction with added thiol/reducing agent. However, such reaction takes much longer to reach steady-state current in buffer as compared to the detection of their LMW counterparts (i.e., 20-30 min vs. 4-5 min). Indeed, the equilibration time for the RSNO sensor to reach steady-state current in blood samples (as well as for subsequent standard RSNO additions) is even shorter, typically 2-4 min. Given this short equilibration time, the contribution of AlbSNO to the detected signal should be small. Therefore, it is likely that the RSNO signal measured with the new RSNO sensor comes predominantly from LMW RSNO species in the blood. Research is underway in this laboratory to develop new RSNO sensors that have similar sensitivity and response times towards both LMW and HMW RSNOs.

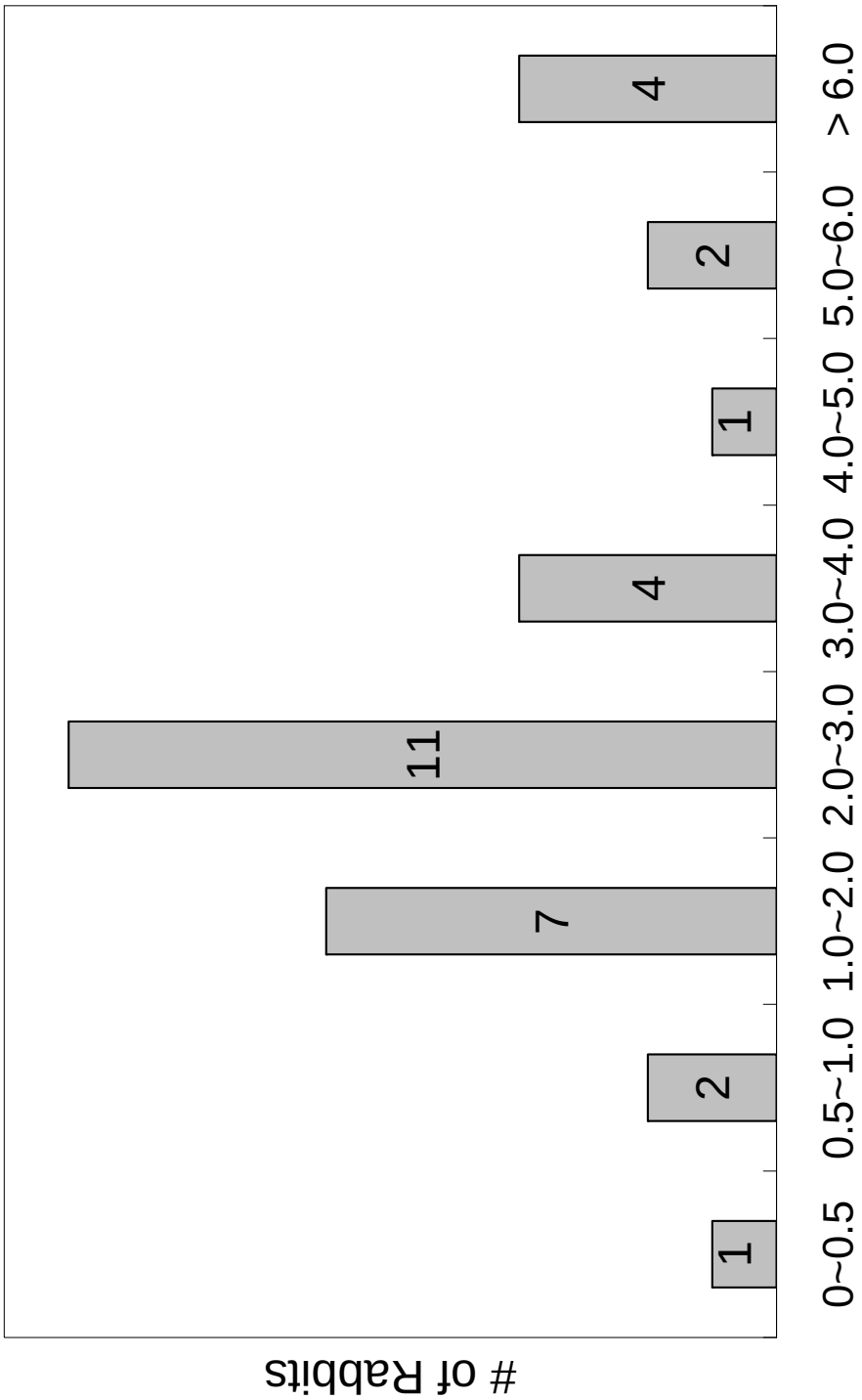

Figure 4.7. The distribution of RSNO concentrations in blood samples from N = 32 rabbits.

4.3.6. Change of RSNO Levels in Rabbits under ECC

Since RSNOs are used as the endogenous substrates for newly-developed NO-generating polymers [55], the change of endogenous RSNO concentrations may serve as an indication of the function of NO-generating polymers. If the RSNO is consumed by the NO-generating polymers at a rate faster than the rate of its biosynthesis in the blood, a gradual decline in endogenous RSNO level can be expected. Obviously, the rate of RSNO consumption is dependent on both the surface area of NO-generating polymer and the volume of circulating blood.

The ECC loops used in this study have a surface of ca. 60 cm^2 in contact with flowing blood and rabbit blood volume is normally 70 mL/kg of body weight [56]. The rabbit blood is passed through a loop with relatively large surface area, and thus the consumption of RSNO is expected to be very fast if the loop has been coated with NO-generating materials. On the other hand, the endogenous RSNO levels should maintain consistent if the ECC loop is coated with control polymers that do not consume RSNOs, or even there is no ECC loop attached to the animal at all. The change of blood RSNO levels over the first hour for rabbits in the ECC study is plotted in Figure 4.8. RSNO levels at Hour 0 are the baseline values and the RSNO levels at Hour 1 have all been normalized to the relative percentage of their respective baseline. After 1 h circulation, the blood RSNO levels in rabbits receiving NO-generating ECC loops drop to 27.3± 14.2% (N=10) of the baseline at Hour 0. But after 1 h, the RSNO levels in rabbits attached to control circuits or no circuits at all are still maintained at 98.9±11.5% (N=7) and 94.9±10.3% (N=5) respectively. It can be seen that the NO-generating ECC loops are functional *in vivo* as they consume considerable amounts of RSNOs within just an

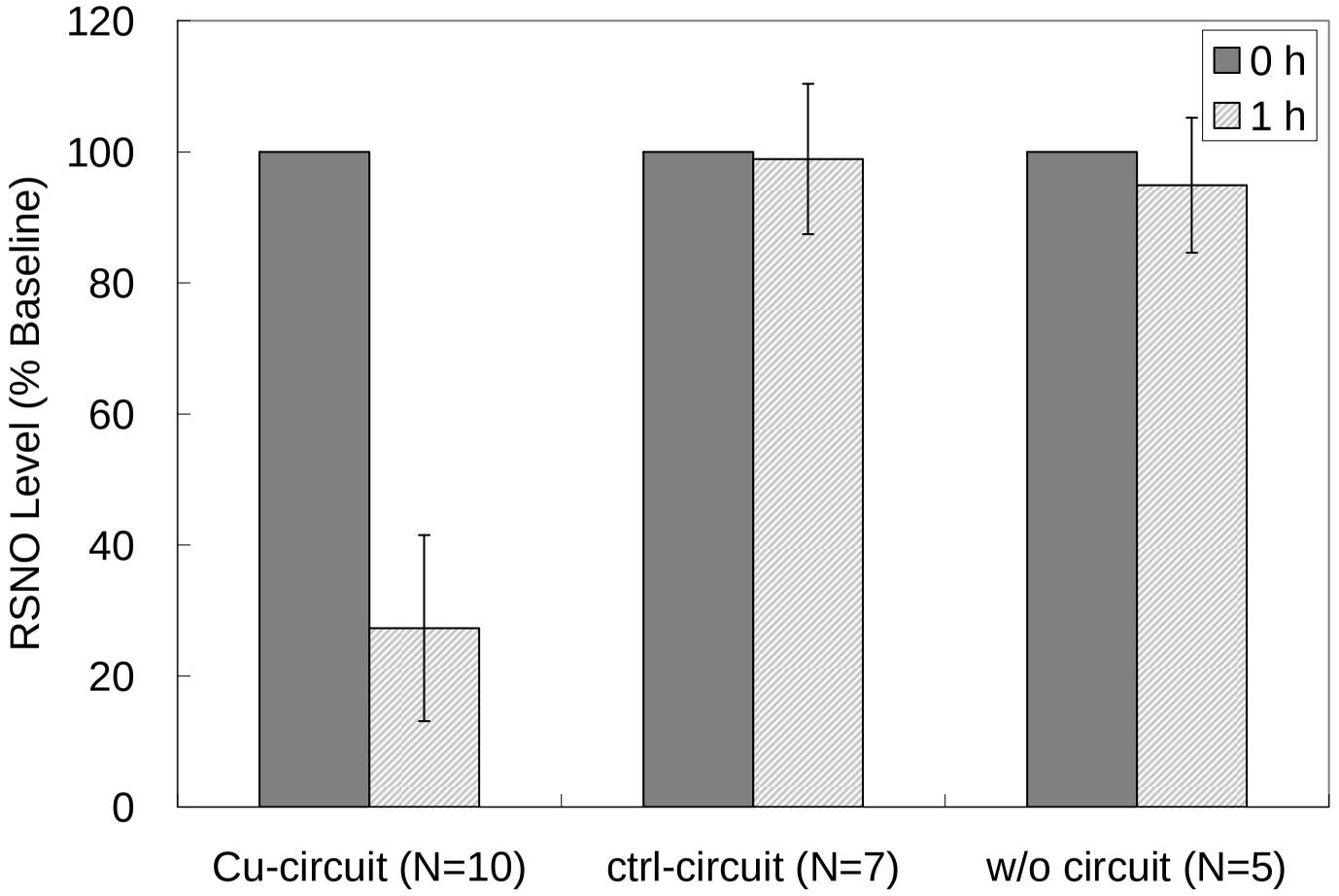

Figure 4.8. Change of blood RSNO levels over the first hour in the three different groups of rabbits in the ECC study

hour. This result also suggests that supplementation of RSNO to rabbits might be necessary to achieve sustainable NO-generation in ECC operations, which normally last 4-6 h.

4.3.7. RSNO Determinations in Pig Blood

Unlike ECC, in some implantable applications of NO-generating polymers such as intravascular sensors or vascular grafts, the contact surface is much smaller and hence the rate of RSNO consumption should be much slower. It has also been reported that a concentration gradient of *S*-nitrosohemoglobin exists between arterial and venous blood [57]. Therefore, in this work, we applied the new RSNO sensor method described above to: 1) examine the change of endogenous RSNO levels, if any, over time when NO-generating vascular grafts are implanted *in vivo*; 2) measure the RSNO concentrations of both arterial and venous blood from the same animal to determine if there is any concentration gradient.

The venous RSNO levels at three time points were monitored, including the RSNO baseline obtained right before the surgical implantation of vascular grafts and the RSNO concentrations 1 week and 3 weeks after the surgery. The baseline RSNO levels in venous pig blood were found to range from 0.6 to 2.7 μM (1.57±0.75 μM, N=9) and the changes in RSNO were normalized with respect to the baseline values (i.e., baseline = 100%). In pigs with NO-generating grafts, the venous RSNO levels dropped to 77.0± 2.2 % (N=2) after 1 week and further decreased to 54.1±11.7% by the end of 3 weeks. On the other hand, the RSNO levels in pigs with control grafts remained relatively constant, being 102.6±2.1% (N=2) after 1 week and 95.3±27.6% (N=3) after 3 weeks.

It can be concluded from these preliminary data that the presence of NO-generating catalyst *in vivo* gradually consumes the endogenous RSNO species. This also serves as indirect evidence that the NO-generating polymers are functioning *in vivo*. The overall change of RSNO concentration results from the different rates of RSNO consumption by NO-generating polymers and the rate of RSNO production by the animal. It is therefore dependent on the ratio of polymer surface area to blood volume. These vascular grafts are 6-8 cm in length and 6 mm in i.d. (surface area ~ 12-15 cm^2), with the NO-generating polymers coated on the inside. Such a surface area lies in between that of intravascular sensors and the surface area of coatings on extracorporeal circuits. It can then be reasonably speculated that the consumption of RSNO would be much slower for NO-generating intravascular sensors, while much faster in the case of NO-generating extracorporeal circuits.

The RSNO concentrations in arterial and venous blood were determined in 3 pigs, with the arterial RSNO levels found to be $94.6 \pm 1.3\%$ of those in the veins. Hence, there is no significant RSNO concentration gradient found between blood in porcine arteries and veins.

4.4. Summary

RSNO species play important roles in the metabolism of NO and they act directly in regulating platelet activity and endothelial function. The measurement of endogenous RSNOs is a popular yet controversial topic. RSNOs are labile species, but currently available techniques to measure RSNOs in blood require methods and associated

treatments which may introduce substantial artifacts. Using a newly developed RSePEI-based amperometric RSNO sensor, the endogenous RSNO (predominantly LMW RSNOs) concentrations in animal (rabbits and pigs) blood can be determined with minimal sample preparation. The sensor results indicate that substantial variations in endogenous RSNO concentrations exist even within the same animal species. The photo-decomposition of RSNOs in blood during the sample collection stage was also examined. The results suggest that even a short exposure to ambient light has detrimental effects on the accuracy in the determination of endogenous RSNOs. These findings emphasize the importance of proper sample handling in obtaining reliable values of endogenous RSNO levels and also suggest a greater potential of the RSNO sensor for clinical applications.

4.5 References

[1] R. J. Singh, N. Hogg, J. Joseph and B. Kalyanaraman, *J. Biol. Chem.*, 271 (1996) 18596-18603

[2] T. Rassaf, P. Kleinbongard, M. Preik, A. Dejam, P. Gharini, T. Lauer, J. Erckenbrecht, A. Duschin, R. Schulz, G. Heusch, M. Feelisch and M. Kelm, *Circ. Res.*, 91 (2002) 470-477

[3] S. C. Askew, A. R. Butler, F. W. Flitney, G. D. Kemp and I. L. Megson, *Bioorg. Med. Chem.*, 3 (1995) 1-9

[4] M. W. Radomski, D. D. Rees, A. Dutra and S. Moncada, *Br. J. Pharmacol.*, 107 (1992) 745-749

[5] M. Moro, V. Darley-Usmar, D. Goodwin, N. Read, R. Zamora-Pino, M. Feelisch, M. Radomski and S. Moncada, *Proc. Nat. Acad. Sci. U.S.A.*, 91 (1994) 6702-6706

[6] D. A. Wink, R. W. Nims, J. F. Darbyshire, D. Christodoulou, I. Hanbauer, G. W. Cox, F. Laval, J. Laval, J. A. Cook and et al., *Chem. Res. Toxicol.*, 7 (1994) 519-525

[7] N. Hogg, *Free Rad. Biol. Med.*, 28 (2000) 1478-1486

[8] D. Jourd'heuil, K. Hallen, M. Feelisch and M. B. Grisham, *Free Rad. Biol. Med*, 28 (2000) 409-417

[9] N. Hogg, *Ann. Rev. Pharmacol. Toxicol.*, 42 (2002) 585-600

[10] D. L. H. Williams, *Acc. Chem. Res.*, 32 (1999) 869-876

[11] H. H. Al-Sa'doni, I. L. Megson, S. Bisland, A. R. Butler and F. W. Flitney, *Br. J. Pharmacol.*, 121 (1997) 1047-1050

[12] P. Root, I. Sliskovic and B. Mutus, *Biochem.J.*, 382 (2004) 575-580

[13] M. P. Gordge, J. S. Hothersall, G. H. Neild and A. A. N. Dutra, *Br. J. Pharmacol.*, 119 (1996) 533-538

[14] Y. C. Hou, Z. M. Guo, J. Li and P. G. Wang, *Biochem. Biophys. Res. Commun.*, 228 (1996) 88-93

[15] J. E. Freedman, B. Frei, G. N. Welch and J. Loscalzo, *J. Clin. Invest.*, 96 (1995) 394-400

[16] T. Ishibashi, J. Yoshida and M. Nishio, *J. Pharmacol. Sci.*, 93 (2003) 409-416

[17] C. Heiss, T. Lauer, A. Dejam, P. Kleinbongard, S. Hamada, T. Rassaf, S. Matern, M. Feelisch and M. Kelm, *J. Am. Col. Cardiol.*, 47 (2006) 573-579

[18] J. A. Cook, S. Y. Kim, D. Teague, M. C. Krishna, R. Pacelli, J. B. Mitchell, Y. Vodovotz, R. W. Nims, D. Christodoulou, A. M. Miles, M. B. Grisham and D. A. Wink, *Anal. Biochem.*, 238 (1996) 150-158

[19] J. K. J. Park and P. Kostka, *Anal. Biochem.*, 249 (1997) 61-66

[20] A. Doctor, R. Platt, M. L. Sheram, A. Eischeid, T. McMahon, T. Maxey, J. Doherty, M. Axelrod, J. Kline, M. Gurka, A. Gow and B. Gaston, *Proc. Natl. Acad. Sci. USA*, 102 (2005) 5709-5714

[21] R. Marley, M. Feelisch, S. Holt and K. Moore, *Free Rad. Res.*, 32 (2000) 1-9

[22] B. K. Yang, E. X. Vivas, C. D. Reiter and M. T. Gladwin, *Free Rad. Res.*, 37 (2003) 1-10

[23] S. R. Jaffrey, H. Erdjument-Bromage, C. D. Ferris, P. Tempst and S. H. Snyder, *Nat. Cell. Biol.* 3 (2001) 193-197

[24] R. Rossi, D. Giustarini, A. Milzani, R. Colombo, I. Dalle-Donne and P. Di Simplicio, *Circ. Res.*, 89 (2001)

[25] R. K. Goldman, A. A. Vlessis and D. D. Trunkey, *Anal. Biochem.*, 259 (1998) 98-103

[26] M. Feelisch, T. Rassaf, S. Mnaimneh, N. Singh, N. S. Bryan, D. Jourd'Heuil and M. Kelm, *FASEB J.*, 16 (2002) 1775-1785

[27] D. Tsikas, *Nitric Oxide-Biol. Chem.*, 9 (2003) 53-55

[28] D. Giustarini, A. Milzani, R. Colombo, I. Dalle-Donne and R. Rossi, *Trends Pharmacol. Sci.*, 25 (2004) 311-316

[29] D. Giustarini, A. Milzani, I. Dalle-Donne and R. Rossi, *J. Chromatogr. B*, 851 (2007) 124-139

[30] A. J. Gow, B. P. Luchsinger, J. R. Pawloski, D. J. Singel and J. S. Stamler, *Proc. Natl. Acad. Sci. USA*, 96 (1999) 9027-9032

[31] B. K. Oh and M. E. Meyerhoff, *Biomaterials*, 25 (2004) 283-293

[32] X. J. Zhang, *Front. Biosci.*, 9 (2004) 3434-3446

[33] T. Malinski and Z. Taha, *Nature*, 358 (1992) 676-678

[34] Y. Lee, J. Yang, S. M. Rudich, R. J. Schreiner and M. E. Meyerhoff, *Anal. Chem.*, 76 (2004) 545-551

[35] W. Cha and M. E. Meyerhoff, *Langmuir*, 22 (2006) 10830-10836

[36] W. Cha, Y. Lee, B. K. Oh and M. E. Meyerhoff, *Anal. Chem.*, 77 (2005) 3516-3524

[37] T. Koch, E. Suenson, U. Henriksen and O. Buchardt, *Bioconjugate Chem.*, 1 (1990) 296-304

[38] J. S. Stamler and J. Loscalzo, *Anal. Chem.*, 64 (1992) 779-785

[39] W. Cha and M. E. Meyerhoff, *Biomaterials*, 28 (2007) 19-27

[40] K. Fang, N. V. Ragsdale, R. M. Carey, T. MacDonald and B. Gaston, *Biochem. Biophys. Res. Comm.*, 252 (1998) 535-540

[41] N. S. Bryan, T. Rassaf, J. Rodriguez and M. Feelisch, *Nitric Oxide*, 10 (2004) 221-228

[42] R. E. Benesch, R. Benesch and S. Yung, *Anal. Biochem.*, 55 (1973) 245-248

[43] D. A. Skoog, F. J. Holler and T. A. Nieman, *Principles of Instrumental Analysis*, 5th ed., Harcourt Brace & Company, 1998, Orlando, FL

[44] A. M. Skrzypchak, N. G. Lafayette, R. H. Bartlett, Zhengrong Zhou, M. C. Frost, M. E. Meyerhoff, M. M. Reynolds and G. M. Annich, *Perfusion*, 22 (2007) 193-200

[45] N. Hogg, *Anal. Biochem.*, 272 (1999) 257-262

[46] X. Liu, M. J. S. Miller, M. S. Joshi, H. Sadowska-Krowicka, D. A. Clark and J. R. Lancaster Jr., *J. Biol. Chem.*, 273 (1998) 18709-18713

[47] R. Grubina, Z. Huang, S. Shiva, M. S. Joshi, I. Azarov, S. Basu, L. A. Ringwood, A. Jiang, N. Hogg, D. B. Kim-Shapiro and M. T. Gladwin, *J. Biol. Chem.*, 282 (2007) 12916-12927

[48] C. Sebastian, R. Romero, E. Olalla, C. Ferrer, J. J. Garcia-Vallejo and M. Munoz, *Eur. Spine J.*, 9 (2000) 458-465

[49] A. Gow, A. Doctor, J. Mannick and B. Gaston, *J. Chromatogr. B*, 851 (2007) 140-151

[50] W. Cha, F. Zhang and M. E. Meyerhoff, *unpublished results*, (2007)

[51] X. Wang, N. S. Bryan, P. H. MacArthur, J. Rodriguez, M. T. Gladwin and M. Feelisch, *J. Biol. Chem.*, 281 (2006) 26994-27002

[52] S. C. Rogers, A. Khalatbari, P. W. Gapper, M. P. Frenneaux and P. E. James, *J. Biol. Chem*, 280 (2005) 26720-26728

[53] N. Fogh-Andersen and P. D'Orazio, *Clin. Chem.*, 44 (1998) 655-659

[54] J. S. Stamler, O. Jaraki, J. Osborne, D. I. Simon, J. Keaney, J. Vita, D. Singel, C. R. Valeri and J. Loscalzo, *Proc. Natl. Acad. Sci. USA*, 89 (1992) 7674-7677

[55] B. K. Oh and M. E. Meyerhoff, *J. Am. Chem. Soc.*, 125 (2003) 9552-9553

[56] R. A. Little, *J. Physiol.*, 208 (1970) 485-497

[57] M. Kelm, *Biochim. Biophys. Acta*, 1411 (1999) 273-289

CHAPTER 5

CONCLUSIONS AND FUTURE DIRECTIONS

5.1. Summary of Results for Dissertation Research

Nitric oxide has been found to be a potent inhibitor of platelet activation and adhesion, as well as an effective vasodilator. Polymers that can continuously release low levels of NO *in vivo* could potentially enhance the biocompatibility of blood-contacting medical devices such as intravascular sensors [1, 2], vascular grafts [3], extracorporeal circuits [4] and hemodialysis filters [5]. In this dissertation research, efforts have been made to develop new strategies to evaluate the biocompatibility of the NO-releasing/generating polymeric materials both *in vitro* and *in vivo*. In addition, due to the critical role of *S*-nitrosothiols (RSNOs) in generating NO at the polymer/blood interface, their endogenous concentrations have also been determined in a number of animals via a novel RSePEI-based electrochemical RSNO sensor.

In Chapter 2, an *in vitro* platelet adhesion assay was developed via the quantification of platelet lactate dehydrogenase (LDH) content to study the *in vitro* biocompatibility of NO-releasing/generating polymeric materials. Through the LDH assay, it was discovered that increasing levels of NO released from plasticized poly(vinyl chloride) films which were doped with DBHD/N_2O_2 could inhibit the adhesion of rabbit platelets to the surface

of such polymers. The highest NO-release flux studied, 7.05 $\times 10^{-10}$ mol cm^{-2} min^{-1}, reduced the adhesion of platelets by as much as 78.9% compared to the control polymers that did not release NO (from 14.0 (±2.1) $\times 10^5$ cells cm^{-2} to 2.96 (±0.18) $\times 10^5$ cells cm^{-2}). This work was the first quantitative *in vitro* assay that proved the enhanced biocompatibility of NO-releasing polymers. The new LDH-based method might potentially serve as a preliminary biocompatibility screening method for new NO-releasing materials that will emerge in the future.

The LDH assay for NO-generating polymers, however, encountered serious challenges. Addition of 5 μM GSNO to plasma samples reduced platelet adhesion. Further, the presence of an NO-generating Cu-DTTCT catalyst did not enhance the biocompatibility when compared to control polymers. The reasons for this result may involve the rapid decomposition of RSNOs by the NO-generating polymers, which was not commensurate with the duration of PRP incubation, or the photo-instability of RSNOs in plasma. Further investigation is required to decipher this observation.

The ideal biocompatibility evaluation methodology for NO-generating polymers is via *in vivo* studies as a continuous supply of RSNOs will be provided by the flowing blood. A proof-of-concept experiment on the enhanced *in vivo* biocompatibility of NO-generating polymers coated on the surfaces of intravascular sensors is described in Chapter 3. The NO-generating coatings were created by impregnating metallic Cu^0 particles of different sizes (i.e., 80 nm or 3 μm) into polymer coatings made of either hydrophobic polyurethane (Tecoflex SG80A, for 80 nm Cu^0 particles) or a mixture of hydrophilic polyurethane (Tecophilic SP-60-D-60) and silicone rubber (RTV-3140, for 3 μm Cu^0 particles). The coatings were applied on the surface of a catheter-type, Clark-

style amperometric oxygen sensors for intravascular implantation. Sensors with either NO-generating coatings or control coatings (polymers without doped Cu^0 particles) were implanted in porcine carotid and femoral arteries and used for continuous monitoring of blood PO_2 levels for up to 20 h. The data suggest that more statistically reliable results are obtained from the NO-generating sensors, with the average of measured PO_2 values falling within 95% confidence interval of the 'true values' read by bench-top blood gas analyzer from discrete blood samples drawn from the animals. The control sensors, however, started to deviate beyond the 95% confidence interval after 10-15 h of implantation. After each experiment, the sensors were carefully removed and examined via the LDH assay for thrombus formation on the surfaces. This surface examination revealed similar results. Although thrombus was still found on ~ 20% of NO-generating sensors evaluated, the average degree of thrombosis was much less than that on the control sensors, which also had a more frequent occurrence of thrombus (~ 80% of the time). This research demonstrated that *in situ* generation of NO at the polymer/blood interface could be utilized to enhance the biocompatibility of implanted medical devices.

Since RSNOs are used as the substrates to generate NO *in vivo*, their concentrations are an important factor in determining whether sufficient NO can be generated at the polymer/blood interface in order to maintain thromboresistance. Consequently, the occasional thrombus formation on the NO-generating sensors examined in Chapter 3 initiated the investigation into the possible variations of endogenous RSNO concentrations in animal blood. Besides the use as biomaterials, the NO-generating polymers can also be employed in detecting RSNOs via the catalytic conversion of RSNOs into NO. Indeed, electrochemical RSNO sensors have already

been designed by modifying amperometric NO sensors with additional catalytic membranes that convert RSNO into NO [6, 7]. The RSePEI-based RSNO sensor has the advantage of being almost equally sensitive to all LMW RSNOs and is thus well suited to assess the overall concentrations of LMW RSNOs in blood. Further characterization of such an RSNO sensor based on immobilized RSePEI catalyst, and its applications in determining the endogenous RSNO concentrations in animal (i.e., rabbits and pigs) blood, were the major focus of Chapter 4.

In this study, an average blood concentration of 3.04 ± 1.93 μM RSNOs (predominantly LMW RSNOs) was determined from a group of 32 rabbits. Considerable variations existed in the measured concentrations of endogenous RSNOs, ranging from 0.37 μM to 7.44 μM. Unlike other methodologies employed in RSNO measurements, the electrochemical RSNO sensor requires virtually no sample preparation and the delay between blood collection and analysis can be minimized. This unique advantage offered the chance to study other factors during the sampling stage that may affect the accurate determination of RSNO concentrations. Specifically, the photo-decomposition of RSNO when blood was passed through a plastic tube during sample collection was studied by either completely covering the tube with Aluminum foil or allowing the tube to be exposed to light. Assuming the covered sample preserved 100% of all RSNOs, the amount of RSNOs remaining in the exposed samples was only 23.6 ± 7.2 % (N=8). This study showed that even very brief exposure to light could have a detrimental effect on the levels of RSNOs in blood. Therefore, the proper handling of blood samples is critical for the accurate measurement of RSNOs. In addition, it also suggests greater potential biomedical applications of the electrochemical RSNO sensors.

5.2. Future Directions

This dissertation research demonstrated the potential of NO-releasing/generating materials in enhancing biocompatibility both *in vitro* and *in vivo*. However, further investigation is still needed to develop more biocompatible materials/devices in the future.

5.2.1. *In Vitro* Biocompatibility Assays

The LDH assay described in Chapter 2 is capable of providing quantitative results on platelet adhesion. However, it merely counts the number of platelets regardless of their state of activation. In many biomedical applications, the degree of platelet activation is an important piece of information, as activated platelets are key to initiate the coagulation cascade, resulting in thrombosis [8]. Therefore, it is necessary to develop an *in vitro* assay to study platelet activation on NO-releasing/generating materials surfaces.

P-Selectin (CD62P), a 140 KDa glycoprotein, is a component of the alpha granule membrane and is expressed at the surface of platelets upon activation [9]. It is regarded by many as a marker for platelet activation [10, 11]. Previous reports have shown that an NO donor, *S*-nitroso-*N*-acetyl-penicillamine (SNAP), could inhibit thrombin-induced platelet activation as determined via an enzyme-linked immunosorbent assay (ELISA) for P-selectin [12]. In the future, it may be possible to design a similar enzyme immunoassay for P-selectin to study platelet activation on the surface of NO-

releasing/generating polymeric films. It should be noted, however, that the locally released NO at the polymer surface might alter the activity of some enzymes, such as horseradish peroxidase (HRP) often used in an ELISA-type assay. In that case, the activities of the enzyme labels on the antibodies bound to NO-releasing/generating polymer surfaces might be considerably different from those of the enzymes on control polymer surfaces. If so, alternative enzyme labels should be sought, or it might be possible to use the soluble P-selectin in plasma [13, 14] as the platelet activation marker and measure it in a similar manner to that in the LDH assay.

5.2.2. *In Vivo* Evaluation of NO-Releasing/Generating Polymers

The NO-generating polymers based on organoselenium catalysts appear promising for *in vivo* applications. A layer-by-layer deposition method of RSePEI onto silicone rubber surfaces is a potential candidate for the next set of *in vivo* studies via the intravascular oxygen sensor model. Nevertheless, challenge still remains for the *in vivo* application of RSe-based NO generation in terms of its catalytic efficiency. When compared to Cu-based NO generation, organoselenium catalysts require much higher RSNO concentrations (i.e., ~ 50 μM, well beyond the endogenous RSNO levels) to generate NO fluxes similar to those produced by the human endothelium. One approach to increase the flux levels generated by the RSe-based catalysts might be the creation of a brush-type structure of the SePEI polymer chain on the polymer surface, such as that has been commercially used on Corline^{TM} surfaces for heparin immobilization [15], in order to maximize the surface density of the catalysts.

As discussed in Chapter 1, needle-type subcutaneous sensors can be used for minimally invasive glucose monitoring in diabetic patients. The schematic of a needle-type NO-releasing glucose sensor based on the NO donor, DBHD/N_2O_2 [3], is shown in Figure 5.1. The biocompatibility of this glucose sensor may also be evaluated in the porcine artery model once it has been more thoroughly characterized *in vitro*. It should be noted that due to their smaller dimension, thrombus is less likely to form on the control glucose sensors compared to the control oxygen sensors. Thrombosis may be induced by a change in blood flow. But the small diameter of the needle-type sensor has little impact on hemodynamics as it will not significantly change the flow of blood around it. In this case, experimental conditions need to be optimized to create contrast between the NO-releasing and control needle sensors to promote thrombosis.

5.2.3. Electrochemical RSNO Sensors

Several questions need to be addressed in the future development of the amperometric RSNO sensors. First and foremost is the detection of HMW endogenous RSNOs such as AlbSNO, since they have been suggested to be the major RSNO reservoirs *in vivo*. In order to determine the overall RSNO concentrations in blood, an RSNO sensor with similar sensitivities and response times towards both LMW and HMW is required. Efforts have been made in this lab to create catalytic membranes from commercial dialysis membranes to improve HMW RSNO sensitivities. It may also be possible to immobilize Se-based catalysts directly on the surfaces of gas-permeable membranes, provided that the leaching of catalysts can be eliminated.

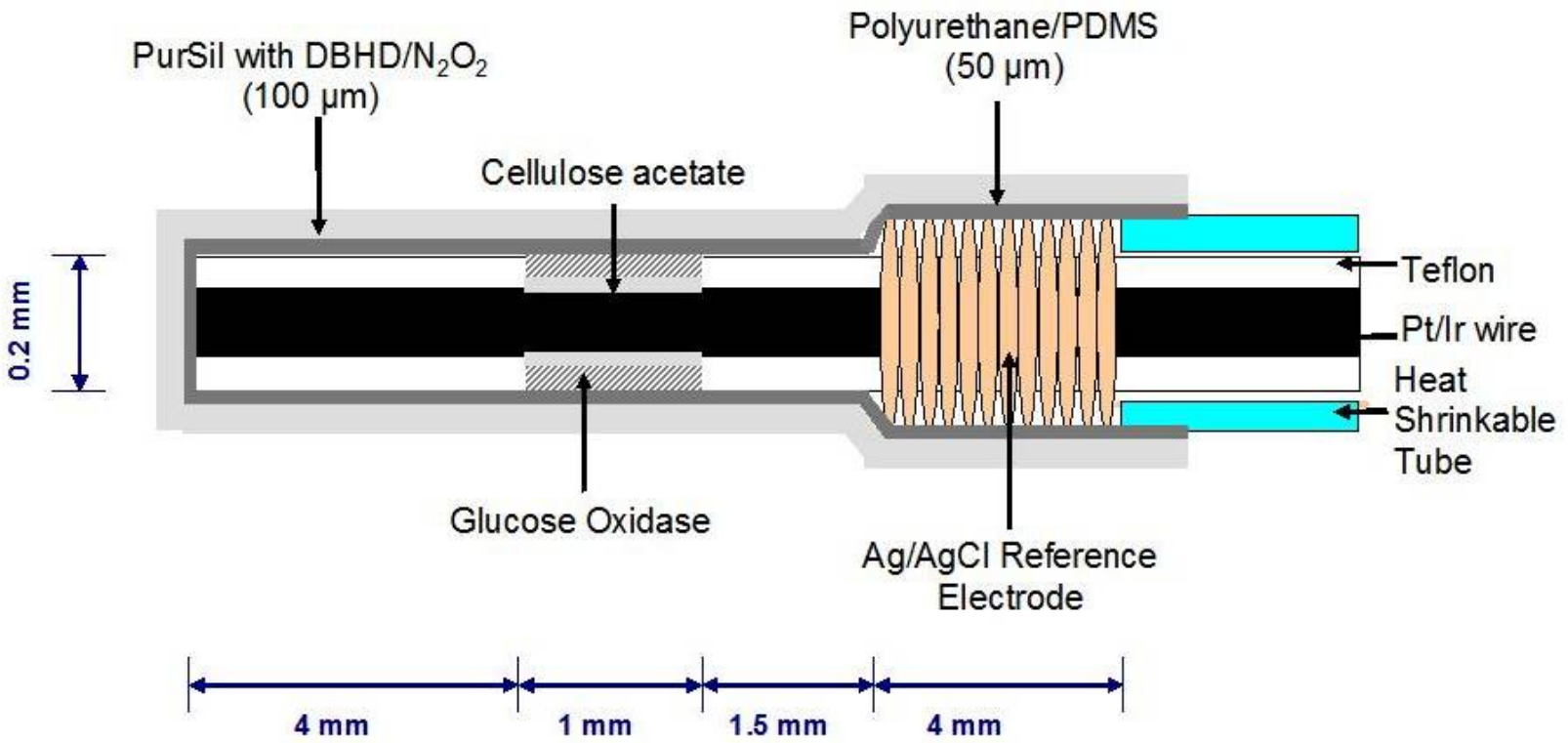

Figure 5.1. Schematic of a NO-releasing needle-type glucose sensor

The second question is the effect of red blood cells. Many researchers are interested in the *S*-nitrosohemoglobin (Hb-SNO) concentrations within the red blood cells. The triiodide assay, which measures the NO liberated from various nitroso compounds in plasma samples via reductive chemiluminescence with acidified iodide/iodine solution, has traditionally been employed in such studies. But it is an area of intense debate as three separate measurements are necessary to differentiate nitrite, RSNO and other nitroso-compounds [16-20]. The RSNO sensor methodology is believed to be advantageous in blood RSNO determinations. It will be exciting if the RSNO sensor can also be used to measure Hb-SNO in the red blood cells. However, precautions need to be taken since hemoglobin is a very complicated molecule and serves multiple roles in the reactions with NO and/or RSNO [16, 21]. In addition to being the acceptor of nitroso- groups, hemoglobin can react with NO or RSNO to form iron-nitrosyl compounds [22], and oxyhemoglobin can scavenge NO to form methemoglobin and nitrate [23]. All of these reactions need to be taken into account when measuring Hb-SNO within red blood cells. Another concern about the red cells is the hematocrit effect. It is not yet clear whether the RSNO concentrations in plasma and red cells are equal. In other words, can the RSNOs (either endogenous or added during standard addition) rapidly diffuse into the red blood cells to achieve a uniform concentration in whole blood? This question needs to be addressed before any statements of 'plasma' or 'whole blood' concentrations of RSNO can be made.

Last but not least, is the elimination of interferences. The RSNO sensor is highly selective against nitrite and other nitroso- species that interfere with other RSNO detection methodologies. The simultaneous use of an NO sensor also helps to reduce the

contribution from interfering endogenous species such as ammonia. However, the RSNO sensor is still subject to its own interference problem, most notably a background current from high concentrations of reduced thiols. An increase in baseline current was often observed after the addition of GSH or cysteine. The identity of this electroactive species produced within the catalytic layer by reduced thiols is largely unknown, although it is suspected to be hydrogen peroxide produced by the oxidation of the thiols in the presence of oxygen [24]. Further research is needed to investigate the origin and nature of this unwanted signal in order to prepare more reliable RSNO sensors.

5.2.4. The Future towards an 'Artificial Endothelium'

To date, the functionality of implantable medical devices such as sensors is still hampered by the adverse biological responses. Numerous attempts have been made to address the physicochemical properties of the materials surface for the development of biocompatible sensors [25]. As discussed in previous chapters, it has been recently shown that the local release/generation of biologically active species such as NO is capable of reducing thrombus formation on intravascular sensors. However, NO alone is unlikely to be the solution to the entire biocompatibility problem. Indeed, the vascular endothelium is a perfectly non-thrombogenic surface due to a number of molecules working synergistically to maintain vascular homeostasis. A biomimetic approach to create an 'artificial endothelium' will likely provide the most promising route to the development of truly biocompatible sensors. NO-releasing/generating polymers are the first step in this direction. Further, surface immobilization of heparin and thrombomodulin, used in conjunction with continuous release of a variety of naturally

occurring antithrombogenic species (including prostacyclin), may enable the implanted devices to exhibit even greater biocompatibility than NO release/generation alone. A dual-functional polymeric coating with surface-immobilized active heparin and NO-release has recently been reported [26]. In addition, it has been found that surface-bound thrombomodulin and heparin on NO-releasing polymers retained their biological function and might be a promising candidate for future development of more biocompatible coatings for implantable sensors [27].

5.3. References

[1] M. C. Frost, S. M. Rudich, H. P. Zhang, M. A. Maraschio and M. E. Meyerhoff, *Anal. Chem.*, 74 (2002) 5942-5947

[2] M. H. Schoenfisch, K. A. Mowery, M. V. Rader, N. Baliga, J. A. Wahr and M. E. Meyerhoff, *Anal. Chem.*, 72 (2000) 1119-1126

[3] M. M. Batchelor, S. L. Reoma, P. S. Fleser, V. K. Nuthakki, R. E. Callahan, C. J. Shanley, J. K. Politis, J. Elmore, S. I. Merz and M. E. Meyerhoff, *J. Med. Chem.*, 46 (2003) 5153-5161

[4] H. P. Zhang, G. M. Annich, J. Miskulin, K. Osterholzer, S. I. Merz, R. H. Bartlett and M. E. Meyerhoff, *Biomaterials*, 23 (2002) 1485-1494

[5] Z. Zhou, G. M. Annich, Y. Wu and M. E. Meyerhoff, *Biomacromolecules*, 7 (2006) 2565-2574

[6] W. Cha, Y. Lee, B. K. Oh and M. E. Meyerhoff, *Anal. Chem.*, 77 (2005) 3516-3524

[7] W. Cha and M. E. Meyerhoff, *Langmuir*, 22 (2006) 10830-10836

[8] J. W. M. Heemskerk, E. M. Bevers and T. Lindhout, *Thromb. Haemost.*, 88 (2002) 186-193

[9] D. Gurney, G. Y. H. Lip and A. D. Blann, *Am. J. Hematol.*, 70 (2002) 139-144

[10] M. Griesshammer, H. Beneke, B. Nussbaumer, M. Grunewald, M. Bangerter and L. Bergmann, *Thromb. Res.*, 96 (1999) 191-196

[11] P. Andre, *Br. J. Haematol.*, 126 (2004) 298-306

[12] P. A. Whiss, R. G. G. Andersson and U. Srinivas, *J. Immunol. Methods*, 200 (1997) 135-143

[13] A. D. Michelson, M. R. Barnard, H. B. Hechtman, H. MacGregor, R. J. Connolly, J. Loscalzo and C. R. Valeri, *Proc. Natl. Acad. Sci. USA*, 93 (1996) 11877-11882

[14] A. Massaguer, P. Engel, V. Tovar, S. March, M. Rigol, N. Solanes, J. Bosch and P. Pizcueta, *Vet. Immunol. Immunopathol.*, 96 (2003) 169-181

[15] K. Christensen, R. Larsson, H. Emanuelsson, G. Elgue and A. Larsson, *Biomaterials*, 22 (2001) 349-355

[16] N. S. Bryan, T. Rassaf, J. Rodriguez and M. Feelisch, *Nitric Oxide*, 10 (2004) 221-228

[17] B. W. Allen and C. A. Piantadosi, *Am. J. Physiol. (Heart Circ. Physiol.)*, 291 (2006) H1507-1512

[18] D. Giustarini, A. Milzani, I. Dalle-Donne and R. Rossi, *J.Chromatogr. B*, 851 (2007) 124-139

[19] M. T. Gladwin, J. H. Shelhamer, A. N. Schechter, M. E. Pease-Fye, M. A. Waclawiw, J. A. Panza, F. P. Ognibene and R. O. Cannon, III, *Proc. Natl. Acad. Sci. USA*, 97 (2000) 11482-11487

[20] A. Gow, A. Doctor, J. Mannick and B. Gaston, *J. Chromatogr. B*, 851 (2007) 140-151

[21] S. Basu, J. D. Hill, H. Shields, J. Huang, S. Bruce King and D. B. Kim-Shapiro, *Nitric Oxide*, 15 (2006) 1-4

[22] N. Y. Spencer, N. K. Patel, A. Keszler and N. Hogg, *Free Rad. Biol. Med.*, 35 (2003) 1515-1526

[23] A. J. Gow, B. P. Luchsinger, J. R. Pawloski, D. J. Singel and J. S. Stamler, *Proc. Natl. Acad. Sci. USA*, 96 (1999) 9027-9032

[24] P. W. Albro, J. T. Corbett and J. L. Schroeder, *J. Inorg. Biochem.*, 27 (1986) 191-203

[25] N. Wisniewski and M. Reichert, *Colloids Surf. B Biointerfaces*, 18 (2000) 197-219

[26] Z. R. Zhou and M. E. Meyerhoff, *Biomaterials*, 26 (2005) 6506-6517

[27] B. Wu, B. Gerlitz, B. W. Grinnell and M. E. Meyerhoff, *Biomaterials*, 28 (2007) 4047-4055